



DE83015792

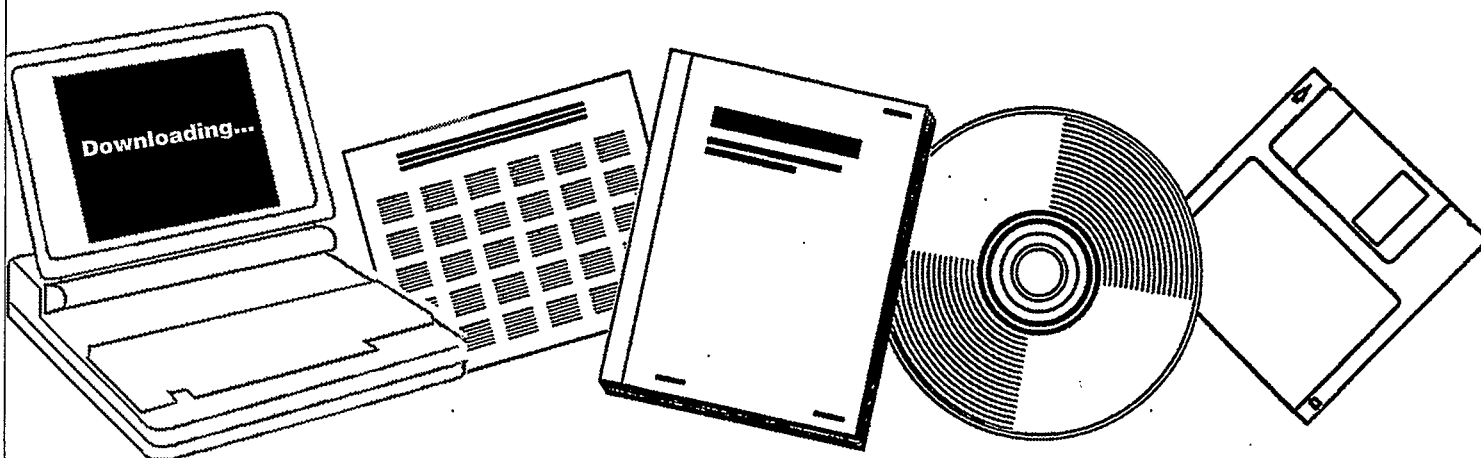
NTIS

One Source. One Search. One Solution.

**CHEMISTRY AND CATALYSIS OF COAL
LIQUEFACTION: CATALYTIC AND THERMAL
UPGRADING OF COAL LIQUID AND HYDROGENATION
OF CO TO PRODUCE FUELS. QUARTERLY PROGRESS
REPORT, APRIL-JUNE 1983**

UTAH UNIV., SALT LAKE CITY. DEPT. OF
MINING AND FUELS ENGINEERING

JUL 1983



U.S. Department of Commerce
National Technical Information Service

DOE/ET/14700-15
(DE83015792)

Distribution Category UC-90d

Chemistry and Catalysis of Coal Liquefaction
Catalytic and Thermal Upgrading of Coal Liquid
and Hydrogenation of CO to Produce Fuels

Quarterly Progress Report
for the Period April-June 1983

Dr. Wendell H. Wiser

University of Utah - Department of
Mining and Fuels Engineering
Salt Lake City, Utah 84112

Date Published - July 1983

Prepared for the United States Department
of Energy
Under Contract No. DE-AC22-79ET14700

CONTENTS

I	Cover Sheet	1
II	Objective and Scope of Work	3
III	Highlights to Date	7
IV	Task 1 Chemical-Catalytic Studies	8
	Task 2 Carbon-13 NMR Investigation of CDL and Coal	16
	Task 3 Catalysis and Mechanism of Coal Liquefaction	17
	Task 4 Momentum, Heat and Mass Transfer in Co-Current Flow	Discontinued
	Task 5 The Fundamental Chemistry and Mechanism of Pyrolysis of Bituminous Coal	20
	Task 6 Catalytic Hydrogenation of CD Liquids and Related Polycyclic Aromatic Hydrocarbons	57
	Task 7 Denitrogenation and Deoxygenation of CD Liquids and Related N- and O- Compounds	58
	Task 8 Catalytic Cracking of Hydrogenated CD Liquids and Related Hydrogenated Compounds	79
	Task 9 Hydropyrolysis (Thermal Hydrocracking) of CD Liquids	80
	Task 10 Systematic Structural-Activity Study of Supported Sulfide Catalysts for Coal Liquids Upgrading	82
	Task 11 Basic Study of the Effects of Coke and Poisons on the Activity of Upgrading Catalysts	88
	Task 12 Diffusion of Polyaromatic Compounds in Amorphous Catalyst Supports	Inactive
	Task 13 Catalyst Research and Development	96
	Task 14 Characterization of Catalysts and Mechanistic Studies	Inactive
V	Conclusion	121

OBJECTIVE AND SCOPE OF WORK

I. The chemistry and Catalysis of Coal Liquefaction

Task 1 Chemical-Catalytic Studies

Coal will be reacted at subsoftening temperatures with selective reagents to break bridging linkages between clusters with minimal effect on residual organic clusters. The coal will be pretreated to increase surface area and then reacted at 25 to 350°C. Reagents and catalysts will be used which are selective so that the coal clusters are solubilized with as little further reaction as possible.

Task 2 Carbon-13 NMR Investigation of CDL and Coal

Carbon-13 NMR spectroscopy will be used to examine coal, coal derived liquids (CDL) and residues which have undergone subsoftening reactions in Task 1 and extraction. Improvements in NMR techniques, such as crosspolarization and magic angle spinning, will be applied. Model compounds will be included which are representative of structural units thought to be present in coal. Comparisons of spectra from native coals, CDL and residues will provide evidence for bondings which are broken by mild conditions.

Task 3 Catalysis and Mechanism of Coal Liquefaction

This fundamental study will gain an understanding of metal salt chemistry and catalysis in coal liquefaction through study of reactions known in organic chemistry. Zinc chloride and other catalytic materials will be tested as Friedel-Crafts catalysts and as redox catalysts using coals and selected model compounds. Zinc chloride, a weak Friedel-Crafts catalyst, will be used at conditions common to coal liquefaction to participate in well defined hydrogen transfer reactions. These experiments will be augmented by mechanistic studies of coal hydrogenation using high pressure thermogravimetric analysis and structural analysis. The results of these studies will be used to develop concepts of catalysis involved in coal liquefaction.

Task 4 Momentum Heat and Mass Transfer in CoCurrent Flow of Particle-Gas Systems for Coal Hydrogenation

A continuation of ongoing studies of heat and transport phenomena in cocurrent, co-gravity flow is planned for a one-year period. As time and development of existing work permits, the extension of this study to include a coiled reactor model will be undertaken. Mathematical models of coal hydrogenation systems will utilize correlations from these straight and coiled reactor configurations.

Task 5 The Fundamental Chemistry and Mechanism of Pyrolysis of Bituminous Coal

Previous work at the University of Utah indicates that coal pyrolysis, dissolution (in H-donor) and catalytic hydrogenation all have similar rates and activation energies. A few model compounds will be pyrolyzed in the range of 375 to 475°C. Activation energies, entropies and pro-

duct distributions will be determined. The reactions will assist in formulating the thermal reaction routes which also can occur during hydro-liquefaction.

II. Catalytic and Thermal Upgrading of Coal Liquids

Task 6 Catalytic Hydrogenation of CD Liquids and Related Polycyclic Aromatic Hydrocarbons

A variety of coal derived (CD) liquids will be hydrogenated with sulfided catalysts prepared in Task 10 from large pore, commercially available supports. The hydrogenation of these liquids will be systematically investigated as a function of catalyst structure and operating conditions. The effect of extent of hydrogenation will be the subject of study in subsequent tasks in which crackability and hydrolysis of the hydrogenated product will be determined. To provide an understanding of the chemistry involved, model polycyclic arenes will be utilized in hydrogenation studies. These studies and related model studies in Task 7 will be utilized to elucidate relationships between organic reactants and the structural-topographic characteristics of hydrogenation catalysts used in this work.

Task 7 Denitrogenation and Deoxygenation of CD Liquids and Related Nitrogen- and Oxygen-Containing Compounds

Removal of nitrogen and oxygen heteroatoms from CD liquids is an important upgrading step which must be accomplished to obtain fuels corresponding to those from petroleum sources. Using CD liquids as described in Task 6, exhaustive HDN and HDO will be sought through study of catalyst systems and operating conditions. As in Task 6, catalysts will be prepared in Task 10 and specificity for N- and O-removal will be optimized for the catalyst systems investigated. Model compounds will also be systematically hydrogenated using effective HDN/HDO catalysts. Kinetics and reaction pathways will be determined. A nonreductive denitrogenation system will be investigated using materials which undergo reversible nitridation. Conditions will be sought to cause minimal hydrogen consumption and little reaction of other reducible groups.

Task 8 Catalytic Cracking of Hydrogenated CD Liquids and Related Polycyclic Naphthenes and Naphthenoaromatics

Catalytic cracking of hydrogenated CD liquid feedstocks will be studied to evaluate this scheme as a means of upgrading CD liquids. Cracking kinetics and product distribution as a function of preceding hydrogenation will be evaluated to define upgrading combinations which require the minimal level of CD liquid aromatic saturation to achieve substantial heteroatom removal and high yields of cracked liquid products. Cracking catalysts to be considered for use in this task shall include conventional zeolite-containing catalysts and large-pore molecular sieve, CLS (cross-linked smectites) types under study at the University of Utah. Model compounds will be subjected to tests to develop a mechanistic understanding of the reactions of hydro CD liquids under catalytic cracking conditions.

Task 9 Hydropyrolysis (Thermal Hydrocracking) of CD Liquids

Heavy petroleum fractions can be thermally hydrocracked over a specific range of conditions to produce light liquid products without excessive hydrogenation occurring. This noncatalytic method will be applied to a variety of CD liquids and model compounds, as mentioned in Task 6, to determine the conditions necessary and the reactivity of these CD feedstocks with and without prior hydrogenation and to derive mechanism and reaction pathway information needed to gain an understanding of the hydropyrolysis reactions. Kinetics, coking tendencies and product compositions will be studied as a function of operating conditions.

Task 10 Systematic Structural-Activity Study of Supported Sulfide Catalysts for Coal Liquids Upgrading

This task will undertake catalyst preparation, characterization and measurement of activity and selectivity. The work proposed is a fundamental study of the relationship between the surface-structural properties of supported sulfide catalysts and their catalytic activities for various reactions desired. Catalysts will be prepared from commercially available. Supports composed of alumina, silica-alumina, silica-magnesia and silica-titania, modification of these supports to change acidity and to promote interaction with active catalytic components is planned. The active constituents will be selected from those which are effective in a sulfided state, including but not restricted to Mo, W, Ni and Co. The catalysts will be pre-sulfided before testing. Catalyst characterization will consist of physico-chemical property measurements and surface property measurements. Activity and selectivity tests will also be conducted using model compounds singly and in combination.

Task 11 Basic Study of the Effects of Coke and Poisons on the Activity of Upgrading Catalysts

This task will begin in the second year of the contract after suitable catalysts have been identified from Tasks 6, 7 and/or 10. Two commercial catalysts or one commercial catalyst and one catalyst prepared in Task 10 will be selected for a two-part study; (1) simulated laboratory poisoning/coking and (2) testing of realistically aged catalysts. Kinetics of hydrogenation, hydrodesulfurization, hydrodenitrogenation and hydrocracking will be determined before and after one or more stages of simulated coking. Selected model compounds will be used to measure detailed kinetics of the above reactions and to determine quantitatively how kinetic parameters change with the extent and type of poisoning/coking simulated. Realistically aged catalysts will be obtained from coal liquids upgrading experiments from other tasks in this program or from other laboratories conducting long-term upgrading studies. Deactivation will be assessed based on specific kinetics determined and selective poisoning studies will be made to determine characteristics of active sites remaining.

Task 12 Diffusion of Polyaromatic Compounds in Amorphous Catalyst Supports

If diffusion of a reactant species to the active sites of the catalyst is slow in comparison to the intrinsic rate of the surface reaction, then only sites near the exterior of the catalyst particles will be utilized effectively. A systematic study of the effect of molecular size on the sorptive diffusion kinetics relative to pore geometry will

be made using specific, large diameter aromatic molecules. Diffusion studies with narrow boiling range fractions of representative coal liquid will also be included. Experimental parameters for diffusion kinetic runs shall include aromatic diffusion model compounds, solvent effects, catalyst sorption properties, temperature and pressure.

III. Hydrogenation of CO to Produce Fuels

Task 13 Catalyst Research and Development

Studies with iron catalysts will concentrate on promoters, the use of supports and the effects of carbiding and nitriding. Promising promoters fall into two classes: (1) nonreducible metal oxides, such as CaO, K₂O, Al₂O₃ and MgO, and (2) partially reducible metal oxides which can be classified as co-catalysts, such as oxides of Mn, Mo, Ce, La, V, Re and rare earths. Possible catalyst supports include zeolites, alumina, silica, magnesia and high area carbons. Methods of producing active supported iron catalysts for CO hydrogenation will be investigated, such as development of shape selective catalysts which can provide control of product distribution. In view of the importance of temperature, alternative reactor systems (to fixed bed) will be investigated to attain better temperature control. Conditions will be used which give predominately lower molecular weight liquids and gaseous products.

Task 14 Characterization of Catalysts and Mechanistic Studies

Catalysts which show large differences in selectivity in Task 13 will be characterized as to surface and bulk properties. Differences in properties may provide the key to understanding why one catalyst is superior to another and identify critical properties, essential in selective catalysts. Factors relating to the surface mechanism of CO hydrogenation will also be investigated. Experiments are proposed to determine which catalysts form "surface" (reactive) carbon and the ability of these catalysts to exchange C and O of isotopically labelled CO. Reactions of CO and H₂ at temperatures below that required for CO dissociation are of particular interest.

Task 15 Completion of Previously Funded Studies and Exploratory Investigations

This task is included to provide for the orderly completion of coal liquefaction research underway in the expiring University of Utah contract, EX-76-C-01-2006.

III Highlights to Date

Task 11 Kinetic studies of catalytic functions have revealed that the overriding deactivation of catalysts used in the H-coal process is due to coke deposits and not metal deposits. Significant deactivation occurs early with the recycle oil used prior to introduction of coal. Thus, the catalyst loses appreciable activity even before coal is processed. However, the catalyst can be successfully reactivated at this stage by a simple air regeneration.

Papers and Presentations

"Comparison of the Chemical Structure of Coal Hydrogenation Products, Athabasca Tar Sand Bitumen and Green River Oil Shale," R. Yoshida, T. Yoshida, Y. Nakata, Y. Hasegawa, M. Huno, Y. Ikawa, M. Makabe and D.M. Bodily, Fuel Proc. Tech., 7, 161 (1983).

Task 1

Comparison of Catalysts for Coal Conversion at Subsoftening Conditions

Faculty Advisor: L.L. Anderson
Graduate Student: T.C. Miin

Introduction

Coal liquefaction at subsoftening conditions by applying the HSAB principle has been completed on the test set of inorganic salts. The results are in the penultimate report. The description of this principle and the explanation of reactions, which presumably occur in the coal liquidfaction process, are also given in that report.

Project Status

A species property has been found (the softness property) that can be used to predict whether a particular candidate reagent will be effective in the reactions involved in the liquefaction.

The HSAB (Hard and Soft Acids and Bases) principle was invented between 1961 and 1967 by R.G. Pearson.¹ Species which includes molecules, ions, radicals, elements and even the portion(s) of a species, is classified into three categories, hard, borderline and soft, according to its electronic softness. This classification, combined with the concept of Lewis Acids and Bases, can determine whether a species is a hard acid (base), a borderline acid (base) or a soft acid (base). A hard acid or base is generally characterized by a small atomic radius, a high effective nuclear charge, and low polarizability; whereas softness implies all the opposite properties. Furthermore, a soft base can be associated with low electronegativity, easy oxidizability, or empty low-lying orbitals.¹ A number of Lewis acids and bases have been assigned to hard or soft groups (see Tables 2.1 and 2.2 in Reference 2). The HSAB principle states that hard acids prefer to bind to hard bases, and soft acids prefer to bind to soft bases. Obviously, the theory implies that borderline acids prefer to bind to borderline bases. However, the softness property should not be over emphasized since the intrinsic strength of acidity (basicity) is also important in a reaction. A four parameter equation is hence proposed by Pearson for governing the reaction. That is, the equilibrium constant of the reaction



is determined by

$$\log K = S_A S_B + \sigma_A \sigma_B$$

where σ_A , σ_B are measures of some characteristics of softness; whereas, S_A , S_B are measures of intrinsic strength of acid A and base B.

In this work only weak acids or bases have been studied, and thus the intrinsic strength of acidity or basicity becomes unimportant, and the above equations can be reduced to

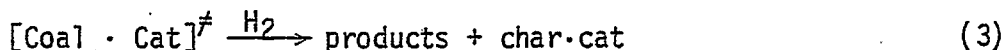
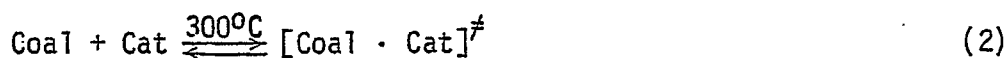
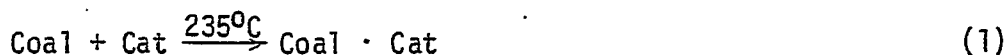
$$\log K = \text{constant} + \sigma_A \sigma_B$$

About 100 reagents have been tested for coal liquefaction by the HSAB principle. The reagents in the coal liquefaction reactions either serve as catalysts alone or do double duty, serving as catalysts and reactants.

About 70 Friedel-Crafts or related reagents were tested as catalysts to liquefy coal at about 300°C and 2000 psig hydrogen pressure. Hiawatha HvB coal, which was pre-extracted with THF, was mixed with the catalyst and reacted in an autoclave for three hours. The liquid yield was defined by the THF soluble material in weight percent of the THF pre-extracted coal. The total yield was the liquid yield plus the gas yield. (Gases were measured by gas chromatography.)

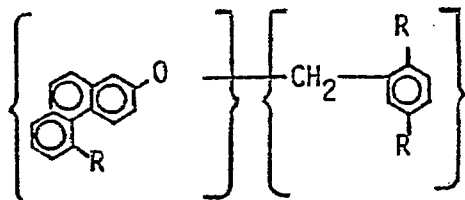
Conversion from the experiments using the 70 catalysts ranged from 5 percent to 99 percent. Results show that only borderline acids (according to the HSAB principle) gave higher conversion (over 20 percent of daf coal). Interestingly, the typical Friedel-Crafts catalysts, e.g., FeCl₃, gave the lowest coal conversion value (5%); whereas weak Lewis acids, e.g., SnI₄, gave the highest conversion value (99%). Explanations of the results are as follows:

The general form of the coal liquefaction reaction mechanism can be represented by



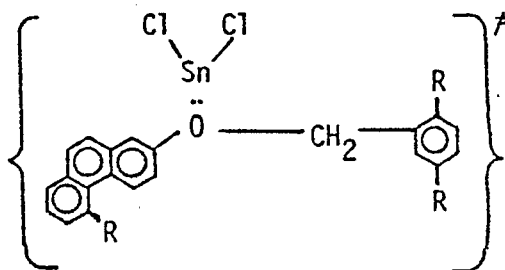
According to Beall's work, halides can penetrate into the coal structure (intercalation) in the first step of the above reactions.³ According to the HSAB principle, borderline catalysts prefer to bind with borderline functional groups of the coal structure. (Wiser's schematic representation, for example, shows that most functional groups and linking units of bituminous coal are expected to belong to the borderline category.)⁴ Soft or hard acids are expected to bind weakly with the structures in coal. Some presumed bond cleavage examples are

Ether linkage cleavage reactions:



in which the phenanthroxy portion is partially electronegative (a borderline

base), and the toluenyl portion is partially electropositive (a borderline acid). According to the HSAB principle, only borderline catalysts can bind stably with such entities, i.e., the halide-ether adduct forms.



The formation of a coordination bond between oxygen and tin would weaken the ether bond ($\text{ArO} - \text{CH}_2\text{Ar}$), which is done at about 230°C .

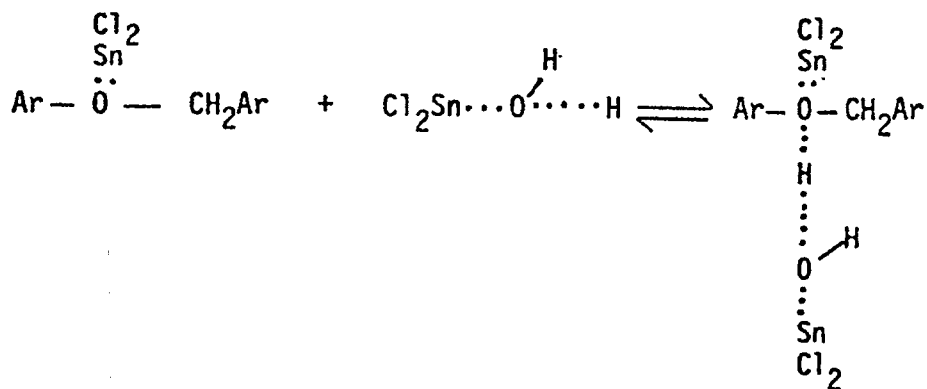


When the temperature is raised above 250°C , Lewis acids attract moisture to form protonic acids or protonic-like adducts. Strong Lewis acids (most strong Lewis acids are hard) ionize H_2O completely to form protonic acids, whereas borderline acids (most borderline acids are weak) form protonic-like adducts with H_2O . Some examples are

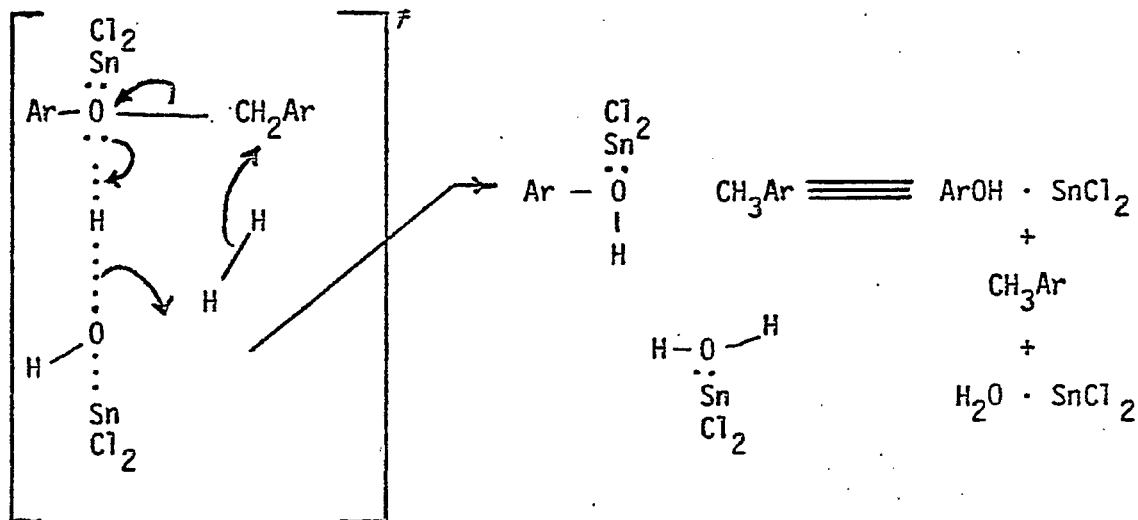
1. Soft acid: $\text{CdCl}_2 + \text{H}_2\text{O} \rightleftharpoons \text{CdCl}_2 \cdots \underset{\text{H}}{\overset{\text{H}}{\text{O}}}$
2. Hard acid: $\text{FeCl}_2 + \text{H}_2\text{O} \rightleftharpoons [\text{Cl}_3\text{FeOH}]^- \text{H}^+$
3. Borderline acid: $\text{SnCl}_2 + \text{H}_2\text{O} \rightleftharpoons \text{Cl}_2\text{Sn} \cdots \underset{\delta^-}{\overset{\text{H}}{\text{O}}} \cdots \underset{\delta^+}{\text{H}}$

Since H^+ is very hard and H^- is very soft, it is logical to say that $\text{H}^{\delta^+}, \text{H}^{\delta^-}$ are borderline. (This should not be confused with $\text{H}\cdot$, which is a free radical, having a free electron which is not attracted by other electrophiles and thus is very polarizable and is soft.)

The borderline proton-like portions (in HSAB terms they are borderline acids) bind stably with borderline coal-Lewis acid adducts to form stable transition states in the second step of the coal liquefaction reaction mechanism, i.e.,

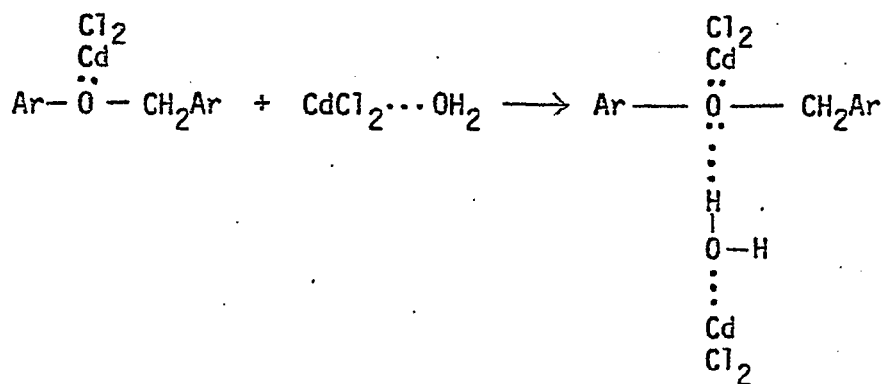


The catalyst-coal adduct is then ready for the hydrogenolysis reaction:



The reaction is believed to occur "concertedly" without any formation of free electron charge. Two reasons can be proposed. First, in the reaction circumstances, any generation of electron charge will create "harder" portions, which are not favored according to the HSAB principle. Second, the free electron charge generation will create carbonium ions which will initiate Friedel-Crafts alkylation and lead to low liquefaction yields, which are contrary to the results.

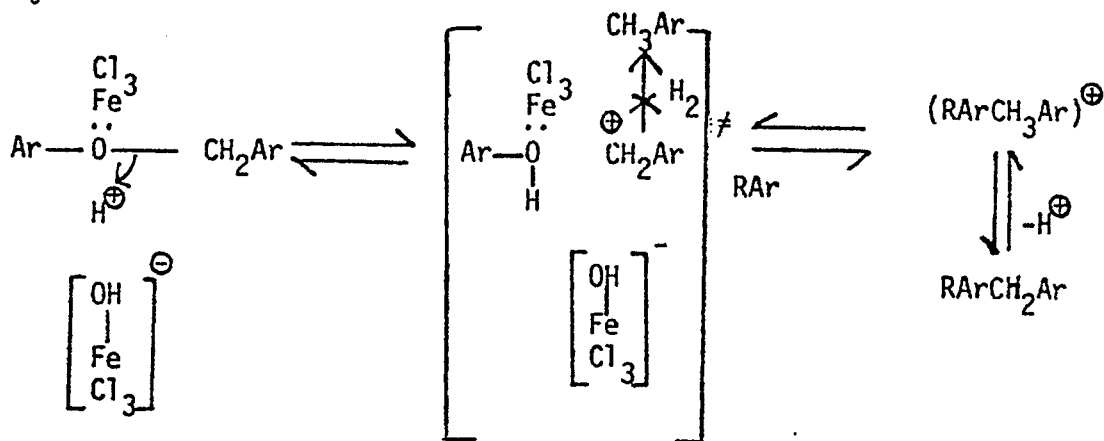
However, the soft acid-coal adduct forms another weak attraction with the soft acid-H₂O adduct:



Since ether linkages are not weakened extensively, reaction (3) of the mechanism is not likely to occur. (However, some facile ether structures still can be cleaved and give small liquefaction yields--less than 20 percent.)

In the case of hard catalysts, the generated proton cannot only catalyze ether linkage cleavage but also can initiate further Friedel-Crafts alkylation reactions. The total effect is that these hard catalysts catalytically break down the large molecular weight coal entities and form high molecular-weight char.

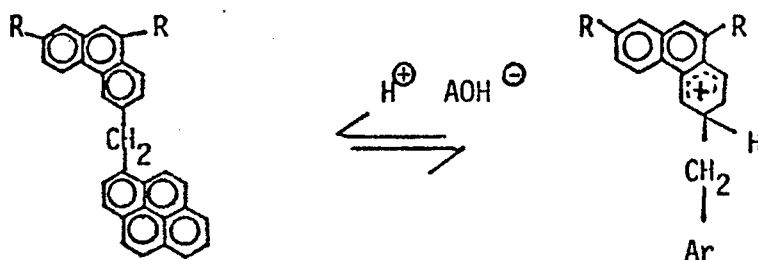
Finally:



In the transition state of the reaction there are large numbers of benzene structures. The short-lived carbonium ion would be easier to attach to benzene structures (alkylation reactions would occur) than to gas-phase hydrogen molecules. The reason for this is that the kinetic concentration of benzene structures is much greater than that of hydrogen. Also, to obtain a hydride ion from a hydrogen molecule requires higher activation energy than to alkylate a benzene structure. One fact to support this argument is that all of the hydroliquefaction processes for coal conversion show positive effects of increasing hydrogen pressure.

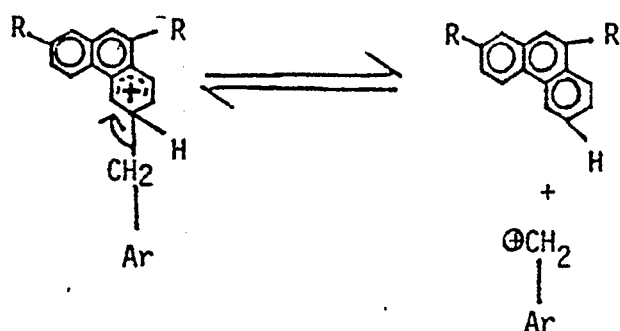
Generally speaking, there are two types of mechanisms for reverse-Friedel-Crafts reactions. The first type involves free carbonium ions (C^+) and the second involves partially-charged alkyl or aralkyl groups ($C^{\delta+}$) which comprise the "concerted" mechanism. Both C^+ and $C^{\delta+}$ are acids according to the HSAB principle. The former is harder than the latter. These two types of mechanism are:

First Type. Free Carbonium Type Mechanism:



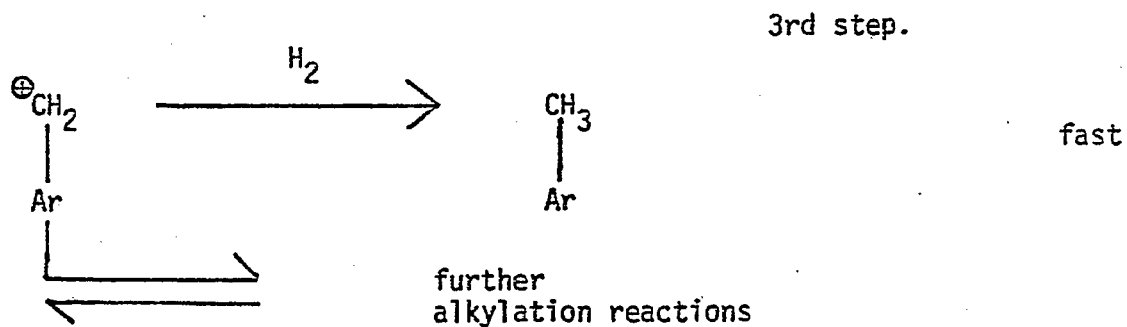
1st step.

fast

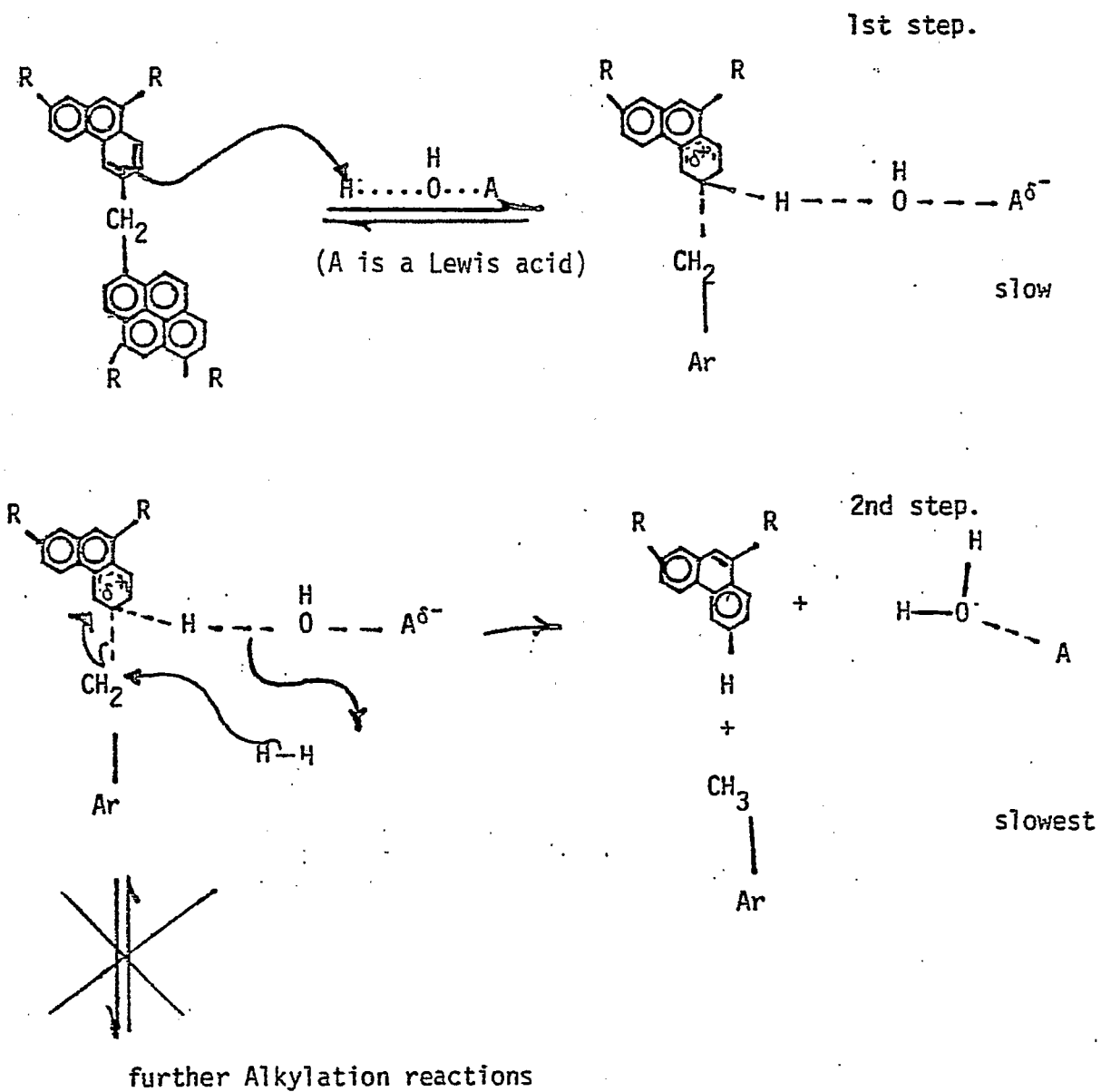


2nd step.

slow



Second Type. Concerted Dearalkylation Mechanism:



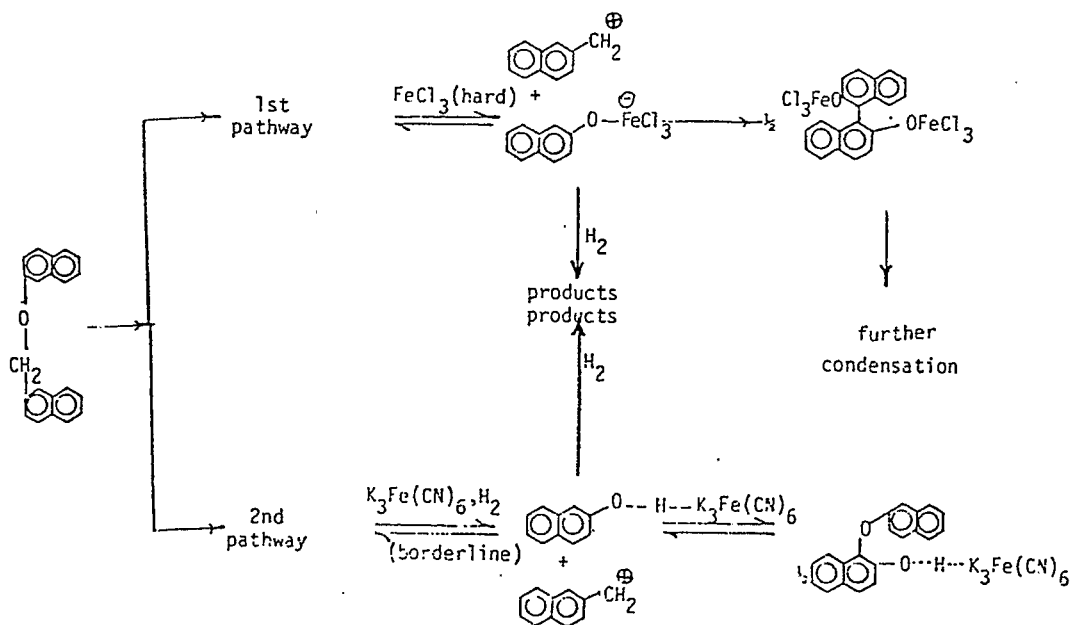
As proposed above, protons (free or bound) are necessary for reverse-Friedel-Crafts reactions. However, mineral acids do not give good conversion yields because all protonic acids are hard. Hard species are simply not favored for binding with borderline coal structures. Also, mineral acids and other hard Lewis acids (both are termed hard acids in the HSAB principle) initiate further aralkylation reactions, which lead to repolymerization of cleaved fragments. However, borderline acids do not have this disadvantage and thus can give better yields of coal conversion products.

Sulfide and disulfide linkages belong to the soft HSAB category and thus are favored to be cleaved by soft catalysts; however, these bonds are comparatively unimportant in coal liquefaction reactions and thus no details are given here.

Hydrogen-bond linkages and other facile linkages are less important and details are not given here. Borderline catalysts favor ether linkage cleavage reactions over reverse-Friedel-Crafts dearalkylation reactions. Hard catalysts favor Friedel-Crafts reactions (polymerization) since to disturb resonance in aromatic rings requires higher energy and thus needs stronger acidity. However, the polymerization reaction initiated by hard acids makes them generally unfavorable for coal conversion processing.

Some of the literature supports for the above argument are the following reactions:

The coupling reactions of phenols²



Naphthol-like structures are formed in the cleavage of ether-linkages which are found in coal structures, during the coal liquefaction process. The Reagent-substrate complex is formed in two pathways. The borderline-borderline reagent-substrate complex in the intermediate step of the second pathway is formed via an outer-sphere attraction in which no strong bonding between the substrate and metal ion exists. The ensuing phenoxy radical is relatively free, and thus the ether linkage formed again in the last step of the second pathway is just like the reverse reaction of the former cleavage of ether linkage. The total effect is that the reagent-substrate complex is serving as an intermediate reaction complex, which loosens the ether bond in the coal structure and makes it easier to perform the later hydrogenolysis reaction. However, the hard-borderline reagent-substrate complex (in the first pathway), having an ionic bond formation between the phenoxy and metal ion, not only prevents the formation of free phenoxy radical but also puts an electron-withdrawing effect on the aromatic ring. Thus the later condensation reaction is reduced. The total effect is that an ether linkage is cleaved first and replaced later by a carbon-carbon linkage. This condensation reaction can continue to form a high molecular weight polymer. This makes the later hydrogenolysis more difficult. The HSAB principle can, therefore, successfully direct the choice of effective inorganic salt(s) for coal liquefaction under mild conditions.

Future Work

The borderline property according to the HSAB principle is not restricted to inorganic compounds. Therefore, organic materials which act with acidic or basic properties are also candidates for reactants for coal liquefactions. Furthermore, "borderline hydrogen" can be predicted using the HSAB principle. Borderline hydrogen will be produced to liquefy coal at the same conditions.

References

1. T.L. Ho, "Hard and Soft Acids and Bases Principle in Organic Chemistry," Academic Press, New York, New York, 1977.
2. W.I. Taylor, eds., "Oxidative Coupling of Phenols," Dekker, New York, New York, 1967.
3. H. Beall, Fuel, 58, 319 (1979).
4. W.H. Wiser, Scientific Problems of Coal Utilization, DOE Symposium Series 46, 232 (1978).

Task 2

Carbon-13 NMR Investigation of CDL and Coal

Faculty Advisor: R.J. Pugmire
Postdoctor Associate: D.K. Dalling
W.R. Woolfenden

Introduction

NMR data has been obtained on a set of 25 samples obtained from the Exxon Coal Data Bank. Progress on the project is still limited by the delay in a graduate student finishing his Ph.D. thesis. Dr. Warner Woolfenden has continued to work part-time on the project. He has now accepted a permanent position and will no longer be available to the project.

Project Status

During the past quarter NMR data has been completed acquiring NMR data on the Exxon Coal Data Bank samples. All 25 samples were analyzed by standard CP/MAS and dipolar dephasing studies.

Employing T_2 values obtained for model compounds and 6 coals that were studied in some detail, we are able to obtain semi-quantitative data on a number of structural parameters on each of the coals. In addition to the normal aromaticity values, we have now calculated $f_a^{A,H}$, $f_a^{A,N}$, f_a^H , f_s^* , and H_{Ar}^* (fraction of aromatic carbon that is protonated, fraction of aromatic carbon that is nonprotonated, fraction of total carbon that is aromatic and protonated, relative fraction of carbon that is aliphatic methyl or aliphatic quaternary carbon, and fraction of protons located on aromatic rings, irrespectively). We are in the process of assessing the degree of variability in these parameters from the different coals. We will attempt to delineate structural variables in the different coals.

Task 3

Catalysis and Mechanism of Coal Liquefaction

Faculty Advisor: D.M. Bodily
Graduate Student: Tsejing Ray

Introduction

Metal halides such as $ZnCl_2$ are well-known to be active catalysts for coal hydrogenation. Zinc chloride has been shown to be a very effective catalyst for coal hydrogenation in the entrained-flow reactor developed at the University of Utah.^{1,2} Bell and co-workers³⁻⁵ have studied the reactions of model compounds with $ZnCl_2$ under conditions similar to those employed in coal hydrogenation. They observed cleavage of C-O and C-C bonds in the model compound and proposed that the active catalytic species is a Bronsted acid formed $ZnCl_2$.

Shibaoka, Russell and Bodily⁶ proposed a model to explain the liquefaction of coal, based on microscopic examination of the solid products from metal halide catalyzed coal hydrogenation. The model involves a competition between hydrogenation and carbonization reactions. The hydrogenation process starts at the surface of vitrinite particles and progresses toward the center. The vitrinite is converted to a plastic material of lower reflectance, which is the source of oils, asphaltenes and preasphaltenes. Concurrently, carbonization occurs in the center of the particles, resulting in vesiculation and a higher reflectance material. The partially carbonized material can be hydrogenated at later stages, but at a lower rate than the original coal.

Thermal and/or catalytic bond rupture occurs during the liquefaction process. The initial products of the bond cleavage reactions may be stabilized by hydrogen addition, resulting in cleavage of bridges between aromatic ring systems and in dealkylation of aromatic rings. If the initial products of the reaction are not stabilized, they may polymerize to form semicoke-like material. This primary semicoke may be isotropic or exhibit a fine-grained anisotropic mosaic texture, depending on the rank of coal. The plastic material formed by stabilization of the initial products may be further hydrogenated or, under hydrogen deficient conditions, may form secondary semicoke. The secondary semicoke is of medium to coarse-grained anisotropic mosaic texture. Bodily and Shibaoka⁷ used this model to explain the nature of the residues from hydrogenation in the short-residence, entrained-flow hydrogenation reactor. The role of the $ZnCl_2$ catalyst is examined in this study.

Project Status

The Clear Creek coal samples heated in hydrogen and in nitrogen were analyzed by optical microscopy. Results of the analysis are summarized in Tables 1 and 2. In hydrogen the $ZnCl_2$ catalyst causes an obvious softening of the coal grains at 350°C. At short reaction times, a reacted rim is observed on the grains. At 20 minutes reaction time and 400°C, the reacted zone is not visible, indicating that the reaction has proceeded through the

entire grain. The initial reactions involve softening of the vitrinite and reaction of exinites. When $ZnCl_2$ is not present, only slight softening occurs prior to carbonization.

In nitrogen, the $ZnCl_2$ also appears to increase the fluidity of the sample during heating, although not to the same extent as in hydrogen. This effect shows up in the size and shape of vesicles.

Future Work

The medium volatile coal will be analyzed by optical microscopy. Reflectance and fluorescence measurements of both coal sample residues will be performed.

References

1. R.E. Wood and W.H. Wiser, Ind. Eng. Chem., Proc. Design Devel., 15, 144 (1976).
2. J.M. Lytle, R.E. Wood and W.H. Wiser, Fuel, 59, 471 (1980).
3. D.P. Mobley and A.T. Bell, Fuel, 58, 661 (1979).
4. N.D. Taylor and A.T. Bell, Fuel, 59, 499 (1980).
5. D.P. Mobley and A.T. Bell, Fuel, 59, 507 (1980).
6. M. Shibaoka, N.J. Russell and D.M. Bodily, Fuel, 61, 201 (1982).
7. D.M. Bodily and M. Shibaoka, Fuel, submitted.

Table 1. Microscopic examination of Clear Creek, Utah coal under H₂.

<u>Temp., °C</u>	<u>Without Catalyst</u>	<u>With Catalyst</u>
300	---	No obvious change
350	No obvious change	Softening occurs at edges, but the spores don't change, reacted rim apparent.
380	No obvious change	Softening at edge, spore still present.
400	Some rounded edges, spores slightly changed, some vesiculation.	Definitive softening at edges, spores start to react. At longer times, no edge effect, reaction occurs through whole grain.
450	The edge is softened in most cases, and the spores reacted, no obvious carbonization.	Softening at edges, some vesiculation, spore reacted, and exinite reacted.

Table 2. Microscopic examination of Clear Creek, Utah coal under N₂.

<u>Temp., °C</u>	<u>Without Catalyst</u>	<u>With Catalyst</u>
350	---	No carbonized reaction, the edge of grains becomes rounded, and softened, reacted rim apparent.
400	Softening starts at edge, grain reacted, no obvious carbonization, some cracking on grain.	Softening at edges, the grains reacted, vesiculations.
450	Exinite gone, carbonized, softened at edge.	Definitively carbonization, softening at edges, vesicles.
500	The grains are reacted, vesiculation, some softened edges.	Severe carbonization, slight softening at edges, more fluid.

Task 5

The Mechanism of Pyrolysis of Bituminous Coal

Faculty Advisor: W.H. Wiser
Graduate Student: J.K. Shigley

Introduction

In the present state of knowledge concerning the fundamental chemistry of coal liquefaction in the temperature range 375-550°C, the liquefaction reactions are initiated by the thermal rupture of bonds in the bridges joining configurations in the coal, yielding free radicals. The different approaches to liquefaction, except for Fischer-Tropsch variations, represent ways of stabilizing the free radicals to produce liquid-size molecules. The stabilization involving abstraction by the free radicals of hydrogen from the hydroaromatic structures of the coal is believed to be the predominant means of yielding liquid size molecules in the early stages of all coal liquefaction processes, except Fischer-Tropsch variations. The objective of this research is to understand the chemistry of this pyrolytic operation using model compounds which contain structures believed to be prominent in bituminous coals:

Project Status

Pyrolysis experiments for 9-benzyl-1,2,3,4-tetrahydrocarbazole (9-BTHC) have been conducted at 360°C. The compiled data are shown in Table 1. The data for each reaction time are the average of at least two experiments. The normalized relative product distribution and the molar ratio of 9-benzylcarbazole/carbazole (9BC/CARB) are shown in Table 2. The normalized relative product distribution vs. reaction time are plotted in Figure 1. The product distribution shows trends very similar to those discussed in the previous report.¹

Kinetic analysis of the data has been performed using integral and differential techniques.² The integral kinetic data are shown in Table 3 and plotted in Figures 2 and 3. The integral analysis shows an interesting result. The data fit the first order plot better than the second order plot but the second order plot shows a downward curvature. The downward curvature suggests that the overall reaction order is greater than two.

In an attempt to clarify the overall reaction order, the data were analyzed by the differential technique. The results of this analysis are shown in Table 4 and are plotted in Figure 4. This analysis suggests that the overall reaction order is at least five and maybe as high as nine. These results suggest that at this temperature (360°C), the reactions are occurring in a mixed phase system (liquid/vapor or solid/liquid/vapor). The resultant complications involved in mixed phase reactions make a simplistic analysis of this nature inadequate.

Experiments have been conducted with 9-BTHC with the specific intent of determining the presence of molecular hydrogen (H₂). Several experiments were conducted with approximately five milligrams of the model compound. The samples were prepared in the standard technique.³ After pyrolysis the

tubes were quenched in liquid nitrogen and placed in a stainless steel gas sampling bottle with several stainless steel ball bearings. The sampling bottle is evacuated and then pressurized to 15 psig with purified helium. This sequence is repeated at least three times before final pressurization with helium to 15 psig. The pyrolysis tube is broken open with the ball bearings inside the sample bottle. The contents are analyzed using a Carle refinery gas analysis gas chromatographic system. No hydrogen was detected with the five milligram samples. In an attempt to understand if this was due to the limits of detection of the system, experiments were conducted with increased sample sizes. Several tubes loaded with at least five milligrams were pyrolyzed and then analyzed simultaneously by the previously described method. Small amounts of hydrogen were detected under these conditions, along with even smaller amounts of methane, ethane and propane. This suggests that dehydrogenation occurs to a small extent and also that some methyl radicals are formed by subsequent cleavage from the initially thermally produced radicals.

Hydrogen (H) balances were calculated for the pyrolysis of 9-BTHC to determine the apparent extent of the aforementioned dehydrogenation. The results of this analysis are shown in Table 5. The H-balance was calculated using 9-BTHC, 9-benzylcarbazole, carbazole, 1,2,3,4-tetrahydrocarbazole and toluene as the only products. The average hydrogen balance for all temperatures (360 to 440°C) is 94.3%. This result, in conjunction, with the results of the hydrogen analysis suggests that the dehydrogenation reactions are occurring to a small extent.

In correlating the pyrolysis of model compounds to coal pyrolysis, the experimental technique most often utilized in coal pyrolysis studies and its effects should be considered. Most coal pyrolysis studies have been conducted by observing the weight loss or rate of weight loss with time for the coal. Kinetics derived from these measurements can be considered as the kinetics of volatile products evolution. The pyrolysis of 9-BTHC has been analyzed by determining the kinetics of toluene, benzene and bibenzyl production. The data were tested using first and second order kinetics. If the rate of production of these compounds can be described by the equation $dx/dt = k_n(a-x)^n$, where

- a = initial moles of starting material
- x = moles of toluene + benzene + bibenzyl produced
- n = overall order of reaction occurring,

then the data can be analyzed with the integrated forms of this equation. If a value for n is assumed, the equation can be easily integrated. If a value of one is assumed for n, the resultant equation is $\ln a/a-x = k_1t$ and if n is assumed to be 2, $x/a(a-x) = k_2t$. The data can be analyzed for the first and second order equations by plotting $\ln a/a-x$ and $x/a(a-x)$ vs. time, respectively, and observing how well the data fit the plotted equations. The results of linear regression analysis of the plotted data are shown in Table 6. The results seem to show no definite trends and suggest that the method is, in some way, insufficient in describing the data. No definite conclusions may be made on the results of this analysis at this time.

Extensive experimentation has been conducted on 9-benzyloxy-1,10-propanophenanthrene (9-BOPP) in an attempt to find a suitable solvent.

Fourteen solvents or solvent systems were tested after a review of pertinent literature. The solvents were tested at ambient and elevated temperatures using manual and ultrasonic methods of mixing. The solvents tested were: carbon disulfide, dichloromethane, chloroform, methanol, ethanol, acetone, diethyl ether, dioxane, pyridine, dimethylsulfoxide, benzene, toluene and super-solvent (diethylether, ethanol, benzene). A known weight of 9-BOPP was placed in a mini-reaction vessel and a predetermined amount of solvent was added to form a one percent (by weight) solution if all the 9-BOPP dissolved. The solutions were then allowed to sit for about one hour with occasional mixing. After an hour two microliters of the solution were injected into a gas chromatograph for analysis. Each solution was analyzed in this manner. The resultant analyses were used for comparison purposes, for each solvent tested. The five apparently best solvents were selected in this manner and they were carbon disulfide, dichloromethane, dioxane, dimethylsulfoxide, and pyridine. These solvents were tested in a more extensive manner both at elevated temperatures and utilizing an ultrasonic bath for mixing. None of these solvents dissolved enough of the 9-BOPP to form a one percent by weight solution. The solvents rated in order of increasing solubility of 9-BOPP are dioxane < dimethylsulfoxide < dichloromethane < carbon disulfide < pyridine.

Another problem discovered with 9-BOPP was its high content of an impurity. The approximate purity of 9-BOPP is 65% with 35% of 1,10-(2-Propeno)phenanthrene-9-ol. The structure of the impurity has been verified by GC/MS analysis.

These two major problems with 9-BOPP necessitated the obtaining of some new model compounds. The model compounds obtained are 1-benzyl-1,2,3,4-tetrahydroisoquinoline (1-BTHIQ), 1-piperidinomethyl-2-naphthol (1-PMN), and 4-benzylpiperidine (4-BPP) are shown in Figures 5-7, respectively. The model compound 1-BTHIQ was chosen because the benzyl group is attached to a naphthenic carbon adjacent to a nitrogen in the compound. This will be valuable for comparing its pyrolysis to that of 9-benzyl-1,2,3,4-tetrahydrocarbazole (9-BTHC). The 1-piperidinomethyl-2-naphthol was chosen for two reasons: (1) if the presence of the hydroxyl group will affect the pyrolysis mechanism and (2) if the fact that the naphthenic portion of the model compound is the smaller cluster of the model compound changes the pyrolysis mechanism. The third new model compound 4-BPP was obtained for two reasons. These reasons are: (1) the attachment of the benzyl group to a carbon para to the nitrogen in the piperidine, and (2) the model compound is two single ring compounds linked through a methylene bridge and is perhaps more similar to a lower rank coal.

The pyrolysis of 1-BTHIQ has been conducted at 623, 611 and 598 Kelvin (350, 338 and 325°C). The conversions and material balance results are shown in Tables 7-9. The normalized product distribution data are tabulated in Tables 10-12 and plotted in Figures 8-10. The product distributions for 1-BTHIQ show trends similar to those of 9-BTHC as discussed in the previous report.¹ The increase in the yield of 1-BIQ with conversion suggests that the thermally produced radicals are being stabilized by abstraction of H from a molecule of 1-BTHIQ. The maximization of the 1-BIQ yield shows that the thermal cleavage of 1-BIQ becomes appreciable and proceeds at a rate faster than the stabilization of the thermally produced radicals. The maximum of 1-BIQ yield varies with temperature and occurs at earlier times the higher the temperature.

The 1-BTHIQ pyrolysis data has been analyzed using the integral technique of analysis.² The tabulated data are shown in Tables 13-15 and are plotted in Figures 11-16. The data at 623 Kelvin are best modeled by first order kinetics and at 598 Kelvin by second order kinetics. The data at 611 Kelvin (338°C) are modeled equally well by the first and second order integrated equations and the actual overall reaction order is probably between one and two.

The data at 611 Kelvin (338°C) were analyzed using the differential technique of analysis and the results are tabulated in Table 16 and plotted in Figure 17. The resulting order of reaction from this technique is 1.5 and supports the results of the integral analysis.

Future Work

Gas chromatographic/mass spectrometric analysis will be performed on 1-BTHIQ, 1-PMN, 4-BPP and the resulting pyrolysis product mixtures. The 1-BTHIQ will be pyrolyzed at one and possibly two more temperatures. Experimentation will be conducted with 1-BTHIQ and 1-PMN similar to that used for 9-BTHC to determine the presence of molecular hydrogen. Hydrogen balance calculations will be made to be used in conjunction with the hydrogen tests for mechanism elucidation. Pyrolysis experiments will be conducted on 1-PMN at a minimum of four temperatures. Pyrolysis of 4-BPP will be conducted if time allows.

References

1. W.H. Wiser et. al., DOE Contract No. DE-AC22-79ET14700, Quarterly Progress Report, Salt Lake City, Utah, Jan-Mar 1983.
2. ibid., Oct-Dec 1982.
3. Octave Levenspiel, "Chemical Reaction Engineering," 2nd Ed., John Wiley & Sons, New York, New York, 1972.

Pyrolysis of 9-Benzy[1,2,3,4-Tetrahydrocarbazole (9-BTHC)

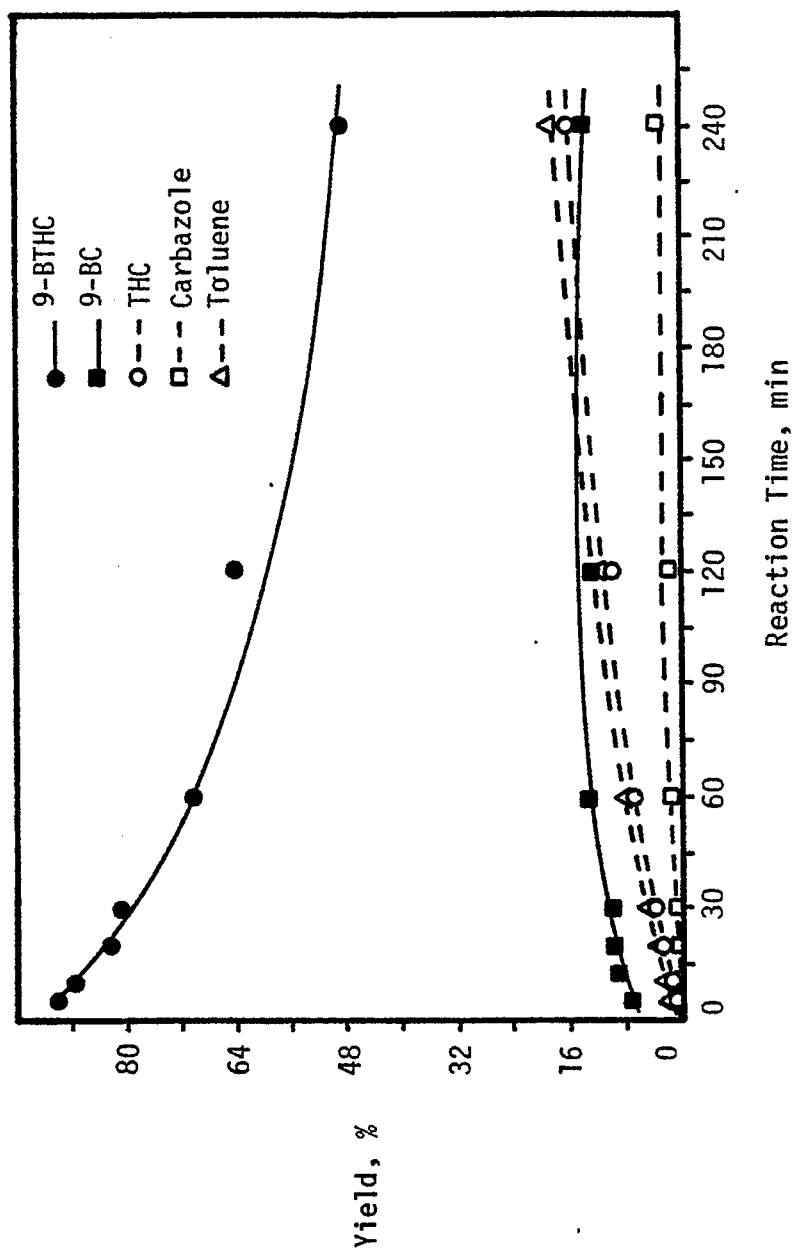


Figure 1. Normalized Product Distribution (%), Temperature, 633 K (360°C).

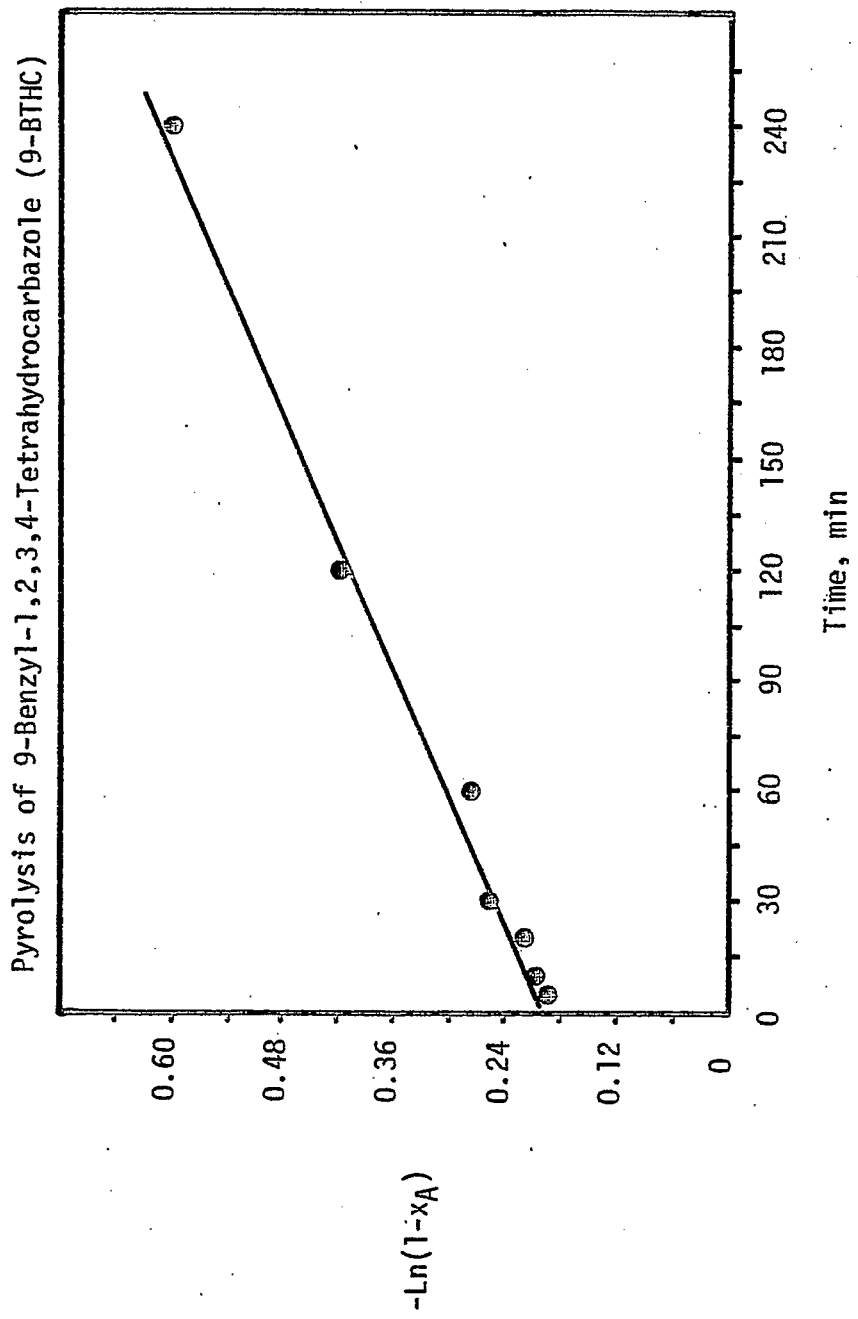


Figure 2. First Order Kinetics Plot. Temperature, 633 K (360°C).

Pyrolysis of 9-Benzy[1,2,3,4-Tetrahydrocarbazole (9-BTHC)

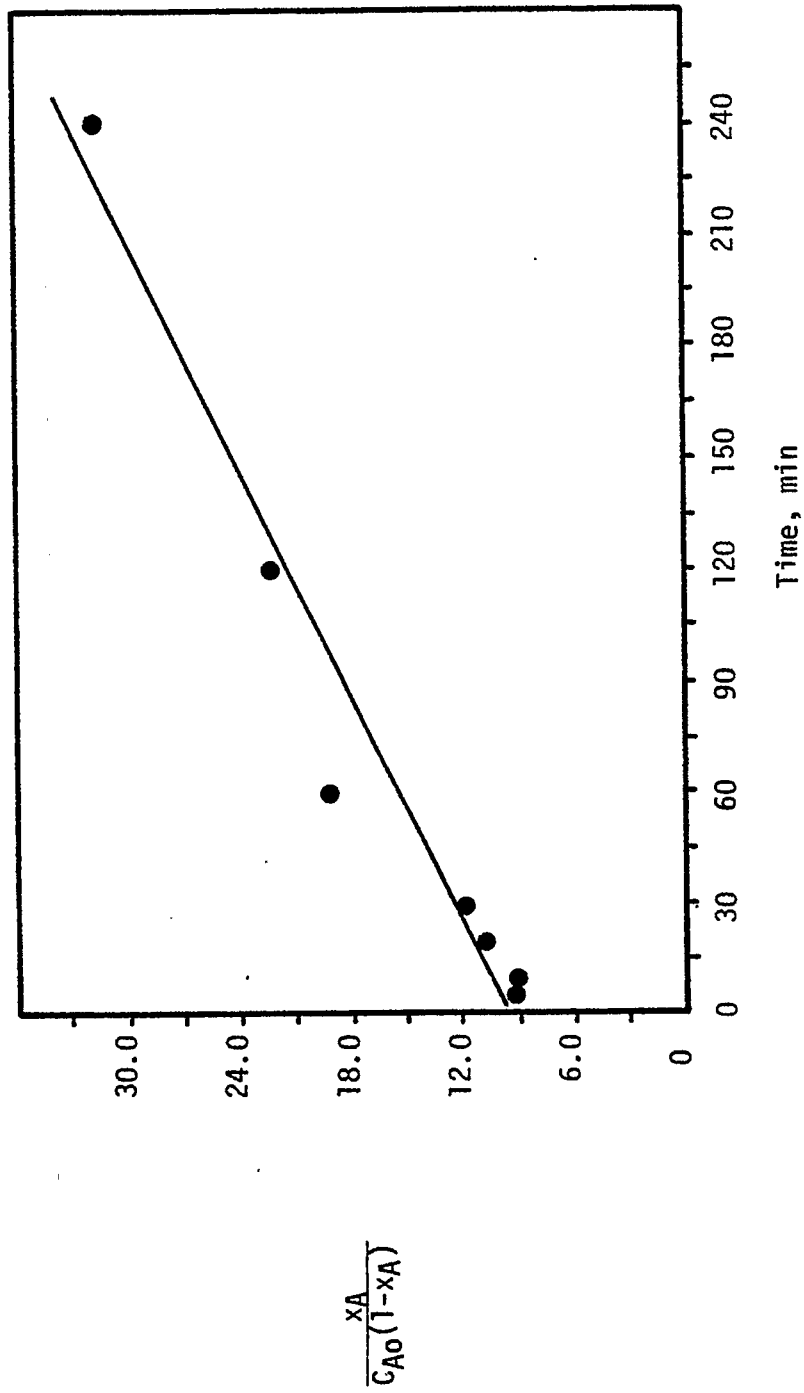


Figure 3. Second Order Kinetics Plot. Temperature, 633 K (360°C).

Pyrolysis of 9-Benzy[1,2,3,3,4-Tetrahydrocarbazole (9-BTHC)

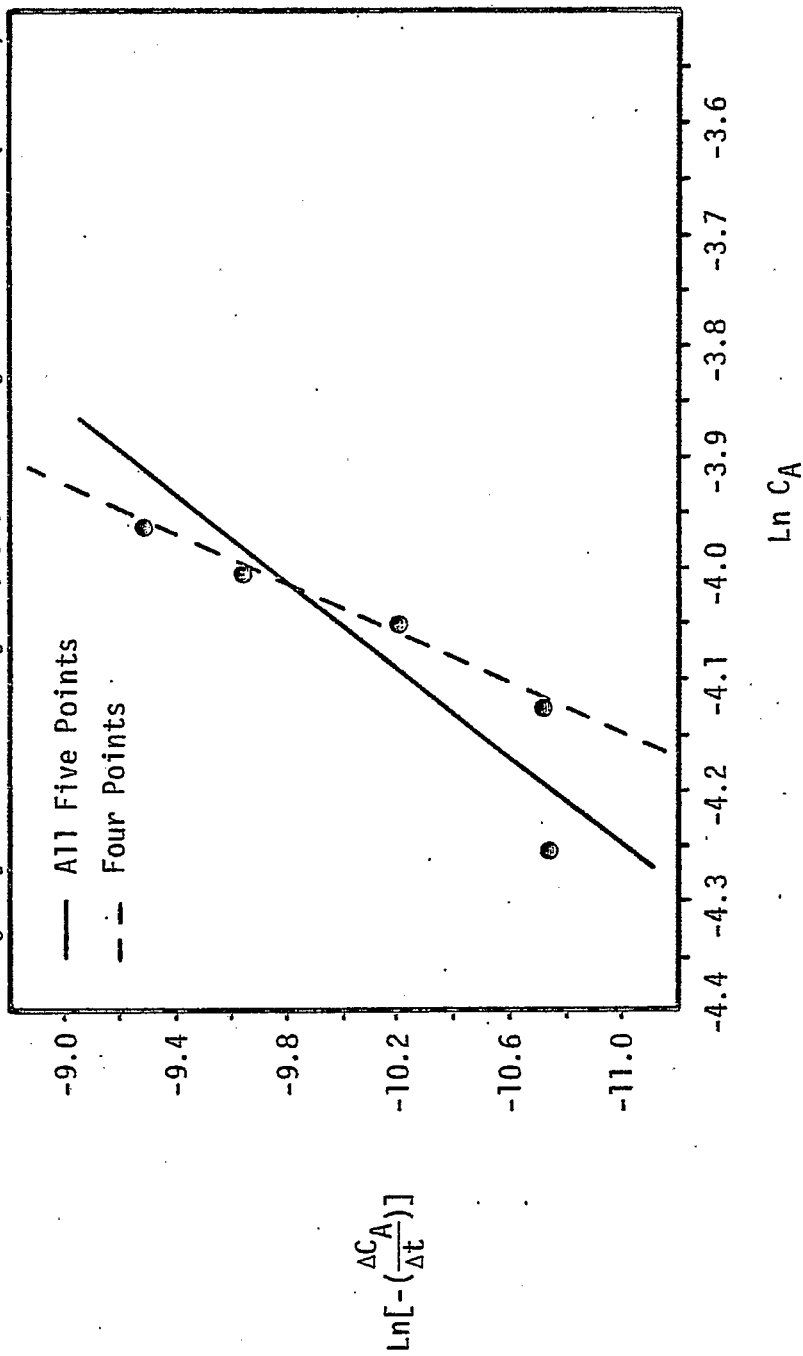
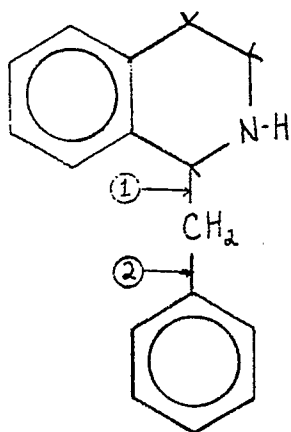


Figure 4. Differential Kinetics Analysis Plot. Temperature, 633 K (360°C).

Figure 5. 1-Benzyl-1,2,3,4-tetrahydroisoquinoline (1-BTHIQ).



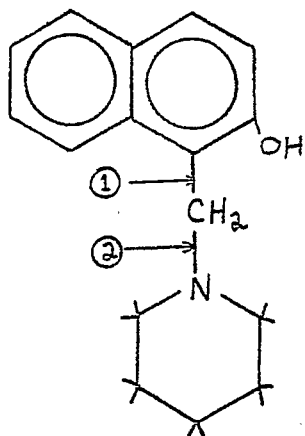
$C_{16}H_{17}N$, FW = 223.32 g/g mole

<u>Bond</u>	<u>\approxBDE, kcal/mole</u>
1	75
2	102

<u>Component</u>	<u>Model Compound, wt %</u>	<u>Bituminous Coal, wt %</u>
C	86.0	77 - 80
H	7.7	4.8 - 6.0
N	7.3	1 - 2
Hydroaromatic C	18.8	15 - 25
Aromatic C	75.0	65 - 75
Aliphatic C	6.2	5 - 10
H/C Atomic Ratio	1.06	0.8 - 0.9

(Utah Coal, H/C \approx 1.0)

Figure 6. 1-Piperidinomethyl-2-naphthol (1-PMN).



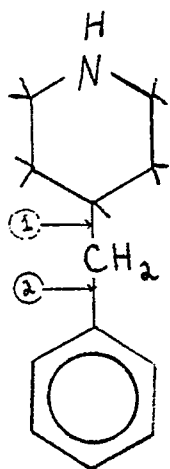
$C_{16}H_{19}NO$, FW = 241.3 g/g mole

<u>Bond</u>	<u>≈BDE, kcal/mole</u>
1	>102
2	< 78

<u>Component</u>	<u>Model Compound, wt %</u>	<u>Bituminous Coal, wt %</u>
C	79.6	77 - 80
H	7.94	4.8 - 6.0
N	5.8	1 - 2
O	6.6	7 - 15
Hydroaromatic C	31.25	15 - 25
Aromatic C	62.5	65 - 75
Aliphatic C	6.25	5 - 10
H/C Atomic Ratio	1.19	0.8 - 0.9

(Utah Coal, H/C ~ 1.0)

Figure 7. 4-Benzylpiperidine.



$C_{12}H_{17}N$, FW = 175.28 g/g mole

MP = 6-7°C, BP = 279°C

<u>Bond</u>	<u>~BDE, kcal/mole</u>
1	80
2	102

<u>Component</u>	<u>Model Compound, wt %</u>	<u>Bituminous Coal, wt %</u>
C	82.2	77 - 80
H	9.78	4.8 - 6.0
N	7.99	1 - 2
Hydroaromatic C	41.7	15 - 25
Aromatic C	50.0	65 - 75
Aliphatic C	8.3	5 - 10
H/C Atomic Ratio	1.4	0.8 - 0.9

(Utah Coal, H/C ~ 1.0)

Pyrolysis of 1-Benzyl-1,2,3,4-tetrahydroisoquinoline (1-BTHIQ)

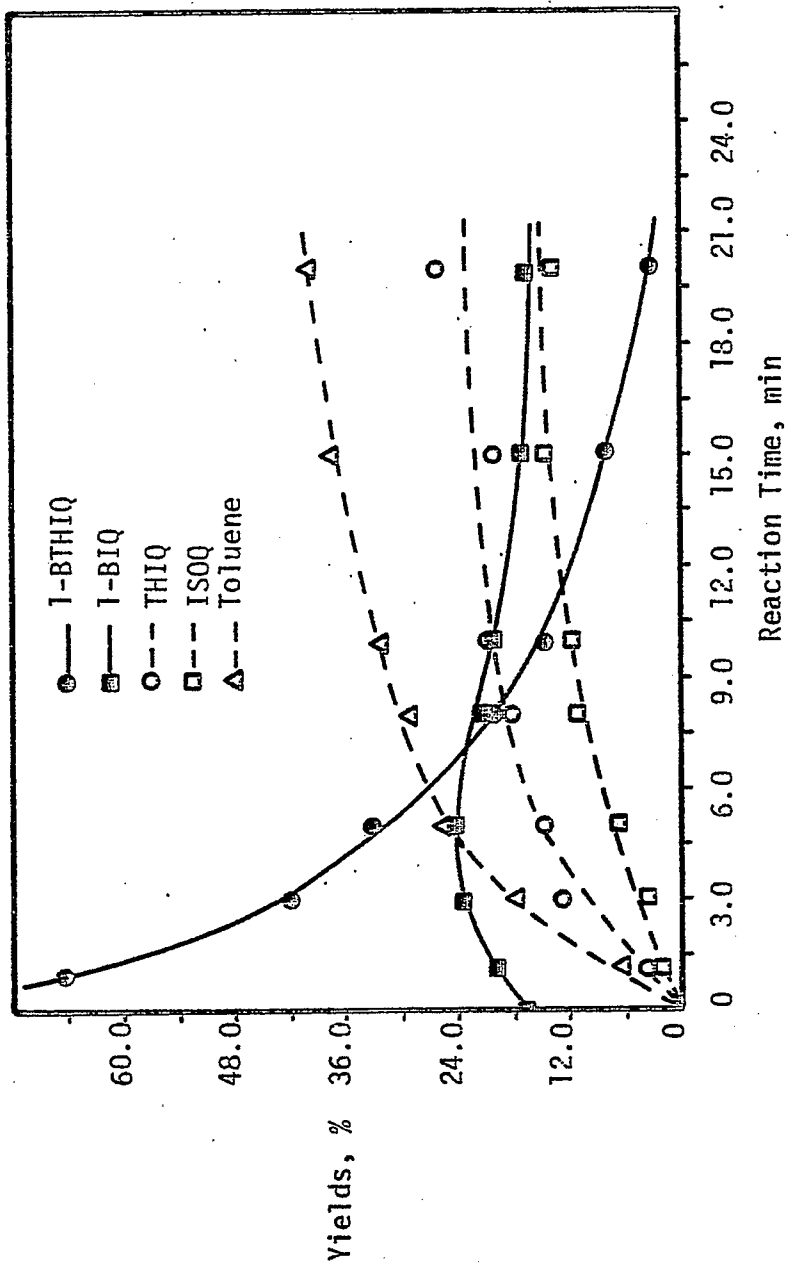


Figure 8. Normalized Product Distribution (%). Temperature, 623 K (350°C).

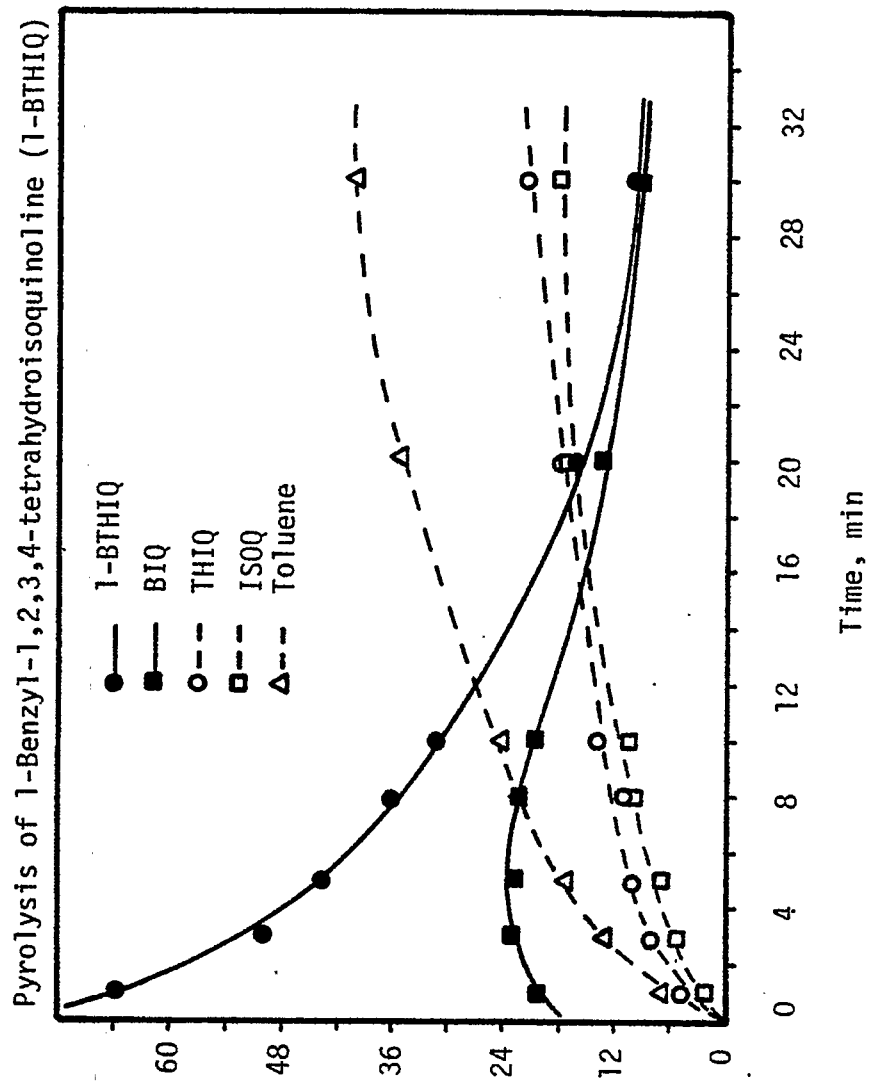


Figure 9. Normalized Product Distribution, %. Temperature, 617 K (338° C).

Pyrolysis of 1-Benzyl-1,2,3,4-tetrahydroisoquinoline (1-BTHIQ)

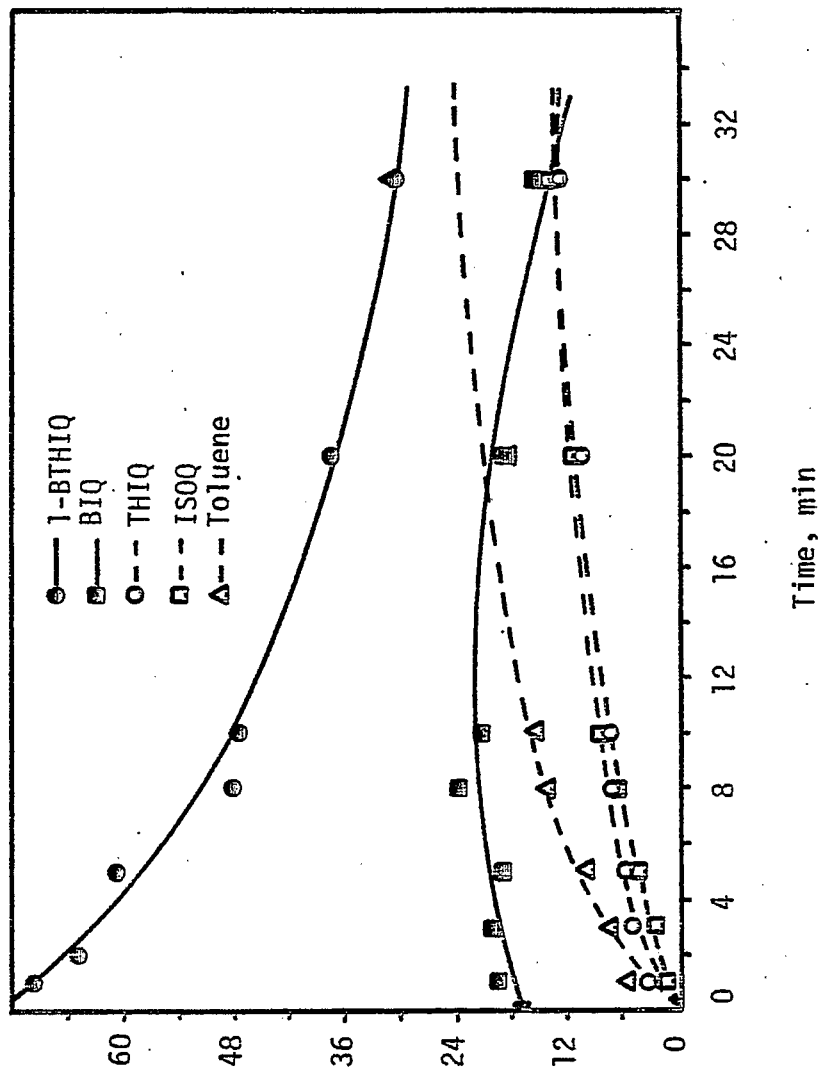


Figure 10. Normalized Product Distribution, %. Temperature, 598 K (325°C).

Pyrolysis of 1-Benzyl-1,2,3,4-Tetrahydroisoquinoline (1-BTHIQ)

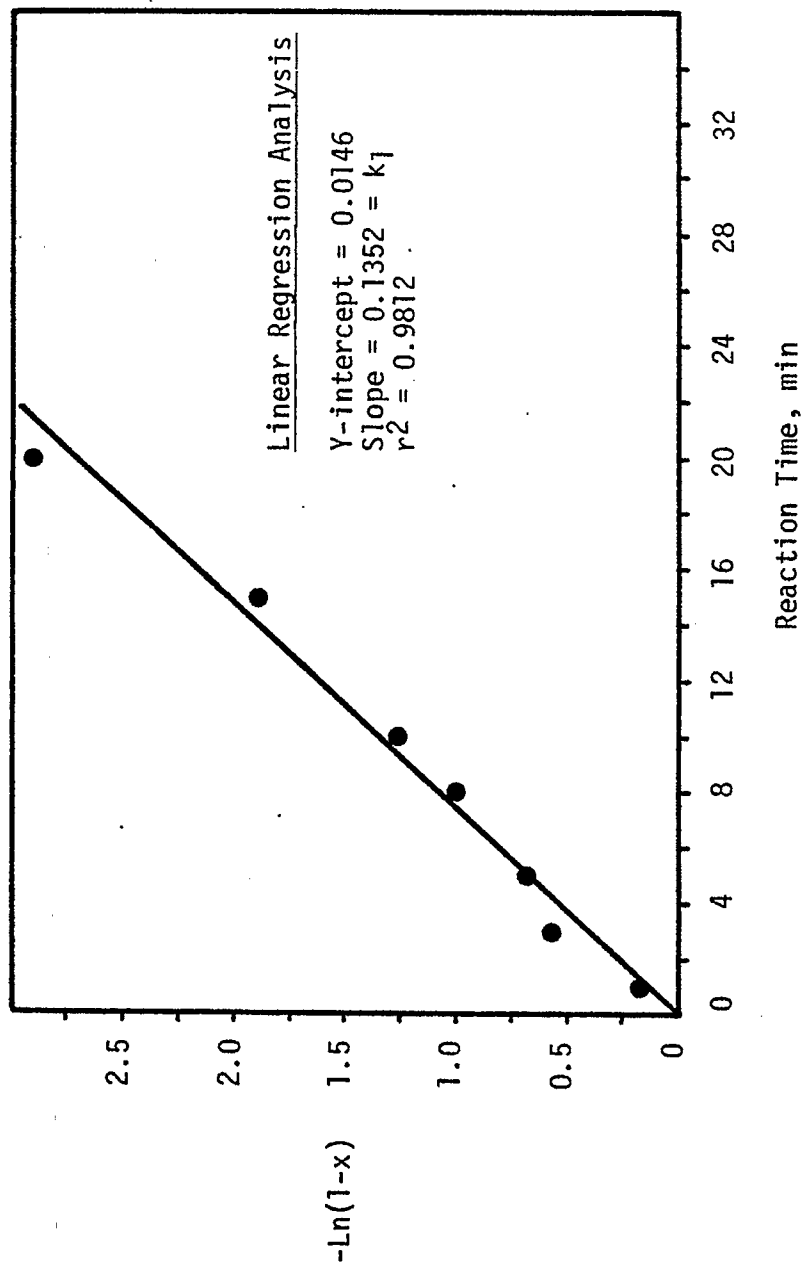


Figure 11. First Order Kinetics Plot, $-\ln(1-x)$ vs. Time. Temperature, 623 K (350°C).

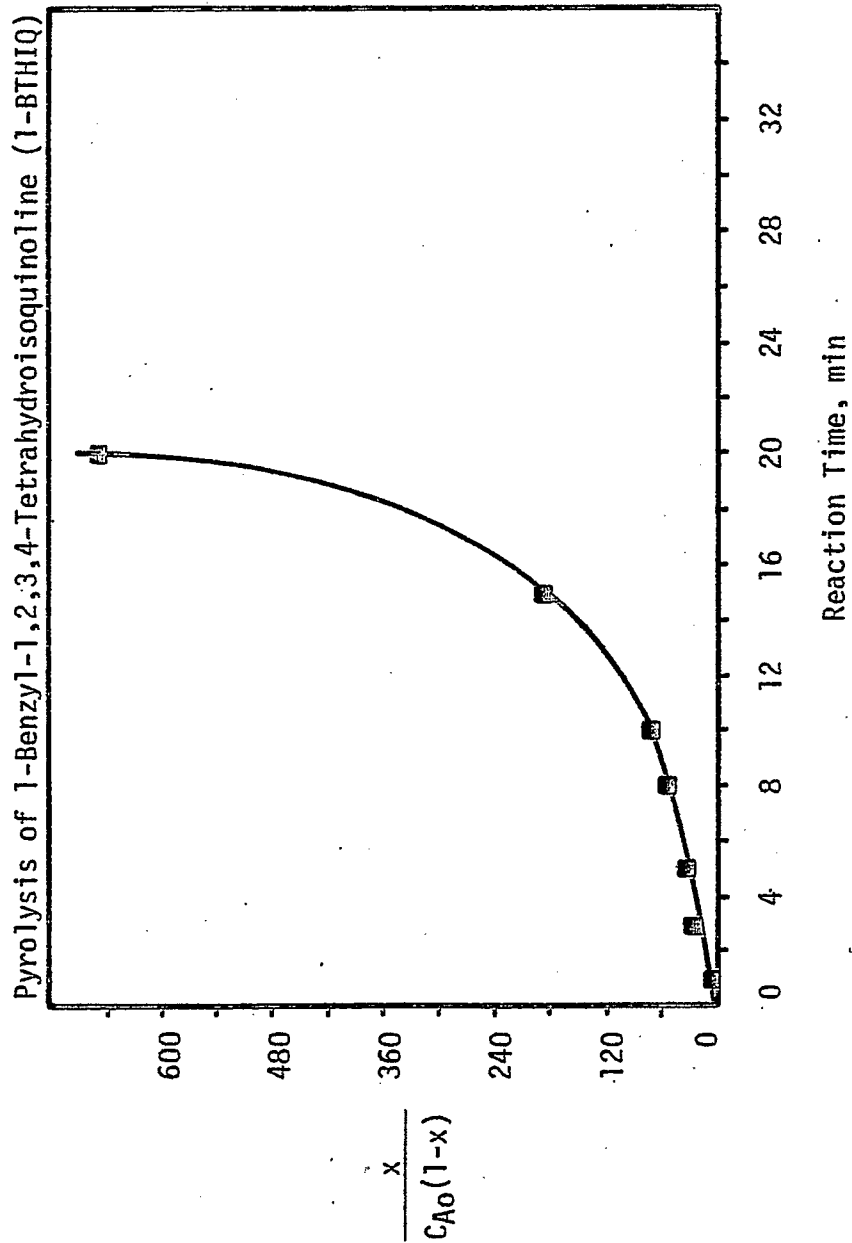


Figure 12. Second Order Kinetics Plot. Temperature, 623 K (350°C).

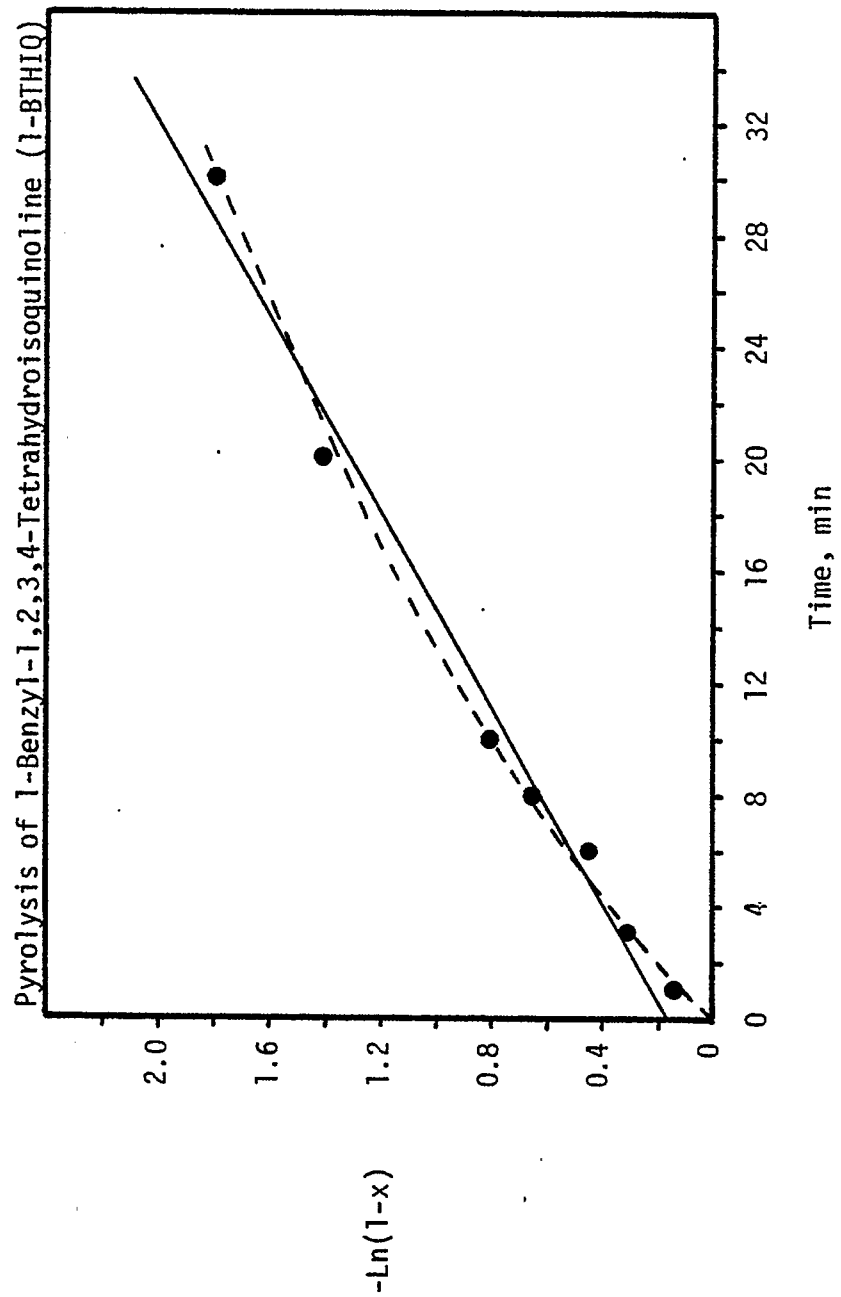


Figure 13. First Order Kinetics Plot. Temperature, 611 K (338°C).

Pyrolysis of 1-Benzyl-1,2,3,4-Tetrahydroisoquinoline (1-BTHIQ)

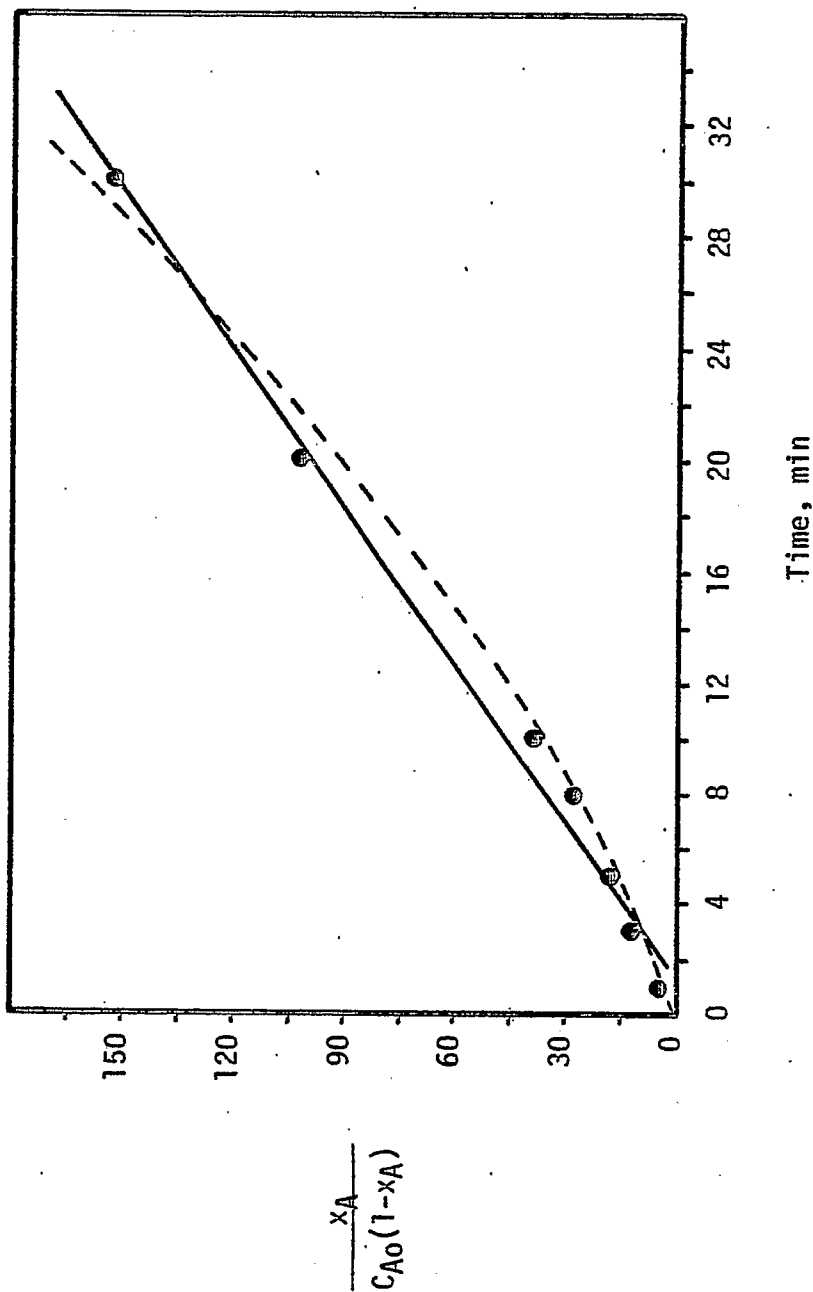


Figure 14. Second Order Kinetics Plot. Temperature, 611 K (338°C).

Pyrolysis of 1-Benzyl-1,2,3,4-Tetrahydroisoquinoline (1-BTHIQ)

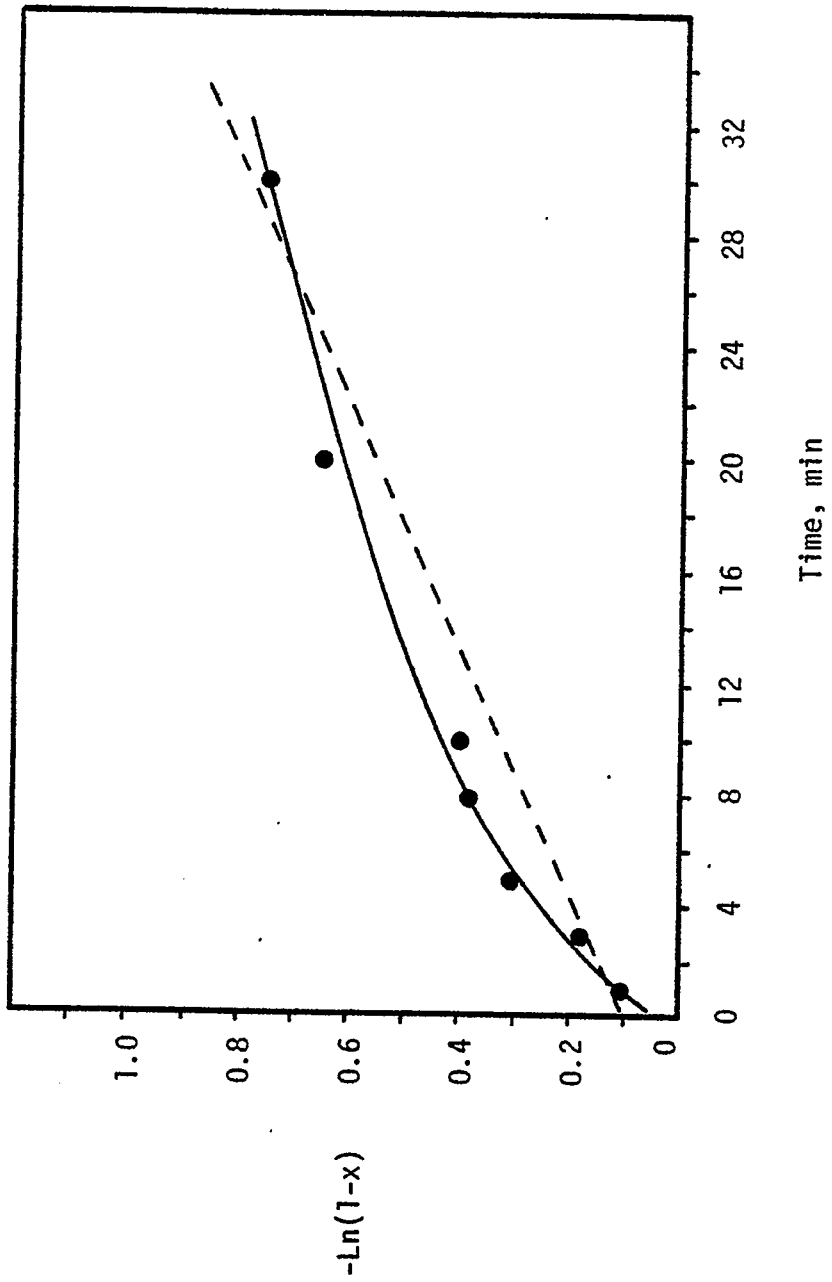


Figure 15. First Order Kinetics Plot. Temperature, 598 K (325°C).

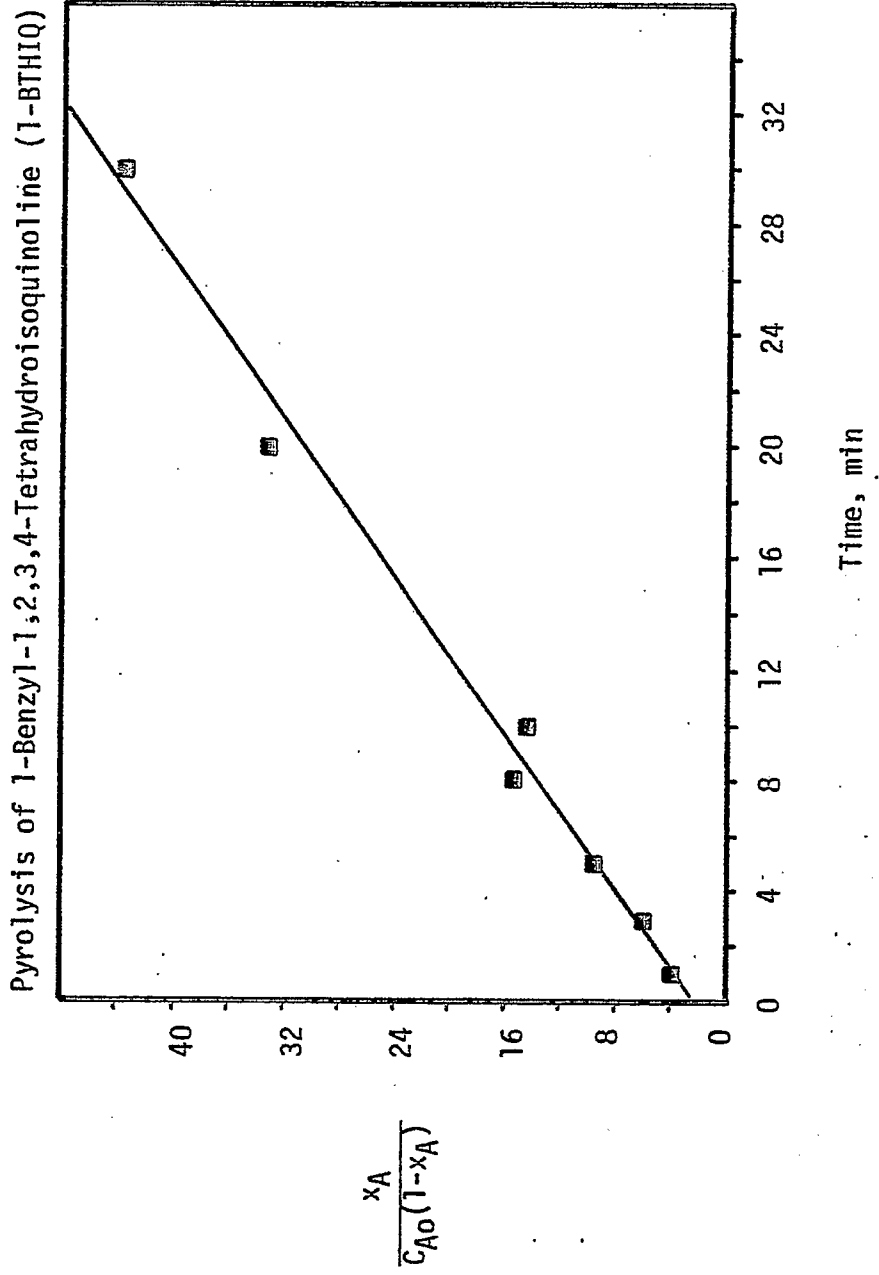


Figure 16. Second Order Kinetics Plot. Temperature, 598 K (325°C).

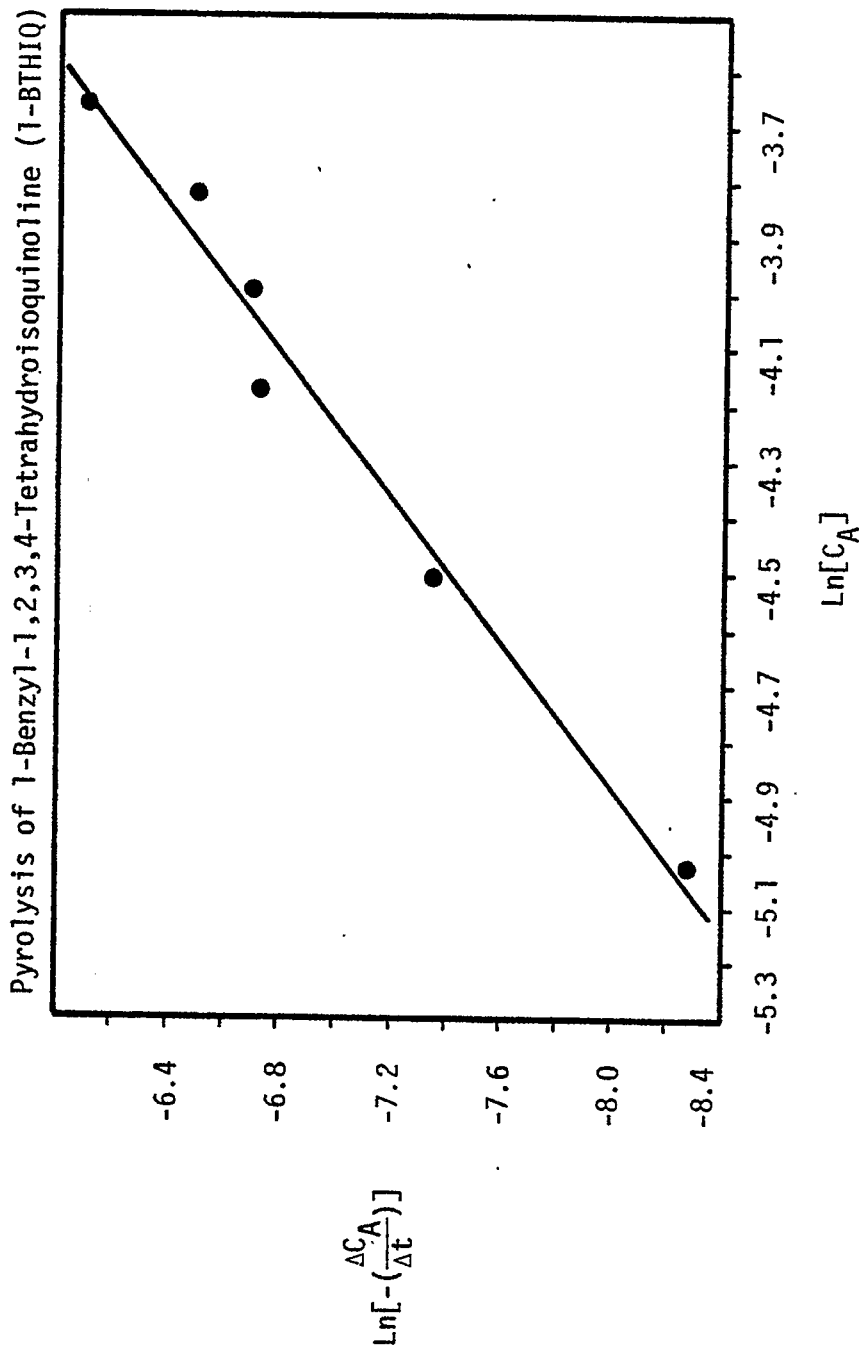


Figure 17. Differential Kinetics Analysis Plot. Temperature, 611 K (338°C).

Table 1.

PYROLYSIS OF 9-BENZYL-1,2,3,4-TETRAHYDROCARBAZOLE (9-BTHC)

Temperature: 633 K (360°C)

<u>Reaction Time, Min</u>	<u>Initial Conc'n of 9-BTHC, mmole/cc</u>	<u>% Material Balance</u>	<u>Conversion of 9-BTHC ± SD</u>
5.0	.02332	91.61	.1764 ± .017
10.0	.02526	92.70	.1855 ± .02
20.0	.02268	94.70	.1971 ± .03
30.0	.02404	91.94	.2239 ± .03
60.0	.02078	93.75	.2861 ± .01
120.0	.02337	90.73	.3424 ± .02
240.0	.02602	93.07	.4525 ± .02

Notes:

$$1. \text{ \% Mat'l Balance} = \left[\frac{N(\text{THC}) + N(\text{CARB}) + N_A + N(\text{9BC})}{N_{A0}} \right] \times 100$$

$$2. \text{ Conversion of 9-BTHC} = 1 - \frac{N_A}{N_{A0}}$$

3. SD = Standard deviation

where, N_A = millimoles of 9-BTHC @ t

N_{A0} = millimoles of 9-BTHC @ t = 0

Table 2

PYROLYSIS OF 9-BENZYL-1,2,3,4-TETRAHYDROCARBAZOLE (9-BTHC)

Reaction Time, min	Conversion of 9-BTHC \pm SD	% Mat'l Balance	Temperature: 633 K (360°C)					9BC/Carb Molar Ratio
			Relative Amounts (% , Normalized)					
			9-BTHC	9-BC	THC	Carb	Toluene	
5.0	.1764 \pm .017	91.61	90.25	7.53	1.11	0	1.11	-
10.0	.1855 \pm .02	92.70	87.37	9.45	1.59	0	1.59	-
20.0	.1971 \pm .03	94.70	82.61	9.76	2.99	.83	3.82	11.8
30.0	.2239 \pm .03	91.94	81.18	9.75	3.46	1.08	4.54	9.06
60.0	.2861 \pm .01	93.75	70.22	13.37	6.72	1.49	8.21	8.98
120.0	.3424 \pm .02	90.73	64.33	12.22	9.68	2.05	11.73	5.97
240.0	.4525 \pm .02	93.07	48.50	13.43	15.96	3.08	19.04	4.36

Table 3

PYROLYSIS OF 9-BENZYL-1,2,3,4-TETRAHYDROCARBAZOLE (9-BTHC)
Overall Reaction(s) Order Determination - Integral Technique

Temperature: 633 K (360°C)

Kinetic Plots Ordinates

<u>Reaction Time, Min</u>	<u>First Order -Ln(1-X_A)</u>	<u>Second Order X_A/[C_{A0}(1-X_A)]</u>
5.0	.1941	9.183
10.0	.2052	9.015
20.0	.2196	10.828
30.0	.2535	12.000
60.0	.3370	19.28
120.0	.4192	22.28
240.0	.6024	31.76

<u>Plot</u>	<u>Y-Intercept</u>	<u>Slope</u>	<u>r²</u>
First Order -Ln(1-X _A)=k ₁ t	.1982	.00174	.9852
Second Order $\frac{X_A}{C_{A0}(1-X_A)} = k_2 t$	9.565	.09771	.9513

where, $k_1 [=] \text{min}^{-1}$; $k_2 [=] \frac{\text{cc}}{\text{mmole-min}}$

X_A = Conversion of 9-BTHC

C_{A0} = Initial conc'n of 9-BTHC, mmole/cc

Table 4

PYROLYSIS OF 9-BENZYL-1,2,3,4-TETRAHYDROCARBAZOLE (9-BTHC)
Overall Reaction(s) Order Determination - Differential Technique

Temperature: 633 K (360°C)

<u>Reaction Time, Min</u>	<u>C_A, mmole/cc</u>	<u>$-\left[\frac{\Delta C_A}{\Delta t}\right]$</u>	<u>$\ln \left[-\left(\frac{\Delta C_A}{\Delta t}\right)\right]$</u>	<u>$\ln [C_A]$</u>
5.0	.01963	2.40×10^{-5}	-10.64	-3.934 ^A
10.0	.01951	9.30×10^{-5}	- 9.28	-3.961
20.0	.01858	6.5×10^{-5}	- 9.64	-4.003
30.0	.01793	3.667×10^{-5}	-10.21	-4.052
60.0	.01683	2.217×10^{-5}	-10.72	-4.125
120.0	.01550	2.167×10^{-5}	-10.74	-4.255
240.0	.01290			

Linear Regression Analysis

$$\ln \left[-\left(\frac{\Delta C_A}{\Delta t}\right) \right] = \ln k + n \ln C_A$$

	<u>Case A</u>	<u>Case B</u>
y-intercept = $\ln k =$	10.45	26.14
slope = $n =$	5.0	9.0
$r^2 =$ correlation coefficient =	.806	.989

Case A: Delete Point #1

Case B: Delete Point #1 & #6

Table 5

HYDROGEN BALANCE ON 9-BTHC PYROLYSIS

<u>Temperature Kelvin (°C)</u>	<u>$\bar{\Sigma}_H \pm SD$</u>	<u>$\bar{\Sigma}_H \pm SD/\%$ Material Balance</u>
633 (360)	0.908 \pm 0.015	0.980 \pm 0.009
648 (375)	0.898 \pm 0.07	0.928 \pm 0.06
673 (400)	0.891 \pm 0.03	0.951 \pm 0.02
683 (410)	0.997 \pm 0.06	0.974 \pm 0.02
698 (425)	0.891 \pm 0.08	0.923 \pm 0.04
713 (440)	0.895 \pm 0.03	0.903 \pm 0.02
Averages	0.910 \pm 0.04	0.943 \pm 0.03

where,

$\bar{\Sigma}_H$ = average hydrogen balance at T

SD = standard deviation

$\Sigma_H = N(9\text{-BTHC}) + 15/19 N(9\text{-BC}) + 13/19 N(\text{THC}) + 9/19 N(\text{CARB}) + 8/19 N(\text{Toluene})$

9-BC = 9-benzylcarbazole

THC = 1,2,3,4-tetrahydrocarbazole

CARB = carbazole

Table 6

9-BTHC PYROLYSIS KINETICS BASED ON VOLATILES PRODUCTION
 LINEAR REGRESSION ANALYSIS ($y = mx + b$)

Temperature Kelvin ($^{\circ}\text{C}$)	First Order Kinetics, $\ln \frac{a}{a-x}$ vs. t			Second Order Kinetics, $\frac{x}{a(a-x)}$ vs. t		
	Slope (m)	Y-Intcpt (b)	r ²	Slope (m)	Y-intcpt (b)	r ²
633 (360)	9.63×10^{-4}	0.014	0.9895	0.0681	1.15	0.9751
648 (375)	3.413×10^{-3}	0.012	0.9887	0.3084	-0.095	0.9803
673 (400)	0.0212	0.042	0.9816	2.489	-0.66	0.9674
683 (410)	0.0386	0.042	0.9653	5.511	-7.2	0.9921
698 (425)	0.0484	0.199	0.7966	7.23	11.66	0.8785
713 (440)	0.1053	0.313	0.8208	22.42	10.3	0.8685

where,

a = initial mmoles of 9-BTHC

x = mmoles of toluene + benzene + 2(bibenzyl) produced

= mmoles of THC + CARB

= mmoles of 9-BTHC cleaved

r² = correlation coefficient

NOTE: Equations are derived from $dx/dt = k_n(a-x)^n$
 by assuming that n=1 or 2 and integrating to
 obtain the resulting equations.

Table 7

PYROLYSIS OF 1-BENZYL-1,2,3,4-TETRAHYDROISOQUINOLINE (1-BTHIQ)

TEMPERATURE: 623 K (350°C)

<u>Reaction Time, Min.</u>	<u>Initial Conc'n mmole/cc</u>	<u>% Material Balance</u>	<u>Conversion of 1-BTHIQ ± SD</u>
1.0	.03075	97.00	.1572 ± .009
3.0	.02937	92.55	.4362 ± .0001
5.0	.03108	99.09	.4941 ± .01
8.0	.03320	101.60	.6346 ± .014
10.0	.03567	106.34	.7172 ± .003
15.0	.03058	98.57	.8500 ± .01
20.0	.02688	94.96	.9417 ± .03

Notes:

1. % Material balance = $[N(\text{THIQ}) + N(\text{ISOQ}) + N(\text{BIQ}) + N_A] / N_{A0} \times 100$

2. Conversion of 1-BTHIQ = $1 - \frac{N_A}{N_{A0}}$

3. SD = Standard Deviation between experiments

where, $N(i)$ = millimoles of i

N_A = millimoles of 1-BTHIQ

THIQ = 1,2,3,4-Tetrahydroisoquinoline

TSOQ = Isoquinoline

BIQ = 1-Benzylisoquinoline

Table 8

PYROLYSIS OF 1-BENZYL-1,2,3,4-TETRAHYDROISOQUINOLINE (1-BTHIQ)
 Temperature: 611 Kelvin (338°C)

Reaction Time, min	Initial Concentration of 1-BTHIQ, mmole/cc	% Material Balance	Conversion of 1-BTHIQ \pm SD
1.0	0.03436	102.4	0.1311 \pm 0.005
3.0	0.03039	104.5	0.2708 \pm 0.01
5.0	0.03204	100.1	0.3648 \pm 0.001
8.0	0.03268	94.56	0.4806 \pm 0.0008
10.0	0.03175	93.36	0.5560 \pm 0.001
20.0	0.03027	93.14	0.7556 \pm 0.02
30.0	0.03286	92.29	0.8345 \pm 0.012

NOTES:

$$1. \text{ \% Material Balance} = \left[\frac{N(\text{ISOQ}) + N(\text{THIQ}) + N_A + N(1\text{-BIQ})}{N_{AO}} \right] \times 100$$

$$2. \text{ Conversion of 1-BTHIQ} = \left[1 - \frac{N_A}{N_{AO}} \right]$$

3. SD = Standard Deviation

where,

N_A = millimoles of 1-BTHIQ at t

N_{AO} = millimoles of 1-BTHIQ at t=0

Table 9

PYROLYSIS OF 1-BENZYL-1,2,3,4-TETRAHYDROISOQUINOLINE (1-BTHIQ)
 Temperature: 598 Kelvin (325°C)

Reaction Time, min	Initial Concentration of 1-BTHIQ, mmole/cc	% Material Balance	Conversion of 1-BTHIQ \pm SD
1.0	0.02895	101.4	0.1025 \pm 0.01
3.0	0.03418	98.50	0.1641 \pm 0.005
5.0	0.03805	94.21	0.2640 \pm 0.01
8.0	0.03053	101.7	0.3168 \pm 0.02
10.0	0.03350	98.88	0.3255 \pm 0.001
20.0	0.02747	94.55	0.4767 \pm 0.02
30.0	0.02566	101.0	0.5276 \pm 0.02

NOTES:

$$1. \text{ \% Material Balance} = \left[\frac{N(\text{ISOQ}) + N(\text{THIQ}) + N(\text{BIQ}) + N_A}{N_{AO}} \right] \times 100$$

$$2. \text{ Conversion of 1-BTHIQ} = 1 - \frac{N_A}{N_{AO}}$$

3. SD = Standard Deviation

where,

N_A = millimoles of 1-BTHIQ @ t

N_{AO} = millimoles of 1-BTHIQ @ t=0

Table 10

PYROLYSIS OF 1-BENZYL-1,2,3,4-TETRAHYDROISOQUINOLINE (1-BTHIQ)
 Normalized Product Distributions
 Temperature: 623 Kelvin (350°C)

Reaction Time, min	Conversion of 1-BTHIQ \pm SD	% Mat'l Balance	Relative Amounts (% , Normalized)					1-BIQ/ISOQ Molar Ratio
			1-BTHIQ	1-BIQ	THIQ	ISOQ	Toluene	
1.0	0.1572 \pm 0.009	97.0	67.70	19.72	4.08	2.21	6.29	9.01
3.0	0.4362 \pm 0.0001	92.55	41.75	23.29	12.68	4.80	17.5	4.92
5.0	0.4941 \pm 0.01	99.09	33.36	23.95	14.65	6.69	25.85	3.62
8.0	0.6346 \pm 0.01	101.6	21.16	20.50	18.10	11.05	29.16	1.86
10.0	0.7172 \pm 0.003	106.3	14.88	19.92	20.83	11.77	32.60	1.82
15.0	0.8500 \pm 0.01	98.57	7.92	17.02	22.81	14.72	37.53	1.18
20.0	0.9417 \pm 0.03	94.96	3.10	17.15	26.18	13.70	39.87	1.25

where,

1-BIQ = 1-Benzyl isoquinoline

THIQ = 1,2,3,4-Tetrahydroisoquinoline

ISOQ = Isoquinoline

Relative Yields = $Ni/(NA_0x)$

Ni = millimoles of i

x = conversion of 1-BTHIQ

NA₀ = initial millimoles of 1-BTHIQ

Table 11

PYROLYSIS OF 1-BENZYL-1,2,3,4-TETRAHYDROISOQUINOLINE (1-BTHIQ)
 Normalized Product Distributions
 Temperature: 611 Kelvin (338°C)

Reaction Time, min	Conversion of 1-BTHIQ \pm SD	% Mat'l Balance	Relative Amounts (% Normalized)				
			1-BTHIQ	1-BIQ	THIQ	ISOQ	Toluene
1.0	0.1311 \pm 0.005	102.4	65.5	20.4	4.74	2.31	7.05
3.0	0.2708 \pm 0.01	104.5	50.0	23.1	8.31	5.11	13.4
5.0	0.3648 \pm 0.001	100.1	43.8	22.5	9.94	6.94	16.9
8.0	0.4806 \pm 0.0008	94.56	36.1	22.3	10.9	9.82	20.8
10.0	0.5560 \pm 0.001	93.36	31.1	20.7	13.8	10.3	24.1
20.0	0.7556 \pm 0.02	93.14	16.2	13.3	17.6	17.7	35.2
30.0	0.8345 \pm 0.012	92.29	10.4	10.0	21.6	18.2	39.8

where,

1-BIQ = 1-Benzylisoquinoline

THIQ = 1,2,3,4-Tetrahydroisoquinoline

ISOQ = Isoquinoline

SD = Standard Deviation

Table 12

PYROLYSIS OF 1-BENZYL-1,2,3,4-TETRAHYDROISOQUINOLINE (1-BTHIQ)
 Normalized Product Distributions
 Temperature: 598 Kelvin (325°C)

Reaction Time, min	Conversion of 1-BTHIQ \pm SD	% Mat'l Balance	Relative Amounts (% Normalized)				
			1-BTHIQ	1-BIQ	THIQ	ISOQ	Toluene
1.0	0.1025 \pm 0.01	101.4	69.70	19.42	3.51	1.92	5.44
3.0	0.1641 \pm 0.005	98.50	65.24	19.88	5.00	2.43	7.44
5.0	0.2640 \pm 0.01	94.21	61.05	19.00	5.67	4.31	9.98
8.0	0.3168 \pm 0.02	101.7	48.13	23.76	7.23	6.82	14.1
10.0	0.3255 \pm 0.001	98.88	47.79	21.01	7.39	8.21	15.60
20.0	0.4767 \pm 0.02	94.55	37.89	18.67	10.74	10.98	21.72
30.0	0.5276 \pm 0.02	101.0	30.21	15.6	13.08	14.02	27.10

where,

1-BIQ = 1-Benzylisoquinoline

THIQ = 1,2,3,4-Tetrahydroisoquinoline

ISOQ = Isoquinoline

SD = Standard Deviation

Table 13

PYROLYSIS OF 9-BENZYL-1,2,3,4-TETRAHYDROISOQUINOLINE (1-BTHIQ)
Overall Reaction(s) Order Determination - Integral Technique

Temperature: 623 Kelvin (350°C)

Reaction Time, min	Kinetic Plots Ordinates	
	First Order $-\ln(1-x_A)$	Second Order $x_A/[C_{A0}(1-x_A)]$
1.0	0.171	6.077
3.0	0.573	26.33
5.0	0.682	31.55
8.0	1.007	52.36
10.0	1.263	71.12
15.0	1.895	186.7
20.0	2.897	668.2

Plot	Y-Intercept	Slope	r^2
First Order $-\ln(1-x_A)=k_1t$	0.015	0.135	0.9812
Second Order $\frac{x_A}{C_{A0}(1-x_A)} = k_2t$	-119	30.2	0.7480

Table 14

PYROLYSIS OF 9-BENZYL-1,2,3,4-TETRAHYDROISOQUINOLINE (1-BTHIQ)
Overall Reaction(s) Order Determination - Integral Technique

Temperature: 611 Kelvin (338°C)

Reaction Time, min	Kinetic Plots Ordinates	
	First Order $-\ln(1-x_A)$	Second Order $x_A/[C_{A0}(1-x_A)]$
1.0	0.1405	4.391
3.0	0.3159	12.23
5.0	0.4538	17.92
8.0	0.6551	28.17
10.0	0.8118	39.44
20.0	1.410	102.4
30.0	1.800	154.0

Linear Progression Analysis

<u>Plot</u>	<u>Y-Intercept</u>	<u>Slope</u>	<u>r²</u>
First Order $-\ln(1-x_A)=k_1t$	0.166	0.0575	0.9860
Second Order $\frac{x_A}{C_{A0}(1-x_A)} = k_2t$	-7.4	5.327	0.9914

Table 15

PYROLYSIS OF 1-BENZYL-1,2,3,4-TETRAHYDROISOQUINOLINE (1-BTHIQ)
Overall Reaction(s) Order Determination - Integral Technique

Temperature: 598 Kelvin (325°C)

Reaction Time, min	Kinetic Plots Ordinates	
	First Order $-\ln(1-x_A)$	Second Order $x_A/[C_{A0}(1-x_A)]$
1.0	0.1081	3.945
3.0	0.1792	5.744
5.0	0.3065	9.427
8.0	0.3810	15.19
10.0	0.3938	14.40
20.0	0.6476	33.16
30.0	0.7500	43.53

Plot	Y-Intercept	Slope	r^2
First Order $-\ln(1-x_A)=k_1t$	0.156	0.0218	0.945
Second Order $\frac{x_A}{C_{A0}(1-x_A)} = k_2t$	2.33	1.417	0.988

where,

$$k_1 [=] \text{min}^{-1}; \quad k_2 [=] \frac{\text{cc}}{\text{mmole} \cdot \text{min}}$$

x_A = Conversion of 1-BTHIQ

C_{A0} = Initial concentration of 1-BTHIQ, mmole/cc

Table 16

PYROLYSIS OF 1-BENZYL-1,2,3,4-TETRAHYDROISOQUINOLINE (1-BTHIQ)
 Overall Reaction(s) Order Determination - Differential Technique
 Temperature: 611 Kelvin (338°C)

<u>Reaction Time, min</u>	<u>C_A, $\frac{\text{mmole}}{\text{cc}}$</u>	<u>$-\left[\frac{\Delta C_A}{\Delta t}\right]$</u>	<u>$\text{Ln}\left[-\left(\frac{\Delta C_A}{\Delta t}\right)\right]$</u>	<u>$\text{Ln}[C_A]$</u>
1.0	0.02785			
		0.002239	-6.102	-3.665
3.0	0.02337			
		1.506×10^{-3}	-6.498	-3.823
5.0	0.02036			
		1.237×10^{-3}	-6.695	-3.990
8.0	0.01665			
		1.208×10^{-3}	-6.719	-4.171
10.0	0.01423			
		6.397×10^{-4}	-7.354	-4.507
20.0	0.007833			
		2.529×10^{-4}	-8.283	-5.025
30.0	0.005304			

Linear Regression Analysis

$$\text{Ln}\left[-\left(\frac{\Delta C_A}{\Delta t}\right)\right] = \text{Ln } k + n \text{ Ln } C_A$$

$$\text{Y-Intercept} = \text{Ln } k = -0.526$$

$$\text{Slope} = n = 1.53$$

$$r^2 = \text{correlation coefficient} = 0.9782$$

Task 6

Catalytic Hydrogenation of CD Liquids and Related Polycyclic Aromatic Hydrocarbons

Faculty Advisor: J. Shabtai
Research Associate: C. Russell

Introduction

The main objective of this research project is to develop a versatile process for controllable hydrotreating of highly aromatic coal liquids, viz., a process permitting production of naphthenic-aromatic feedstocks containing variable relative concentrations of hydroaromatic vs. aromatic ring structures. Such feedstocks, including the extreme case of a fully hydrogenated coal liquid, are suitable starting materials for catalytic cracking, as applied for preferential production of light liquid fuels. The overall objective of this project and of a parallel catalytic cracking study is, therefore, to develop and optimize a hydrotreating-catalytic cracking process sequence for conversion of coal liquids into conventional fuels.

The present project includes also a study of metal sulfide-catalyzed hydrogenation of model polycyclic arenes present in coal liquids, e.g., phenanthrene, pyrene, anthracene and triphenylene, as a function of catalyst type and experimental variables.¹ This part of the study provides basic information on the rate, mechanism and stereochemistry of hydrogenation of structurally distinct aromatic systems in the presence of sulfided catalysts.

Project Status

The systematic studies of metal sulfide-catalyzed hydrogenation of phenanthrene, pyrene, anthracene, triphenylene, and chrysene, have been completed and the results obtained are being prepared for publication. The study of the hydrogenation kinetics of a representative coal liquid (SRC-II middle-heavy distillate) is continuing.

Future Work

The study of the hydrogenation kinetics of a typical coal liquid (SRC-II middle-heavy distillate) and of a tetracyclic model compound, i.e., chrysene, will be continued and completed.

References

1. J. Shabtai, C. Russell, L. Veluswami and A.G. Oblad, paper in preparation.

Task 7

Denitrogenation and Deoxygenation of CD Liquids and Related N- and O- Containing Compounds

Hydrodenitrogenation of Coal-Derived Liquids and Related N-Containing Compounds

Faculty Advisor: J. Shabtai
Graduate Student: J. Yeh

Introduction

The main objective of this research project is to develop effective catalyst systems and processing conditions for hydrodenitrogenation (HDN) of coal-derived liquids (CDL) in a wide range of nitrogen contents and structural type composition. This is of particular importance in view of the higher concentration of nitrogen-containing compounds in CDL as compared to that in petroleum feedstocks. For a better understanding of denitrogenation processes, the project includes systematic denitrogenation studies not only of CDL but also of related model N-containing compounds found in such liquids, e.g., phenanthridine, 1,10-phenanthroline, carbazoles, acridines, etc., as a function of catalyst type and experimental rate, mechanism and stereochemistry of HDN of structurally distinct N-containing aromatic systems in the presence of sulfided catalysts.

Project Status

The observed rate constant of a catalytic reaction depends on the following five steps:¹

1. Diffusion of reactants into catalyst.
2. Adsorption of reactant.
3. Chemical reaction.
4. Desorption of product.
5. Diffusion of product out of catalyst.

Diffusion resistance is more important for larger sized catalyst particles. To minimize diffusion resistance, the effect of catalyst particle size on the rate constant is being studied. The effect of catalyst particle size on the rate of hydrogenation of the pyridine ring in 5,6-benzoquinoline is given in Table 1 and in Figure 1. The reaction conditions are indicated in the footnote of Table. This rate constant changes little when catalyst particle size is about 650 microns or smaller (Figure 1). This means that there is little diffusion resistance when the particle size is about 650 microns or smaller.

Katzer found that a small amount of CS₂ in solution will stabilize sulfided catalysts, increase HDN activity and decrease hydrogenation activity in the hydrogenation reaction of quinoline.² The effect of different concentrations of CS₂ on 5,6-benzoquinoline HDN kinetics has been studied. A typical GC chromatogram of the 5,6-benzoquinoline hydrogenation products is given in Figure 2. The reaction network is shown in Figure 3, and the effect of CS₂ concentration on the rate constants is summarized in Table 2. Figure 4 shows hydrogenolysis activity vs. concentration of CS₂. Figure 5 shows hydrogenation activity vs. CS₂ concentration. The ratios of k₂/k₃

and k_5/k_6 are given in Table 3 and Figures 6 and 7.

Generally, a higher concentration of CS_2 will increase hydrogenolysis activity (k_2, k_5) and reduce hydrogenation activity (k_3, k_6, k_7) (see Table 2, Figures 4 and 5). Figures 6 and 7 show that k hydrogenolysis/ k hydrogenation increases with increased CS_2 concentrations.

In the previous report, rate constants in the reaction network of Figure 3 were determined using 5 grams of reactant over prepared catalysts. Those rate constants (Figure 3) were also studied using smaller amounts of reactants over prepared catalysts, with a small amount of CS_2 added (5 drops/100 cc dodecane) to stabilize sulfided catalysts. The results are given in Table 4. The composition and methods of preparation of the catalysts are indicated in the footnotes of Table 4, while details are provided elsewhere.³ Comparison of rate constants using different amounts of reactant is shown in Table 5. The experimental conditions are given in the footnotes of these Tables.

Kinetic rate constants (Table 4) were obtained for a reaction pressure of 2500 psig and at a reaction temperature of 300°C. The rate of hydrogenation of the pyridine ring in 5,6-benzoquinoline (1), k_1 , is large, so most of the reactant is consumed before taking the sample. C-N hydrogenolysis of the first reaction intermediate, 1,2,3,4-tetrahydro-5,6-benzoquinoline (2), is a very slow reaction with all catalysts examined, although the catalyst 2-5 are somewhat active for this step. Ring hydrogenation of 2, yielding two octahydrobenzoquinolines (3), is much faster than cleavage, and catalysts 3 and 5 are more active for this step. Compound 3 is much more susceptible to C-N hydrogenolysis (compared to 2), yielding the denitrogenated products 6. Catalyst 3 is the least active in this C-N hydrogenolysis step. Compound 3 also undergoes less active ring hydrogenation (compared with k_5) to yield perhydro-5,6-benzoquinoline (4), which is ultimately denitrogenated to 7. The F-addition catalyst (catalyst 5) has higher hydrogenation activity, k_3 and k_6 , than standard impregnation catalyst 1. Stepwise addition of Co of Ni in catalysts 2 and 6 produces lower hydrogenation activity, k_6 , than for the standard impregnated catalysts 1 and 4.

From Table 5, k_5 for 0.5 gram of reactant is about 5 times the k_5 for 5 grams of reactant, which suggests that a second order polymerization reaction deposits coke which deactivates some active sites on the catalysts.

References

1. O.H. Hougen and K.M. Watson, "Chemical Process Principle-Part III".
2. S.S. Shih, J.R. Katzer, H. Kwart and A.R. Stiles, "Symposium on Refining of Synthetic Crudes," Chicago meeting, 1977, pp 919-940.
3. G. Muralidhar, F.E. Massoth and J. Shabtai, submitted for publication in J. Catalysts.

Table 1. The effect of catalyst particle size^{a)} on rate constant k_1 for 5,6-benzoquinoline hydrogenation reaction

<u>Catalyst No.</u>	<u>Mesh opening (microns)</u>	<u>Conversion^c</u>	<u>k_1^b</u>
1	2021	.441	1.163
2	1265	.470	1.270
3	637.5	.681	2.286
4	362.5	.682	2.293
5	231	.688	2.332
6	181	.681	2.285

^aCommercial Ni-Mo Catalyst (Nalco NM-504)

^bRate constants are based on first order assumption; unit is 1/hr.

^cExperimental conditions: T:150°C, H₂ pressure:2500 psig, Reactant:.3g, Catalyst:.2g, CS₂ concentration:1 drop/100 cc dodecane, Solvent:dodecane 20cc, Reactor:batch autoclave

Table 2: The effect of CS₂ concentration on the HDN reaction^a of 5,6-benzoquinoline

Concentration of CS ₂ (drops/100cc of dodecane)	<u>Rate constants^c</u>							
	<u>k₁</u>	<u>k₂</u>	<u>k₃</u>	<u>k₄</u>	<u>k₅</u>	<u>k₆</u>	<u>k₇</u>	<u>k₈</u>
0 drops (unsulfided catalyst)	--	.007	.616	--	.032	.019	--	--
0 drops (sulfided catalysts)	--	.021	.968	--	.301	.117	.234	--
5 drops ^b	--	.033	1.144	--	.421	.126	.171	--
10 drops ^b	--	.034	1.114	.177	.591	.075	.136	--
15 drops ^b	--	.041	.500		.762	.093	.047	--

^acatalyst is 6%Co, 8%Mo/γAl₂O₃, prepared by impregnation (3); Reaction conditions: T:300°C, H₂ pressure:2500 psig, Reactant:.5g benzoquinoline, Solvent:dodecane 100cc, Catalyst:2 grams

^bSulfided catalyst is used

^cUnit: 1/hr (see Figure 2)

Table 3. The effect of CS₂ concentration on k₂/k₃ & k₅/k₆ for 5,6 benzoquinoline^a

Concentration of CS ₂ (drops/100cc dodecane)	k ₂ /k ₃	k ₅ /k ₆
0 drops (unsulfided catalyst)	.011	1.71
0 drops (sulfided catalyst)	.022	2.56
5 drops	.029	3.35
10 drops	.031	7.92
15 drops	.082	8.194

^aCatalyst: 6%Co, 8%Mo/γ-Al₂O₃ prepared by impregnation (3).

Table 4. Rate constants in the reaction network of Figure 2 (for 5,6-benzoquinoline) using prepared catalyst - different amounts of reactant.

Catalyst No. ^a	Rate Constant ^b							
	k_1	k_2	k_3	k_4	k_5	k_6	k_7	k_8
3Co8Mo/ γ -Al ₂ O ₃ (I) ^c	--	.012	.521	--	.668	.055	.125	--
(step)3Co8Mo/ γ -Al ₂ O ₃ (II) ^d	--	.029	.561	--	.625	<<.05	.083	--
6Co8Mo/ γ -Al ₂ O ₃ (III)	--	.033	1.144	--	.421	.126	.171	--
3Ni8Mo/ γ -Al ₂ O ₃ (IV)	--	.025	.344	--	.610	.093	.046	--
.5F3Co8Mo/ γ -Al ₂ O ₃ (V) ^e	--	.030	1.430	.107	.615	.251	<.043	.457
(step)3Ni8Mo/ γ -Al ₂ O ₃ (VI) ^f	--	.015	.715	--	.621	.031	--	--

^aConcentration levels are 8% by wt of Mo in catalysts 1-6, .5% by wt of F and 3% by wt of Co in catalyst 5; 3% by wt of Ni in catalyst 6; the rest are the same as in Table 5A.

^bUnit:1/hr. Experimental conditions: H₂ pressure:2500 psig, Reactant:.5 grams, Catalyst:2 grams, Solvent:100cc dodecane, CS₂ concentration:5 drops/100cc dodecane.

^cPrepared by a standard impregnation procedure (3).

^dPrepared by a stepwise addition of Co to Mo impregnated γ -Al₂O₃(3).

^ePrepared by addition of F to Co-Mo impregnated γ -Al₂O₃.

^fPrepared by a stepwise addition of Ni to Mo impregnated γ -Al₂O₃(3).

Table 5 . Comparison of rate constants in the reaction network of Figure 2 using different amounts of reactant.

Reactant Amount	Rate Constants ^{a,b}							
	k_1	k_2	k_3	k_4	k_5	k_6	k_7	k_8
5 g	1.923	.011	1.025	.314	.069	.075	.369	.370
.5 g	--	.021	.968	--	.301	.117	.234	--

^aUnit is hr^{-1} . Experimental conditions: H_2 Pressure:2500 psig, Catalyst:2 grams, Solvent:100 cc dodecane, Temp.:300°C.

^bCatalyst is 6%Co-8%Mo/ $\gamma\text{Al}_2\text{O}_3$ (III). Particle size is 637 microns.

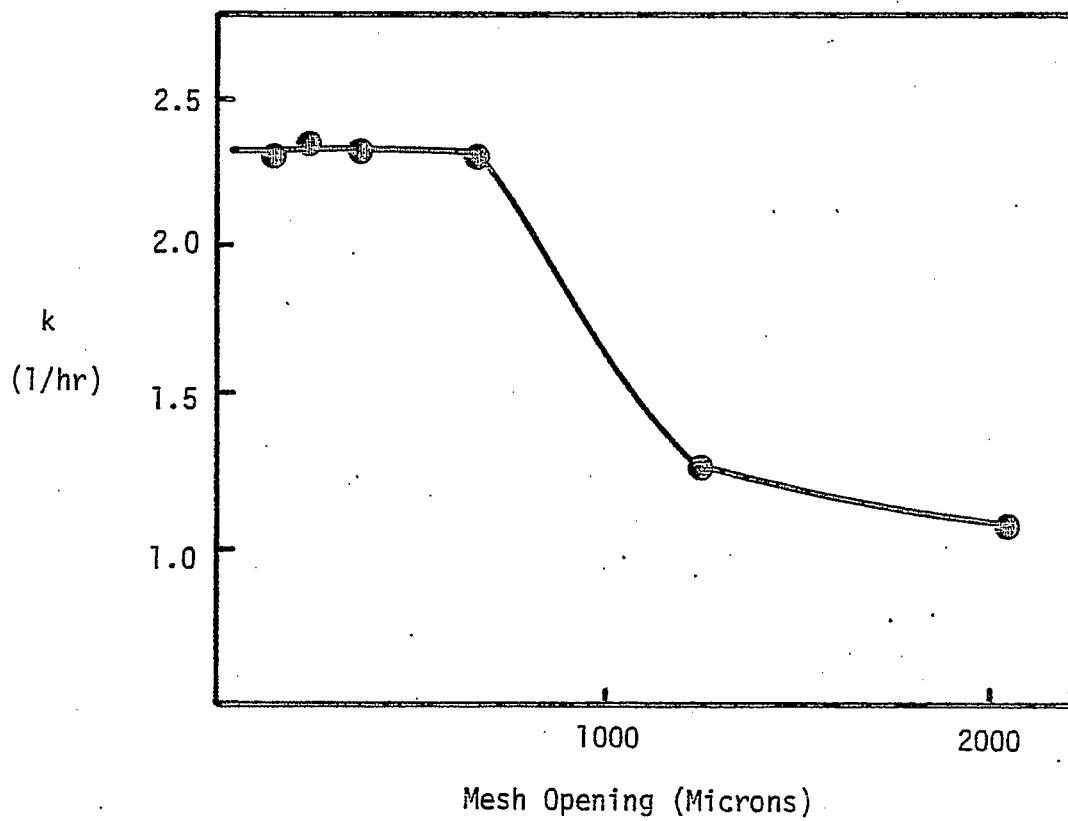


Figure 1. The effect of catalyst particle size on rate constant k_1 for 5,6-benzoquinoline.

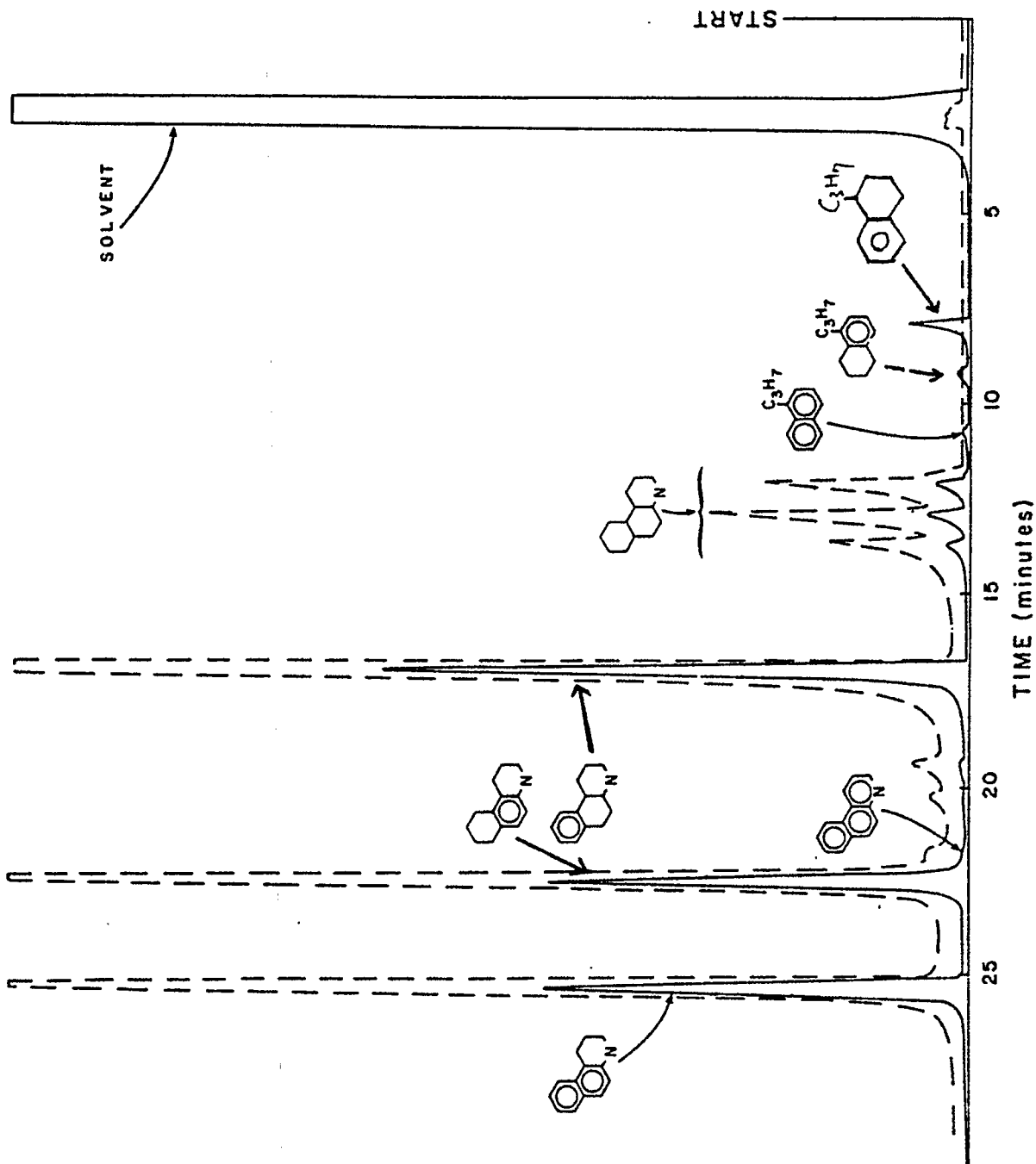


Figure 2: Typical G.C. chromatogram for 5,6-benzoquinoline hydrogenation products

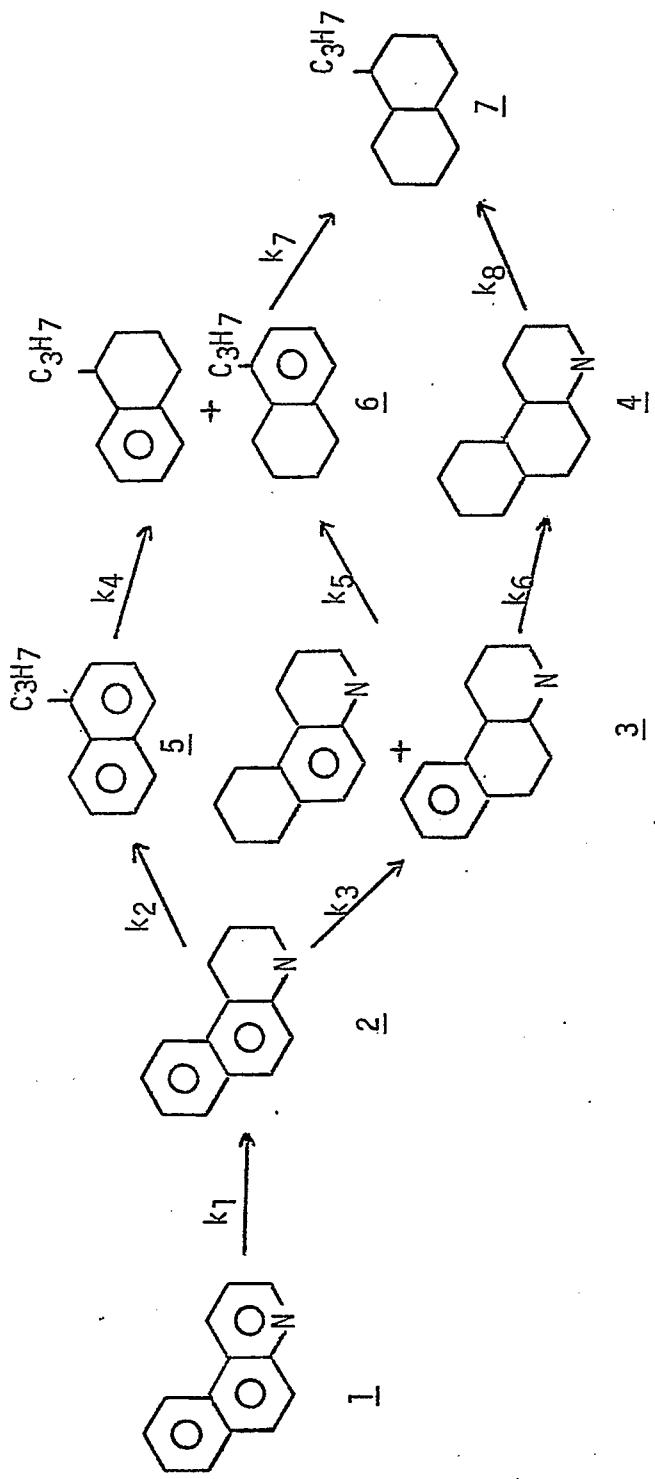


Figure 3. The reaction network for HDN of 5,6-benzoquinoline.

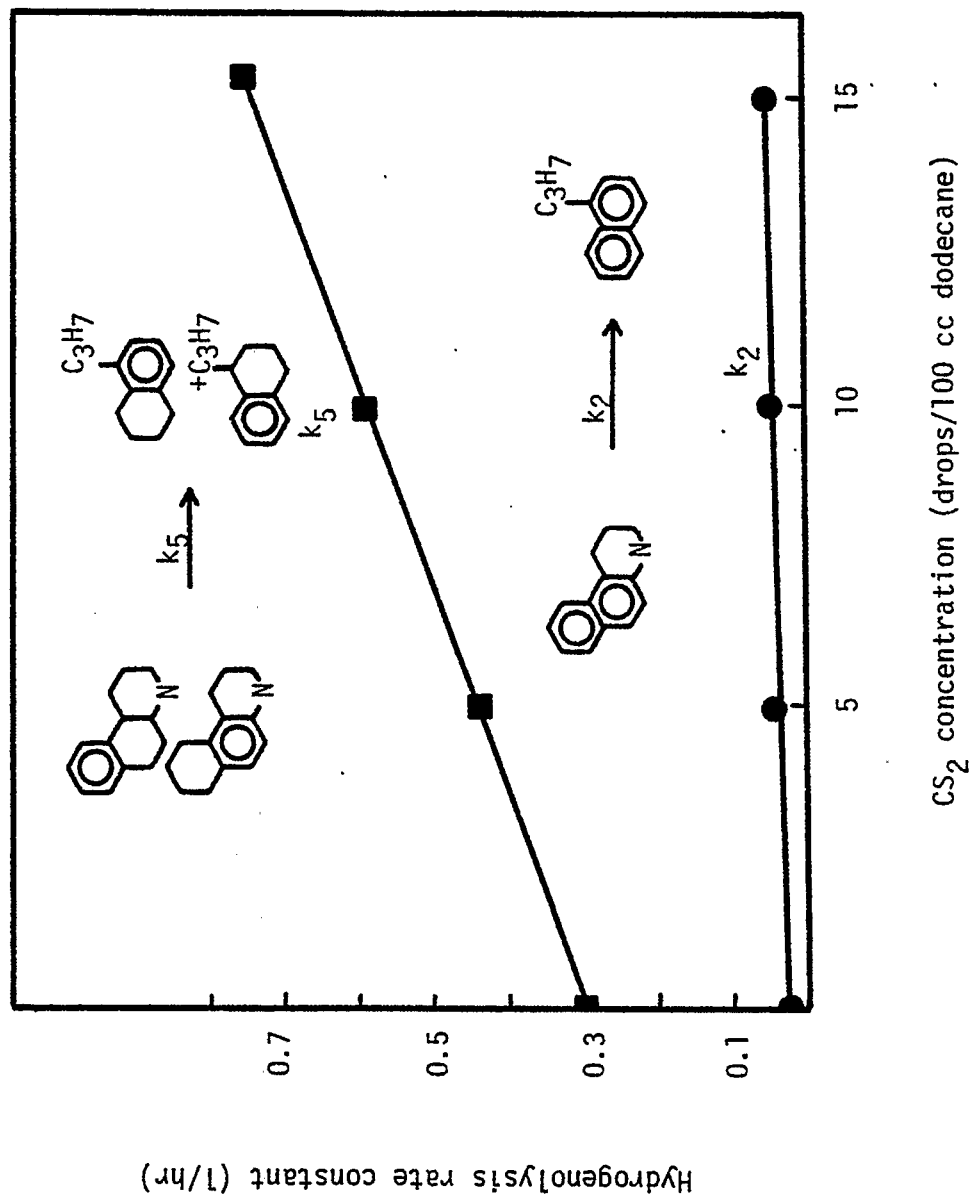


Figure 4. The hydrogenolysis activity vs. CS₂ concentration for 5,6-benzoquinoline.

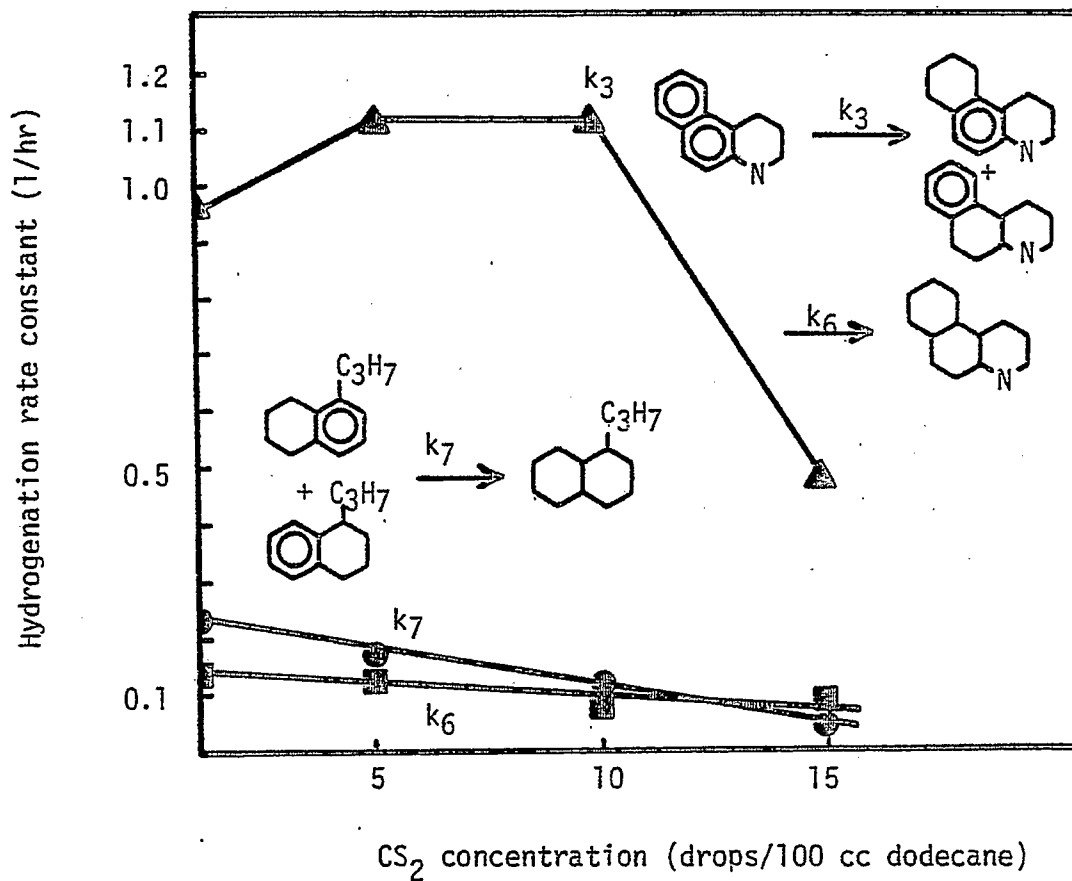


Figure 5. The hydrogenation activity vs. CS₂ concentration for 5,6-benzoquinoline.

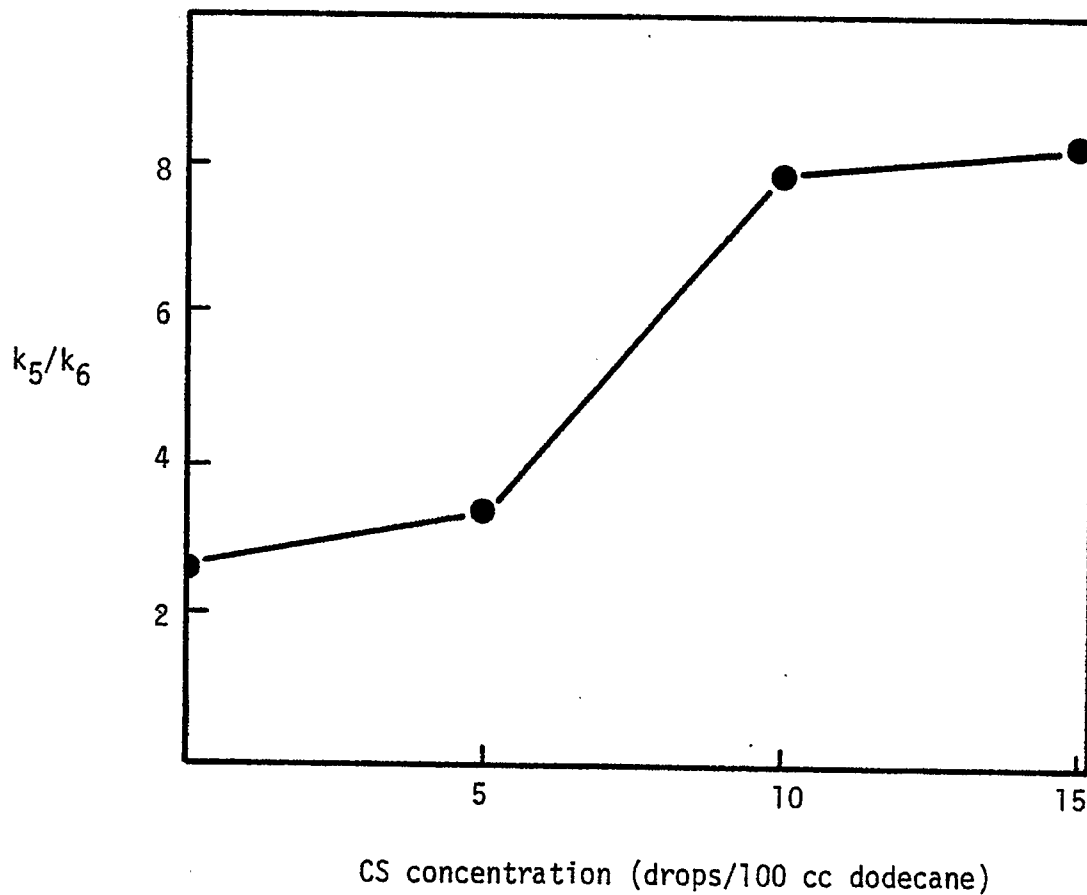


Figure 6. k_5/k_6 vs. CS_2 concentration for 5,6-benzoquinoline.

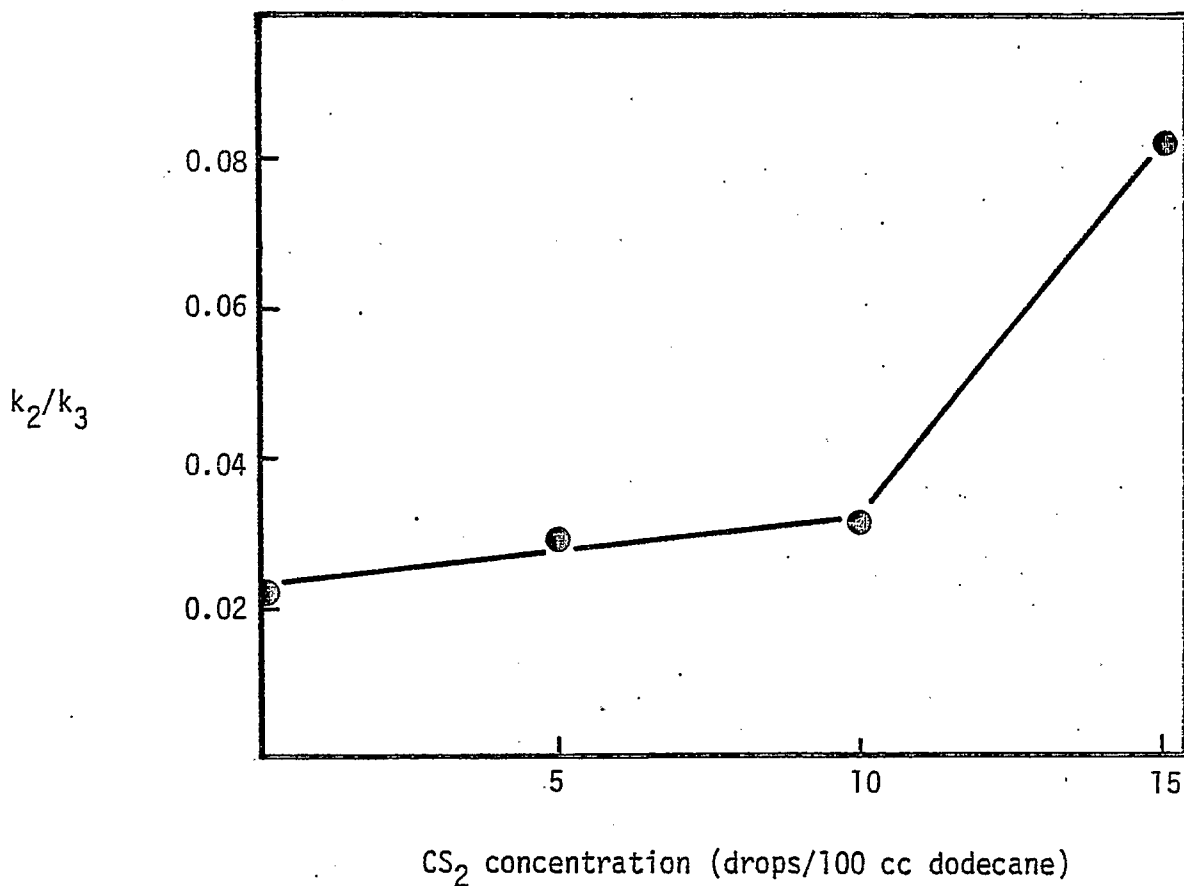


Figure 7. k_2/k_3 vs. CS_2 concentration for 5,6-benzoquinoline.

Task 7

Catalytic Hydrodeoxygenation of Coal-Derived Liquids and Related Oxygen-Containing Model Compounds

Faculty Advisor: J. Shabtai
Graduate Student: Y. Shukla

Introduction

Coal-derived liquids are characterized by the presence of a considerable concentration of oxygen-containing components. Therefore, a systematic catalytic hydrodeoxygenation (HDO) study of coal-derived liquids and related model compounds is being carried out. This study provides information not only on the mechanism of HDO as related to the subject of catalytic upgrading of coal-derived liquids, but also on the role of oxygen-containing compounds in primary coal liquefaction processes.

Project Status

The catalytic HDO reactions of three representative aryl and aryl-alkyl ether, i.e., dibenzyl ether, diphenyl ether, anisole and two furans, i.e., 2,3-benzofuran and dibenzofuran, are presently being investigated. Results obtained with diphenyl ether (6) as feed are presented in this report. The change in product composition as a function of experimental conditions, e.g., reaction temperature, hydrogen pressure and catalyst types, is being studied. The experiments were performed in a shaken autoclave reactor.¹ The products obtained were identified and quantitatively analyzed by gas chromatography and mass spectrometry.

The reactions of 6 in the presence of sulfided Co-Mo/ γ -Al₂O₃ and Ni-Mo/ γ -Al₂O₃ catalysts were first investigated as a function of reaction temperature in the range of 170 - 320°C, keeping all other experimental conditions constant.² The results obtained with sulfided Co-Mo/ γ -Al₂O₃ and Ni-Mo/ γ -Al₂O₃ are summarized in Figures 1 and 2, respectively. As seen in Figure 1, the conversion of 6 increases rapidly between 200 - 290°C (from 1.20% at 200°C to 79.2% at 290°C) and then moderately from 290°C to 320°C. At lower temperatures cyclohexylphenylether (39) is the main intermediate which upon cleavage of the C-O bond forms phenol (5) and cyclohexane (2). In the middle temperature range, an intermediate of M.W. 92 and benzene (3) are formed. At higher temperatures phenol (5) and benzene (3) are formed. Traces of methylcyclopentane (1), cyclohexyl benzene (8), cyclohexyl phenols (10) and dicyclohexyl phenols (13) are also formed.

Different compositions are observed with the sulfided Ni-Mo/ γ -Al₂O₃ catalyst (Figure 2). As seen with this catalyst, cyclohexane (2) is the main product at lower temperatures, which could have been formed from cyclohexyl phenyl ether or bicyclohexyl ether. At lower temperatures phenol (5) hydrogenation forms cyclohexane (2), while at higher temperatures, where hydrogenation-dehydrogenation equilibrium favors dehydrogenation, (C-O) bond cleavage forms benzene (3). Small amounts of cyclohexene (22) methyl cyclopentane (1), cyclohexyl phenol (10), dicyclohexyl phenols and cyclohexyl diphenyl ether (12) are also formed.

The reactions of 6 in the presence of the sulfided Co-Mo/ γ -Al₂O₃ and Ni-Mo/ γ -Al₂O₃ catalysts were also investigated as a function of hydrogen pressure in the range of 250 - 1500 psig (total reaction time, 0.5 hr; amount of reactant, 5.0 g; amount of catalyst, 1.0 g; reaction temperature with sulfided Co-Mo catalyst, 260°C and with sulfided Ni-Mo catalyst, 320°C). Results obtained are summarized in Figures 3 and 4, respectively.

As seen in Figure 3, with the sulfided Co-Mo catalyst, the concentration of benzene (3) first slowly decreases as pressure increases, but the concentration of phenol (5) remains constant. At higher pressures (1250 - 1500 psig) the concentration of phenol (5) decreases while the concentration of benzene (3) increases. Small amounts of methylcyclopentane (1), cyclohexane (2), cyclohexyl benzene (8), cyclohexyl phenols, dicyclohexyl phenols and cyclohexyl phenyl ether are also formed.

As seen in Figure 4, with sulfided Ni-Mo, the concentration of benzene (3) slowly decreases as pressure increases, but the concentration of cyclohexane (2) increases. At higher pressures the concentration of benzene (3) again increases while the concentration of cyclohexane (2) remains constant. The concentration of phenol (5) slowly decreases through out the pressure range. Small amounts of methyl cyclopentane (1), cyclohexyl phenol and cyclohexyl phenyl ether are also formed.

The change in product composition as a function of reaction temperature, hydrogen pressure and catalyst type can be rationalized in terms of the mechanism proposed in Figure 5. With sulfided Co-Mo, at lower temperatures one of the rings hydrogenates and forms cyclohexyl phenyl ether (39) from which (C-O) hydrogenolysis yields phenol (5) and cyclohexane (2). In the middle temperature ranges an intermediate of M.W. 92 and benzene is formed. This intermediate of M.W. 92 is very reactive and its molecular structure is now being determined. At higher temperatures the reaction path A is favored where cleavage of the (C-O) bond forms phenol and benzene.

With sulfided Ni-Mo, cyclohexane is the main product at lower temperatures, which could have been formed from cyclohexyl phenyl ether or bicyclohexyl ether. (These could have been formed by hydrogenation of either one benzene ring or both benzene rings.) At lower temperatures phenol (5) hydrogenation could form cyclohexane while at higher temperatures the hydrogenation-dehydrogenation equilibrium that favors dehydrogenation yields benzene.

Future Work

Kinetic studies of dibenzyl ether, diphenyl ether and dibenzofuran with both commercial catalysts and catalysts synthesized in this laboratory are in progress.

References

1. G. Haider, Ph.D. Thesis, University of Utah, Salt Lake City, Utah, 1981.
2. W.H. Wiser et al., DOE Contract No. DE-AC01-79ET14700, Quarterly Progress Report, Salt Lake City, Utah, Oct - Dec 1981.

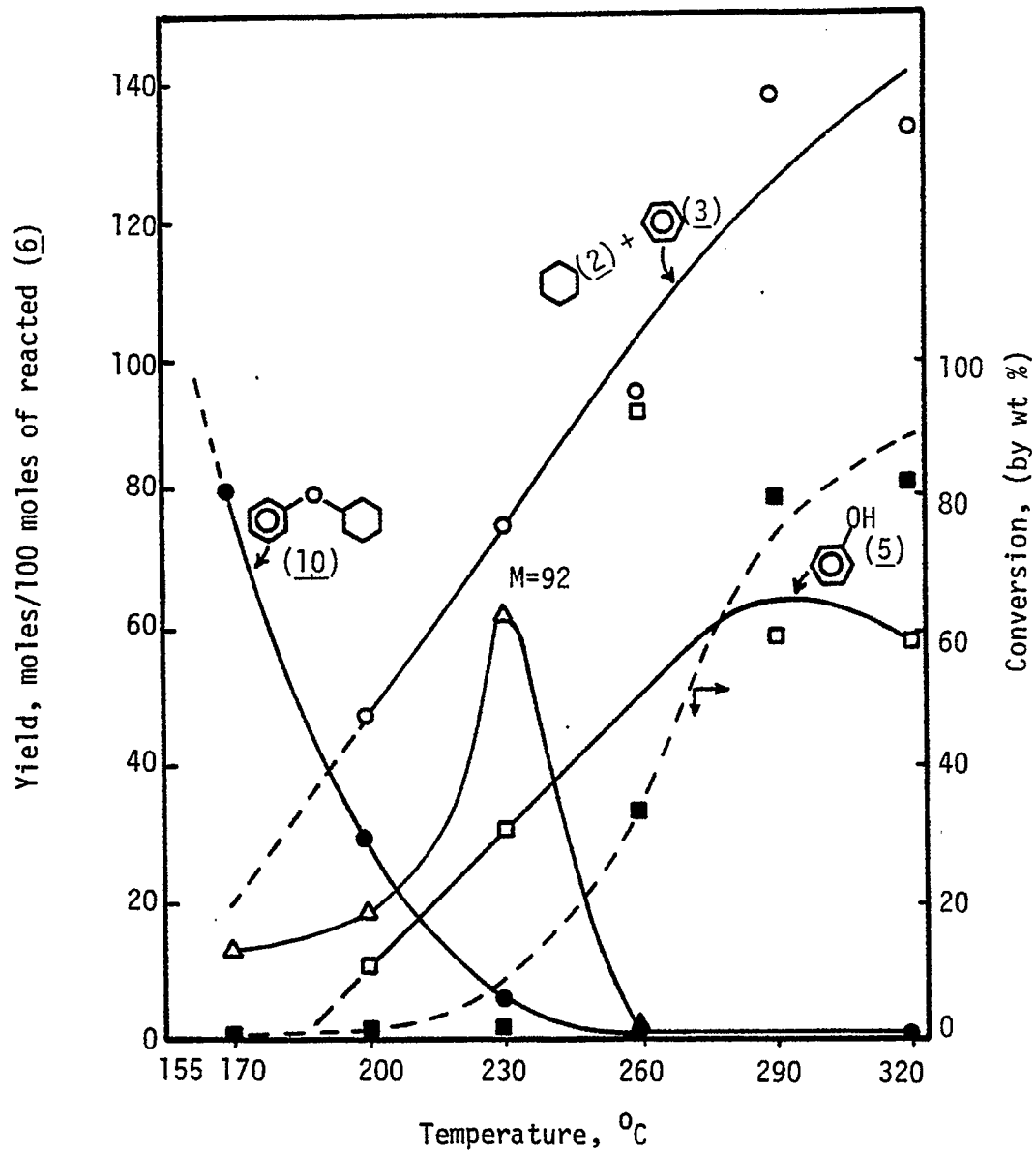


Figure 1. Change in product composition from hydrodeoxygenation of diphenyl ether, (6), c1ccc(Oc2ccccc2)cc1 as a function of reaction temperature. Catalyst, sulfided Co-Mo/ γ -Al₂O₃ (Nalco #471); hydrogen pressure, 1000 psig; total reaction time, 0.5 hr.

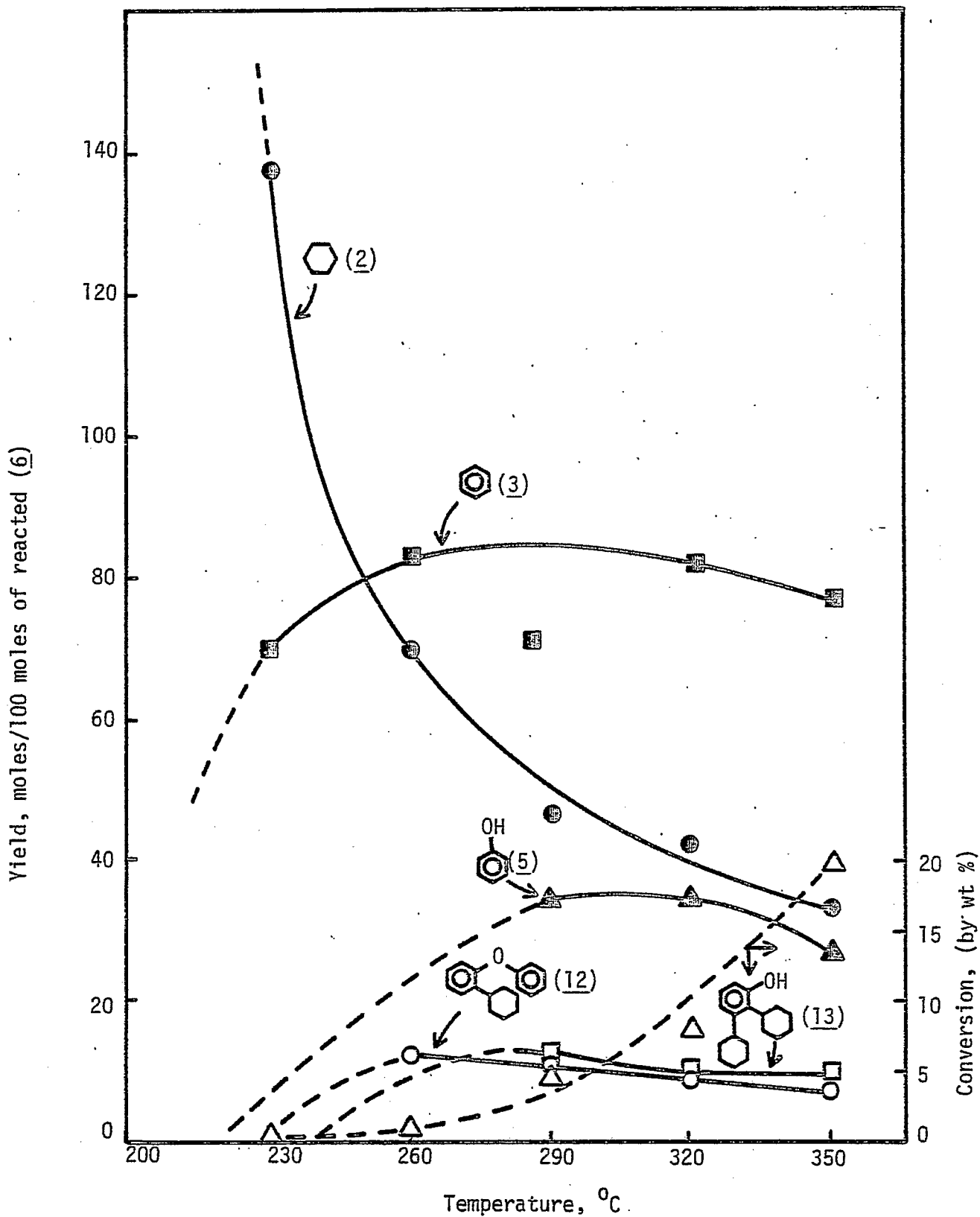


Figure 2. Change in product composition from hydrodeoxygenation of diphenyl ether, (6) c1ccc(cc1)-c2ccccc2 as a function of reaction temperature. Catalyst, sulfided Ni-Mo/ γ -Al₂O₃ (Nalco #504); hydrogen pressure, 1000 psig; total reaction time, 0.5 hr.

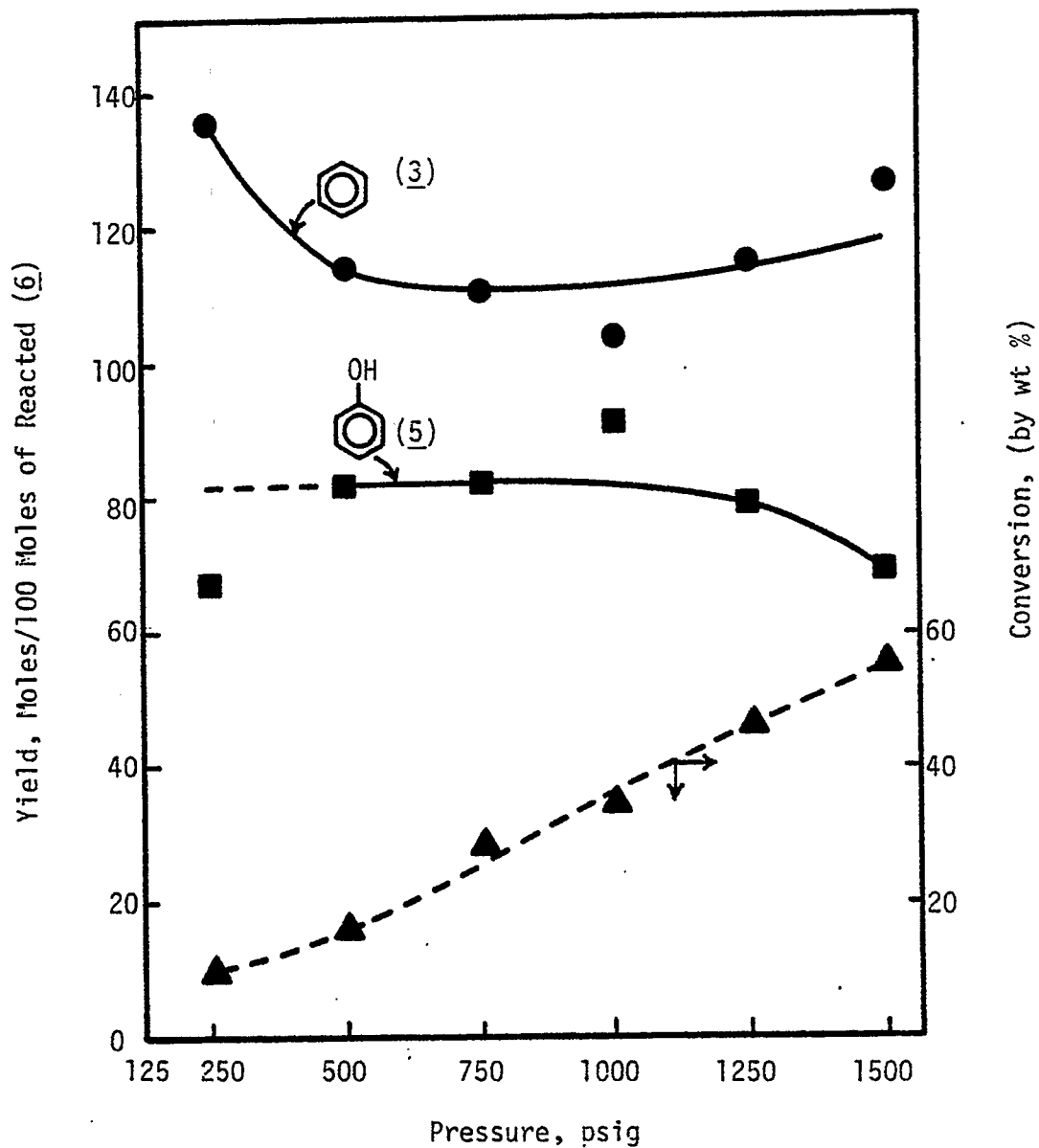


Figure 3. Change in product composition from hydrodeoxygenation of diphenyl ether (5) c1ccc(cc1)-c2ccccc2 as a function of hydrogen pressure. Catalyst, sulfided Co-Mo/ γ -Al₂O₃ (Nalco #471); reaction temperature, 260°C; total reaction time, 0.5 hr.

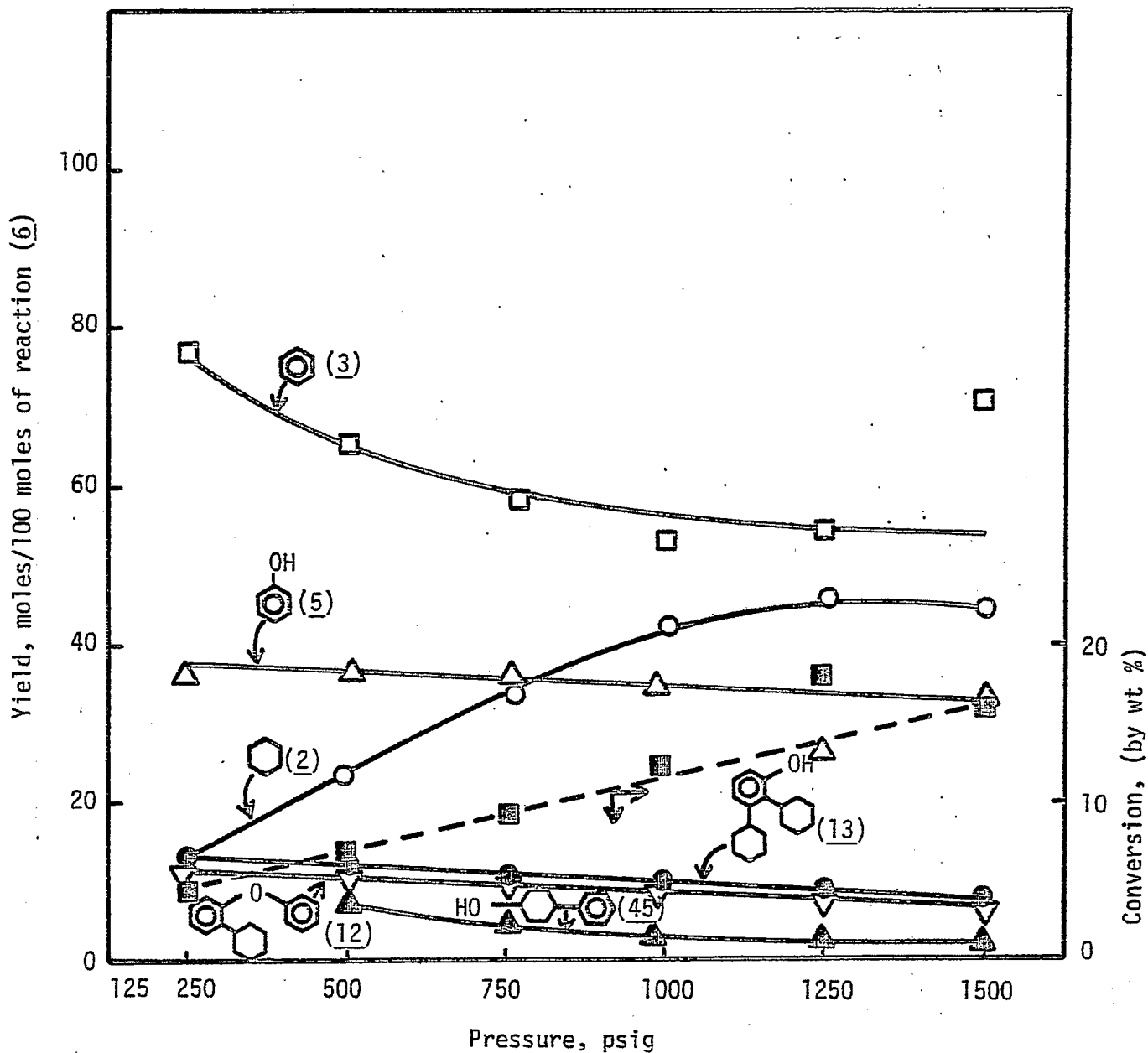


Figure 4. Change in product composition from hydrodeoxygenation of diphenyl ether (6) c1ccc(cc1)-c2ccccc2 as a function of hydrogen pressure. Catalyst sulfided Ni-Mo/ γ -Al₂O₃ (Nalco #504); reaction temperature, 320°C; total reaction time, 0.5 hr.

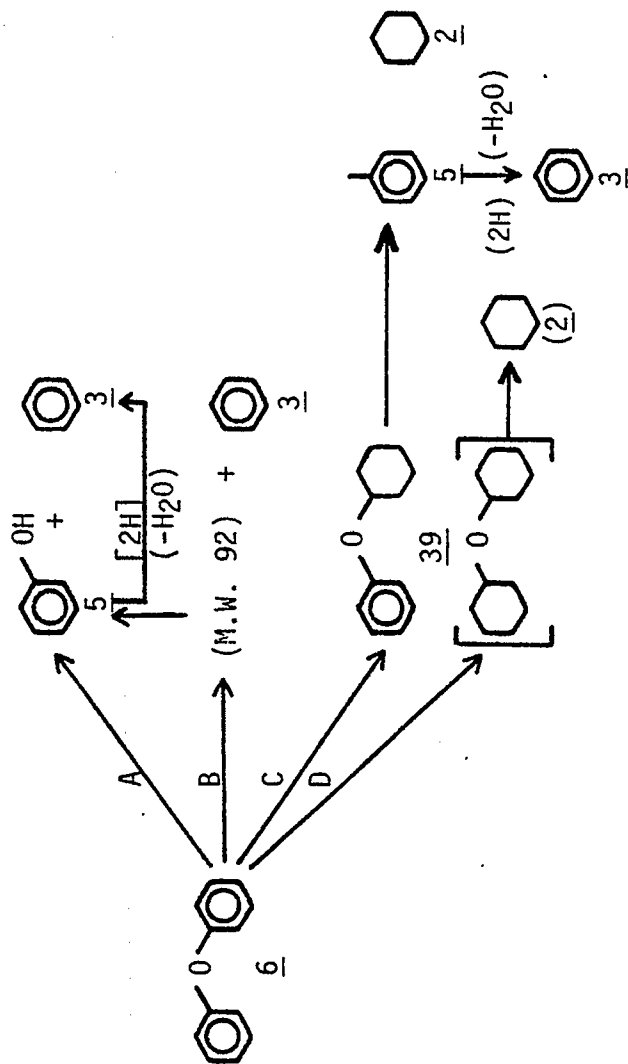


Figure 5. Indicated pathways in the H₂O reaction of diphenyl ether (6) in the presence of sulfided catalysts.

Reaction path A&B: favored at higher temperature with Co-Mo/ γ -Al₂O₃.

Reaction path C: favored at lower temperature with Co-Mo/ γ -Al₂O₃ and Ni-Mo/ γ -Al₂O₃.

Reaction path D: favored with Ni-Mo/ γ -Al₂O₃.

Task 8

Catalytic Cracking of Hydrogenated Coal-Derived Liquids and Related Compounds

Faculty Advisor: J. Shabtai
A.G. Oblad
Graduate Student: John McCauley

Introduction

Hydrogenation followed by catalytic cracking provides a feasible process sequence for conversion of coal liquids into conventional fuels. Such a sequence has certain advantages in comparison with a hydrocracking-catalytic reforming scheme.

The present project is concerned with the following interrelated subjects: (1) systematic catalytic cracking studies of polycyclic naphthenes and naphthenoaromatics found in hydrogenated coal liquids and (2) systematic catalytic cracking studies of hydrotreated coal-derived liquids.

Project Status

The systematic catalytic cracking studies, using newly synthesized cross-linked smectite (CLS) molecular sieves are being completed and results obtained are being summarized in the framework of the thesis of the Mr. John McCauley. A copy of the thesis will be submitted to the sponsor upon its completion.

Future Work

The thesis work of Mr. John McCauley on the above indicated subject will be completed.

References

1. J. Shabtai, U.S. Patent 4,238,364 (1980).
2. J. Shabtai, R. Lazar and A.G. Oblad, Proc. 7th International Congress on Catalysis, Tokyo, Japan, 1980, pp 828-840.

Task 9

Hydropyrolysis (Thermal Hydrocracking) of CD Liquids

Faculty Advisors: J. S. Shabtai
A. G. Oblad
Graduate Student: J. Williams

Introduction

This project is concerned with a systematic investigation of hydro-pyrolysis (thermal hydrocracking) as an alternative processing concept for upgrading of heavy coal-derived liquids (CDL) into light liquid products. The high efficiency and versatility of hydro-pyrolysis has been indicated in previous studies with heavy CDL feedstocks and with model compounds.¹⁻³ The present project is an extension of this previous work for the purpose of (a) further developing and enlarging the scope of the hydro-pyrolytic process, and (b) optimizing the operating conditions for different types of feedstocks, e.g., coal liquids from different liquefaction processes, partially hydrotreated coal liquids, and relevant model compounds. The project includes systematic studies of reaction kinetics, product composition, and coking tendencies, as a function of operating variables. The work with model compounds provides necessary data for further elucidation of mechanistic aspects of the hydro-pyrolysis process.

Project Status

Systematic studies of thermal hydrocracking reactions have been undertaken using as model compounds diaryl, diaralkyl and arylalkyl ethers, e.g., diphenyl ether, dibenzyl ether and anisole. Process variables investigated include reaction temperature and contact time. Results obtained indicate that in the temperature range of 400° to 550°C diaryl ethers have a much higher resistance to cleavage than diaralkyl ethers with arylalkyl ethers being somewhat in between. Further studies for the elucidation of reaction mechanisms are in progress.

The above studies allow for examination of the feasibility of upgrading (viz., deoxygenation and molecular weight reduction) of coal-derived liquids by a combination of mild hydrotreatment and subsequent hydro-pyrolysis.

Future Work

The potential for the use of gas phase catalysts such as hydrogen chloride and hydrogen sulfide will be explored.

References

1. J. Shabtai, R. Ramakrishnan and A.G. Oblad, *Advances in Chemistry*, No. 183, Thermal Hydrocarbon Chemistry, Amer. Chem. Soc., 1979, pp 297-328.
2. R. Ramakrishnan, Ph.D. Thesis, University of Utah, Salt Lake City, Utah, 1978.

3. A.G. Oblad, J. Shabtai and R. Ramakrishnan, U.S. Patent 4,298,457 (1981).

Task 10

Systematic Structural Activity Study of Supported Sulfided Catalysts for Coal Liquids Upgrading

Faculty Advisors: F.E. Massoth
J. Shabtai
Post-Doctoral Fellow: N.K. Nag
Graduate Student: K. Baluswamy

Introduction

The objective of this research is to develop an insight into the basic properties of supported sulfide catalysts and to determine how these relate to coal liquids upgrading. The proposed program involves a fundamental study of the relationship between the surface-structural properties of various supported sulfide catalysts and their catalytic activities for various types of reactions. Thus, there are two clearly defined and closely related areas of investigation, viz., (1) catalyst characterization, especially of the sulfided and reaction states and (2) elucidation of the mode of interaction between catalyst surfaces and organic substrates of different types. The study of subject (1) will provide basic data on sulfided catalyst structure and functionality, and would allow the development of catalyst surface models. Subject (2), on the other hand, involves systematic studies of model reactions on sulfide catalysts, and the utilization of data obtained for development of molecular level surface reaction models correlating the geometry (and topography) of catalyst surfaces with the steric conformational structure of adsorbed organic reactants. The overall objective of the project is to provide fundamental data needed for design of specific and more effective catalysts for upgrading of coal liquids.

Atmospheric activity tests using model compounds representative of hydrodesulfurization (thiophene), hydrogenation (hexene) and cracking (isooctene) were employed to assay changes in the catalytic functions of various supported CoMo catalysts. It was found that hydrodesulfurization (HDS) and hydrogenation (HYD) activities were generally unaffected by the type of alumina used or by the cobalt salt used in the preparation; whereas, cracking (CKG) activity varied considerably. Increase in Co or Ni content at a fixed Mo content of 8% resulted in considerably higher promotion of HDS activity than HYD activity. Addition of additives at 1/2% level to the standard CoMo/Al₂O₃ catalyst generally increased HDS and CKG for acidic additives and decreased these functions for basic additives, HYD being unaffected. At 5% level, the additives decreased all functions, basic additives decreasing activities more severely. In a series of catalysts employing silica-alumina as the support, the HDS and hydrogenation functions decreased with increasing silica content, while cracking went through a maximum in activity. Catalysts prepared by supporting CoMo on TiO₂, SiO₂·MgO and carbon showed low activities, except for high cracking activity for the two former catalysts.

Oxide precursors of CoMo and Mo catalysts supported on various silica-aluminas evaluated by ESCA showed that support-active component interaction decreased with increase of silica in the support. It was also found that cobalt did not influence the Mo dispersion. On alumina, the Mo phase was found to be dispersed in essentially a monoatomic form.

Several catalysts, which were evaluated in the atmospheric pressure test unit, were subsequently tested at elevated pressure (34 atm) using dibenzothiophene (HDS), naphthalene (HYD) and indole (HDN). The high pressure runs were carried out sequentially in the order indicated to assess the separate catalytic functionalities. Repeat runs of HDS and HYD after HDN gave appreciably lower activities for HDS and HYD which was found to be due to strongly adsorbed residues containing nitrogen. The effect of increasing H₂S was to appreciably decrease HDS, moderately decrease HYD, and moderately increase HDN conversions.

Comparison of high pressure results for HDS of dibenzothiophene and HYD of naphthalene with atmospheric results for HDS of thiophene and HYD of hexene carried out in the same reactor showed good correlations, signifying that the low pressure tests reasonably reflect catalytic activity under high pressure test conditions, at least for the model compounds used.

The sulfided catalysts, depending on their compositions, showed that the hydrogenation of naphthalene and tetralin is stereospecific. Detailed investigation with multiring aromatic and N-heterocyclic compounds are expected to provide insight into the nature and geometry of the active sites for the hydrogenation reactions that occur under hydroprocessing conditions.

Project Status

The studies on the stereospecific hydrogenation of naphthalene to decalins have been extended to the quinolines on sulfided CoMo/Al, NiMo/Al and Ni-W/Al hydroprocessing catalysts under high H₂ pressure (2300 psig). The same experimental procedure as reported in the previous report was used for every run, unless otherwise specified. The results are given in Tables 1-3.

In contrast to the hydrogenation results of naphthalene and tetralin to decalins,¹ the present works on quinolines show that the stereospecific hydrogenation of the latter is less susceptible to the catalyst composition (see Table 1). This immediately leads one to appreciate the involvement and importance of the N-atom in these reactions. While MoS₂ or Mo/Al catalyst have comparable activity and selectivity with promoted catalysts, Ni or Co/Al catalyst have much lower activity for all the hydrogenation reactions.

From Table 3 it is observed that the course of hydrogenation (i.e., the selectivity towards various partially hydrogenated products included the DHQ's) varies widely depending on the position(s) of the substituent(s).

The dramatic effect of H₂S on the product distribution and the relative ease of trans- or cis-addition is depicted in Table 2. It

appears that the sites responsible for the trans-addition are preferentially poisoned by H₂S. Moreover, HDN is greatly enhanced by H₂S. From the present results the following conclusions are derived:




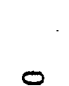

- (1) Catalyst composition has only minor effect on the stereospecific hydrogenation of quinolines. This is contrary to the naphthalene hydrogenation results.¹
- (2) Substituents on both the benzenoid and pyridinoid rings and H₂S in the reacting system lead to dramatic change in the stereospecific hydrogenation of these compounds.

References

1. W.H. Wiser et al., DOE Contract No. DE-AC01-79ET14700, Quarterly Progress Report, Salt Lake City, Utah, Jan - Mar 1983.

Table 1

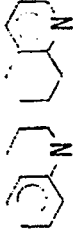

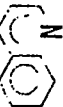

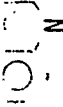
Experiments with quinoline and tetrahydroquinolines on various catalysts^a

Run No.	Feed	Catalyst ^b (Sulfided)	Conversion, %	Selectivity (%) to:					
							trans	cis	Hydro-carbons + others
21		CoMo/Al (6:8)	~ 100	87	1	10	2	0.5	5.8:1
31		NiMo/Al (6:8)	~ 99.5	70	1	24	4.5	0.5	5.1:1
43		NiW/Al (6:16)	99	70.5	4	22	4	Trace	5.5:1
37		Mo/Al (8)	95	-	-	77	16	7	5.5:1
57		MoS ₂ (Bu1k)	51	-	-	82	18	-	4.6:1
35		Co/Al (6)	32.5	-	-	76.5	23.5	-	3.4:1
36		Ni/Al (6)	20.5	-	-	77	23	-	3.4:1

^a 1 wt % of reactant in n-heptane, 300°C, 164 atm H₂, 2.5 h.^b Numbers are wt % supported on Al₂O₃.

Table 2

Experiments with quinoline and 5,6,7,8-tetrahydroquinoline in presence of H₂S with various catalysts^a

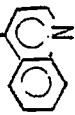



Run No.	Feed	Catalyst ^b (Sulfided)	Conversion, %	Selectivity (%) to				Remarks		
						trans N H	cis		Hydro- carbons + others	trans cis
26		NiW/Al	99	89	4	5.2	1.3	< 0.5	4.1:1	Very little H ₂ S added
59		CoMo/Al	98	87	11	1	0.5	0.5	3.5:1	Very little H ₂ S added
60		CoMo/Al	80	-	-	25	15.5	59.5	1.4:1	Large excess of H ₂ S

^a1 wt % of reactant in n-heptane, 300°C, 164 atm H₂, 2.5 h.

^bNumbers are wt % supported on Al₂O₃.

Table 3

Experiments with methyl - quinolines^a

Run No.	Feed	Catalyst ^b (Sulfided)	Conversion, %	Selectivity (%) to					Hydro-carbons + others	$\frac{\text{trans}}{\text{cis}}$
				1,2,3,4-THQ ^c	5,6,7,8-DHQ ^c	Trans DHQ ^c	cis DHQ ^c			
45		NiMo/Al (6:8)	98	0	34	52	8.2	6	6.3:1	
46		NiMo/Al (6:8)	100	30	2	53	4.5	9	12:1	
62		NiMo/Al (6:8)	98	56.5	1.3	27	6.3	8.5	4.3:1	
63		NiMo/Al (6:8)	99.5	43.5	0.3	36.5	11.5	8.5	3.2:1	

^a 1 wt 5 of reactant in n-heptane, 300°C, 164 atm H₂, 2.5 hr.^b Numbers are wt % supported on Al₂O₃.^c Corresponding methyl or dimethyl derivative of the feed.

Task 11

Basic Study of the Effects of Poisons on the Activity of Upgrading Catalysts

Faculty Advisor: F.E. Massoth
Post-Doctoral Fellow: J. Miciukiewicz

Introduction

The importance of cobalt-molybdena catalysts for hydrotreating and hydrodesulfurization of petroleum feedstocks is well-known. These catalysts are also being studied for hydrodesulfurization and liquefaction of coal slurries and coal-derived liquids. However, such complex feedstocks result in rapid deactivation of the catalysts. To gain an insight into the deactivation mechanism, the detailed kinetics of reactions of model compounds representative of heteroatom hydrogenolysis and hydrogenation are compared before and after addition of various poisons and coke precursors. The studies are carried out using a constant stirred microbalance reactor, which enables simultaneous measurement of catalyst weight change and activity. Supplementary studies are made to gain additional insight into the effect of poisons on the active catalyst sites. Finally, catalysts aged in an actual coal pilot plant run are studied to compare with laboratory studies.

Previous work on this project has shown that catalyst poisoning by pyridine or coke results in loss of active sites for benzothiophene HDS, but that the remaining unpoisoned sites retain their original activity. Pyridine appeared to be site selective in poisoning effect whereas coke was nonspecific. Furthermore, at least two HDS sites were indicated from the pyridine poisoning studies.

Poisoning of a commercial CoMo/Al₂O₃ catalyst by several nitrogen containing compounds gave the following order of deactivation of hexene hydrogenation (HYD): quinoline > pyridine = 3,5-lutidine > indole > aniline. Thiophene hydrodesulfurization (HDS) was deactivated more than hexene hydrogenation, but was less sensitive to the type of poison adsorbed. Poisoning with 2,6-lutidine gave opposite results, hydrogenation being deactivated more than HDS, showing that steric and inductive effects are important in the effect of specific poisons on catalyst deactivation. Adsorption of 2,6-lutidine at low concentrations resulted in an increase in HDS activity rather than the decrease expected, while at the same time hexene HYD decreased. However, this effect was considerably less pronounced for a laboratory-prepared CoMo catalyst using a pure γ -Al₂O₃ support.

Project Status

Kinetic studies were completed for reactions of thiophene and of isooctene (2,4,4-trimethylpentene-1) on commercial aged catalysts which had been used in an H-coal process run (PDU-9). The samples were obtained from Sandia Laboratories. One sample had been exposed to start-up recycle oil only for one day and the other to two days on recycle oil plus one day on coal. The former catalyst contained about 12% coke and 0.8% metals (mostly Ti and Fe), while the latter contained about 14% coke and 1.3% metals. In addition, kinetic runs were made on the aged catalysts after subjecting them to a coke burnoff at 500°C.

The aged catalysts represent samples taken early in the PDU-9 run, which lasted 30 days. They were chosen because they showed significant activity decline in other tests,¹ and thus their study should reveal causes of early catalyst deactivation in the H-coal process. Samples taken later in the PDU run had such low residual activity that their study would have been difficult because of low conversions.

The apparatus, procedure and data analyses were described in the last quarterly progress report. All runs were carried out in a stirred-tank reactor at 350°C and atmospheric pressure, using one-half gram of catalyst. Reactants were introduced into the reactor by saturation bubblers at 0°C with a H₂ flow. Auxillary H₂ and H₂S flows were added to change partial pressures of the feeds, maintaining a total flow of 100 cm³/min. The data were analyzed by nonlinear least squares analysis to obtain parameters from the generalized rate expression,

$$r_i = \frac{k_i p_i p_H}{(1 + K_i p_i + K_S p_S)^n} \quad (1)$$

where r is the measured reaction rate, k the global rate constant, p the partial pressure and K the adsorption constant, subscript i referring to reactant, H to hydrogen, and S to H₂S; n is a constant, either 1 or 2.

The kinetic parameters obtained for reaction of thiophene with the various catalysts are given in Table 1. The primary reaction of thiophene is HDS to give n-butenes, with subsequent partial hydrogenation (HYD) of the butenes to n-butane. Since the reaction is carried out in a stirred-tank reactor, the rates of HDS and HYD can be individually determined and separately analyzed. It was found that better fits were obtained for $n=2$ in Equation (1) for HDS. For n-butene HYD, the contributions of the K_p terms in the denominator of Equation (1) were negligible, giving a pseudo first-order reaction in n-butene concentration.

In order to compare the reactivities of the aged and regenerated catalysts, the respective parameters were normalized to the fresh catalyst basis. The results are given in Table 2. Thus, if there is no change in the parameter value between the aged or regenerated catalyst and the fresh catalyst, a value of unity within the experimental 95% confidence limits should be obtained. Inspection of Table 2 for the thiophene HDS shows that the rate constant, k_T , and the thiophene adsorption constant, K_T , both decrease in the aged catalysts and increase in the regenerated catalysts; a reverse trend is observed in the H₂S adsorption constant, K_S , although not as marked. The overall rate of HDS (not shown) was significantly lower for the aged catalysts, and somewhat higher for the regenerated catalysts, compared to the fresh catalyst. This indicates that the metals alone do not cause catalyst deactivation, but rather the coke (or perhaps coke + metals) is the cause of deactivation.

The global rate constant, k_i , in Equation (1) actually contains K_i , according to the standard derivation of this equation based on the Langmuir-Hinshellwood treatment. By dividing k_i by K_i , an intrinsic rate constant, k_i^0 , is obtained. Surprisingly, these values appear to be the same for HDS for all the catalysts. This intrinsic rate constant has in it the number of active sites and possibly a K_H term for hydrogen adsorption. Since

the aged catalysts were less reactive, it would be expected that some of the active sites would be covered by coke, giving a lower k_T^0 value. That this was not observed may be due to a compensating increase in the intrinsic reaction constant per unit active site or an increase in K_H .

A similar analysis for the butene HYD reaction accompanying the thiophene HDS reaction could not be made because of the small K values obtained (within experimental error). The relative first-order rate constants (Table 2) show significantly lower reactivity for the aged catalysts and higher activity for the regenerated catalysts. Again, it is obvious that the coke is responsible for loss in hydrogenation activity, since the metal deposits without coke present (regenerated catalysts) actually promote the HYD reaction of butenes.

Results of the isooctene runs (carried out on the same catalyst charge after the thiophene run) are given in Table 3. (Time did not permit running the oil + coal catalyst.) Isooctene reacts in two parallel paths, viz., (1) by hydrogenation to isooctane and (2) by cracking (CKG) to isobutene, which subsequently undergoes partial hydrogenation to isobutane. Isooctane does not undergo cracking under the reaction conditions employed. Kinetic analyses revealed that H_2S had a negligible effect on isooctene CKG and HYD and was eliminated from the kinetic analysis. The parameter values in Table 3 are for $n=1$ in Equation (1). Secondary isobutene HYD was best fit by a pseudo first-order reaction.

Comparisons of relative rate parameters for the isooctene runs are presented in Table 4. The aged catalyst showed a much depressed CKG activity compared to the fresh catalyst, which is reflected in the lower rate constant and adsorption constant. Undoubtedly, the coke has caused appreciable loss of active cracking sites (low k_G^0), especially in view of the promoting effect of the metals in the regenerated catalyst. These results are quite different from those obtained for HDS discussed above, and are in accordance with the view that different sites are used in HDS and cracking.²

The secondary isobutene HYD response is similar to that obtained for *n*-butene HYD from thiophene, i.e., lower reactivity for the aged catalyst and promoted activity for the regenerated catalyst. However, the isooctene HYD reaction gave a different response (Table 4). The global rate constant k_{OH} , was not significantly different between the aged or regenerated and the fresh catalyst, while the isooctene adsorption constant was lower for the aged and higher for the regenerated catalysts. Consequently, the intrinsic constant, k_{OH}^0 , actually appears to be higher for the aged catalyst and lower for the regenerated catalyst, a result difficult to understand. It should be appreciated, however, that considerably higher error was experienced in this particular analysis and the results should be considered tenuous. Nevertheless, it does seem unusual that the isooctene HYD response was so different from that of butene/isobutene HYD results.

The results of this study are interesting on several counts. First, the catalyst exposed to recycle oil for only one day before introducing coal already showed appreciable deactivation of all catalytic functions tested, especially cracking. The recycle oil used contained metals and coke precursors, as evidenced by the metal deposits and coke on the catalyst. Catalyst deactivation was caused by the coke, not the metal deposits. In fact, the metal deposits improved catalyst activity when the coke was removed (regenerated samples).

Second, deactivation of the HDS and butene HYD functions for the sample exposed to two-days recycle oil and one-day coal, was only slightly greater than the one-day recycle oil sample. This is reflected in the fact that the coke level was only marginally higher in this sample, the coke again being entirely responsible for deactivation. Apparently, the coke made from the recycle oil used is the main cause of high initial activity loss of the catalyst in this process.

Third, the regenerated catalyst results show that catalysts deactivated early in the process can be successfully reactivated. However, other studies revealed that aged samples taken later in the process run suffer the same permanent deactivation which can not be reactivated.

Future Work

1. F.E. Massoth and T.L. Cable, Final Report, University of Utah Project 5-20414, February 1983, to Sandia Laboratories (Contract 68-8584).
2. F.E. Massoth, Fourth Intern. Conf. Chemistry and Uses of Molybdenum, Golden, Colorado, August 1982, p 343.

Table 1. Kinetic parameters for thiophene runs with fresh, aged, and aged-regenerated catalysts. a,b

Catalyst:	Fresh		Oil Only		Oil + Coal	
	Aged	Regen.	Aged	Regen.	Aged	Regen.
<u>Thiophene HDS (n=2)</u>						
k_T	233 ± 12	172 ± 12	480 ± 53	150 ± 10	410 ± 39	
K_T	15.8 ± 3.3	7.6 ± 3.8	27.8 ± 8.2	11.1 ± 3.7	29.7 ± 7.4	
K_S	4.6 ± 0.7	7.0 ± 1.0	4.0 ± 1.5	6.8 ± 1.0	2.4 ± 1.2	
k_T^0	14.8 ± 3.2	22.6 ± 11.4	17.3 ± 5.4	13.5 ± 4.6	13.8 ± 3.7	
<u>n-Butene HYD (1st order)</u>						
k'_{BH}	98 ± 7	35 ± 5	151 ± 6	27 ± 4	131 ± 13	

^aDimensions are: k_T -cm³/g min atm²; K_T , K_S -atm; k_T^0 -cm³/g min atm; k'_{BH} -cm³/g min atm².

^bValues in ± are 95% confidence intervals.

Table 2. Kinetic parameters relative to fresh catalyst for thiophene runs.^a

Catalyst:	Oil Only		Oil + Coal		Effect	
	Aged	Regen.	Aged	Regen.	Aged	Regen.
<u>Thiophene HDS</u>						
RK _T	0.74 ± 0.06	2.06 ± 0.12	0.64 ± 0.08	1.76 ± 0.11	↓	↑
RK _T	0.48 ± 0.26	1.76 ± 0.64	0.70 ± 0.28	1.88 ± 0.61	↓	↑
RK _S	1.52 ± 0.32	0.87 ± 0.35	1.48 ± 0.31	0.52 ± 0.27	↑	↓
RK _T ⁰	1.53 ± 0.84	1.17 ± 0.45	0.91 ± 0.37	0.93 ± 0.34	=	=
<u>n-Butene HYD</u>						
RK _{BH}	0.36 ± 0.16	1.54 ± 0.08	0.28 ± 0.16	1.34 ± 0.12	↓	↑

^aAll values are dimensionless ratios, ± indicates 95% confidence intervals.

Table 3. Kinetic parameters for isooctene runs with fresh, aged, aged-regenerated catalysts. ^{a,b}

Catalyst:	Oil Only		
	Fresh	Aged	Regen.
<u>Isooctene CKG (n=1, K_S=0)</u>			
k _C	1070 ± 85	68 ± 16	2090 ± 146
K _{OE}	147 ± 60	50 ± 57	217 ± 65
k _C ⁰	7.3 ± 3.0	1.36 ± 1.60	9.6 ± 3.0
<u>Isooctene HYD (n=1, K_S=0)</u>			
k _{OH}	99 ± 8	89 ± 14	92 ± 7
K _{OE}	111 ± 57	29 ± 33	213 ± 67
k _{OH} ⁰	0.90 ± 0.40	3.1 ± 3.7	0.43 ± 0.14
<u>i-Butene HYD (1st order)</u>			
k _{iBE} ¹	155 ± 25	76 ± 15	201 ± 38

^aDimensions are: k_C, k_{OH}, k_{iBE}¹-cm³/g min atm²; K_{OE}-atm; k_C⁰, k_{OH}⁰-cm³/g min atm.

^bValues in ± are 95% confidence intervals.

Table 4. Kinetic parameters relative to fresh catalyst for isooctene runs.^a

Catalyst:	Oil Only		Effect	
	Aged	Regen.	Aged	Regen.
<u>Isooctene CKG</u>				
Rk _C	0.06 ± 0.02	1.95 ± 0.21	↓	↑
Rk _{OE}	0.34 ± 0.41	1.48 ± 0.75	↓	= (?)
Rk _C ⁰	0.19 ± 0.23	1.32 ± 0.68	↓	↑
<u>Isooctene HYD</u>				
Rk _{OH}	0.90 ± 0.16	0.93 ± 0.11	=	=
Rk _{OE}	0.30 ± 0.39	1.92 ± 1.16	↓	↑(?)
Rk _{OH} ⁰	3.48 ± 4.49	0.49 ± 0.29	?	↓
<u>i-Butene HYD</u>				
Rk _{iBH}	0.49 ± 0.12	1.32 ± 0.32	↓	↑

^a All values are dimensionless ratios, ± indicates 95% confidence intervals.

Task 13

Catalyst Research and Development

Hydrogenation of Carbon Monoxide Over Raney Fe-Mn Catalyst

Faculty Advisor: F.V. Hanson
Graduate Student: K.R. Chen

Introduction

The objectives of this project are to determine the kinetics of the caustic leaching of alumina from iron-aluminum alloys and to determine the optimum process operating conditions for the production of low molecular weight olefins from hydrogen and carbon monoxide over Raney iron-manganese catalysts.

A single phase Al-Fe (53/47, wt %) alloy was prepared for the leaching kinetics study. The leaching conditions were: leaching temperature 303-353 K, alloy granule particle size 30-325 mesh, 5% NaOH and alloy sample size 5 g. The volumetric flow rate of the hydrogen evolved was determined with a wet test meter.

A Raney iron-manganese catalyst, prepared from an Al-Fe-Mn (59/138.3, 363 K leaching) alloy, was used to evaluate the activity and selectivity of the catalyst. Catalyst loading and stability tests were conducted prior to the process variable study.

Project Status

The results of leaching kinetics, loading and stability tests were discussed in the previous report. A schematic of the process variable study apparatus is presented in Figure 1. The operating conditions and the data are presented in Table 1. The coefficients and reduced coefficients of the product selectivities are presented in Tables 2 and 3. In Table 3, the C₂-C₄ O/P ratio is expressed as a response equation:

$$Y_1 = 3.407 - 2.43X_1 + 0.319X_2 - 0.884X_4 + 0.026X_1^2 + 0.003X_2^2 + 0.111X_4^2 + 0.164X_1X_4 - 0.223X_2X_4$$

where

Y_1 = C₂-C₄ O/P ratio response factor

X_1 = Pressure

X_2 = Temperature

X_4 = H₂/CO ratio.

From this equation, the C₂-C₄ O/P ratio under the operating ranges can be predicted.

In Figure 2, the C₂-C₄ O/P ratio decreases from 3.77 at 1378 kpa to 2.74 at 4134 kpa. In the equilibrium equation $C_nH_{2n} + H_2 \rightleftharpoons C_nH_{2n+2}$, the olefinic products are favored at the lower pressure. The experimental results follow the stoichiometric prediction. In Figure 3, the temperature effect on the product selectivity on the C₂-C₄ O/P ratio is presented. The O/P ratio increases as the temperature increases, from 2.75 at 443 K to 3.70 at 483 K. The CO₂ selectivity increases as the temperature increases. In Figure 4, the C₂-C₄ O/P ratio remains constant from a space velocity of 3 to a space velocity of 15. The space velocity effect was eliminated in the response equation of the C₂-C₄ O/P ratio. In Figure 5, the C₂-C₄ O/P ratio is very sensitive to the H₂/CO ratio. The C₂-C₄ O/P ratio increases from 1.58 at the H₂/CO ratio of 5 to 5.61 at the H₂/CO ratio of 0.2. The combined effects of the H₂/CO ratio and temperature and of the H₂/CO ratio and pressure were observed. In Table 3, B₁₄ is equal to 0.164 and B₂₄ is equal to -0.223.

As discussed, a lower H₂/CO ratio, higher temperature and lower pressure may produce a higher C₂-C₄ O/P ratio. To avoid carbon deposits on the catalyst, the H₂/CO ratio was limited to 0.5 in the optimal experiment. The calculated optimal operating conditions and their predicted O/P ratio value were 1378 kpa, 473 K, space velocity of 12, H₂/CO ratio of 0.5 and C₂-C₄ O/P value of 5.4. After the test run, the result was a C₂-C₄ value of 6.4, higher than expected.

Future Work

The Raney iron-manganese catalyst in the slurry bed reactor system will be used to optimize the C₂-C₄ olefinic products.

- A: CO Supply
- B: H₂ Supply
- C: Helium Supply
- D: Valve
- E: Pressure Gauge
- F: Mass Flow Meter
- G: Reactor
- H: High Temperature Furnace
- I: Heating Tape
- J: Glove Loader
- K: Liquid Collector
- L: Wet-Test Meter

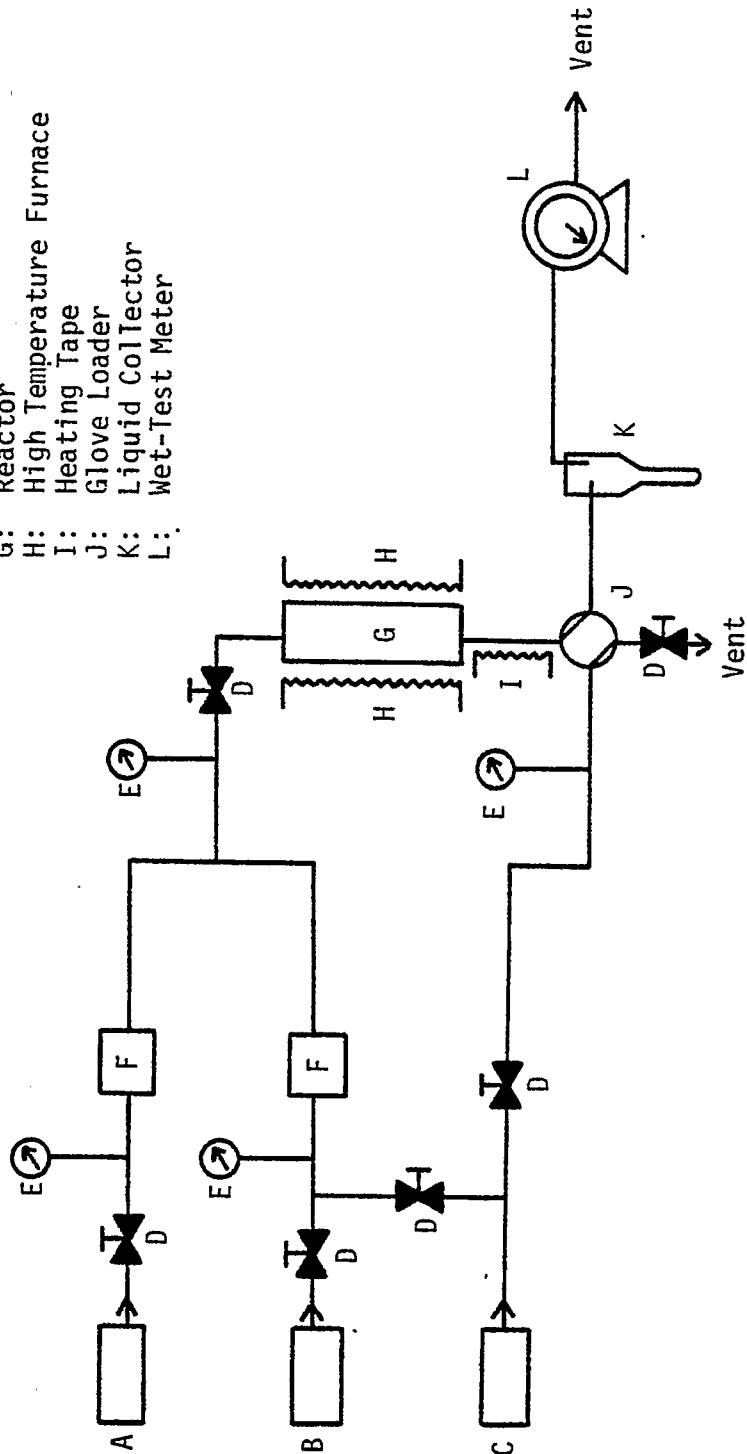


Figure 1. A Schematic of the process variable study apparatus.

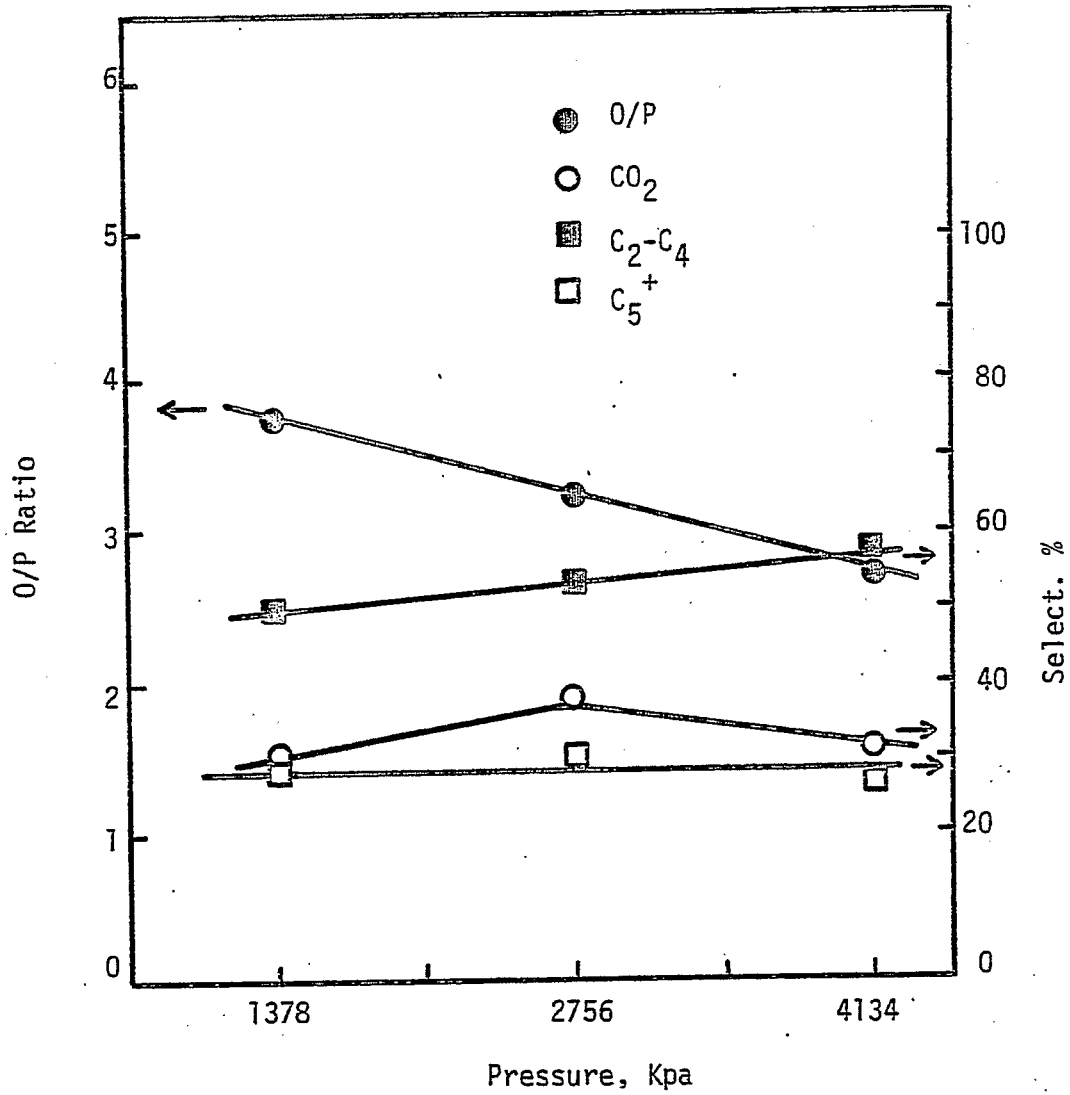


Figure 2. Pressure effect on product selectivity and C₂-C₄ O/P Ratio
 463 K, H/CO Ratio = 1/1
 Space Velocity = 9 cm³g⁻¹s⁻¹

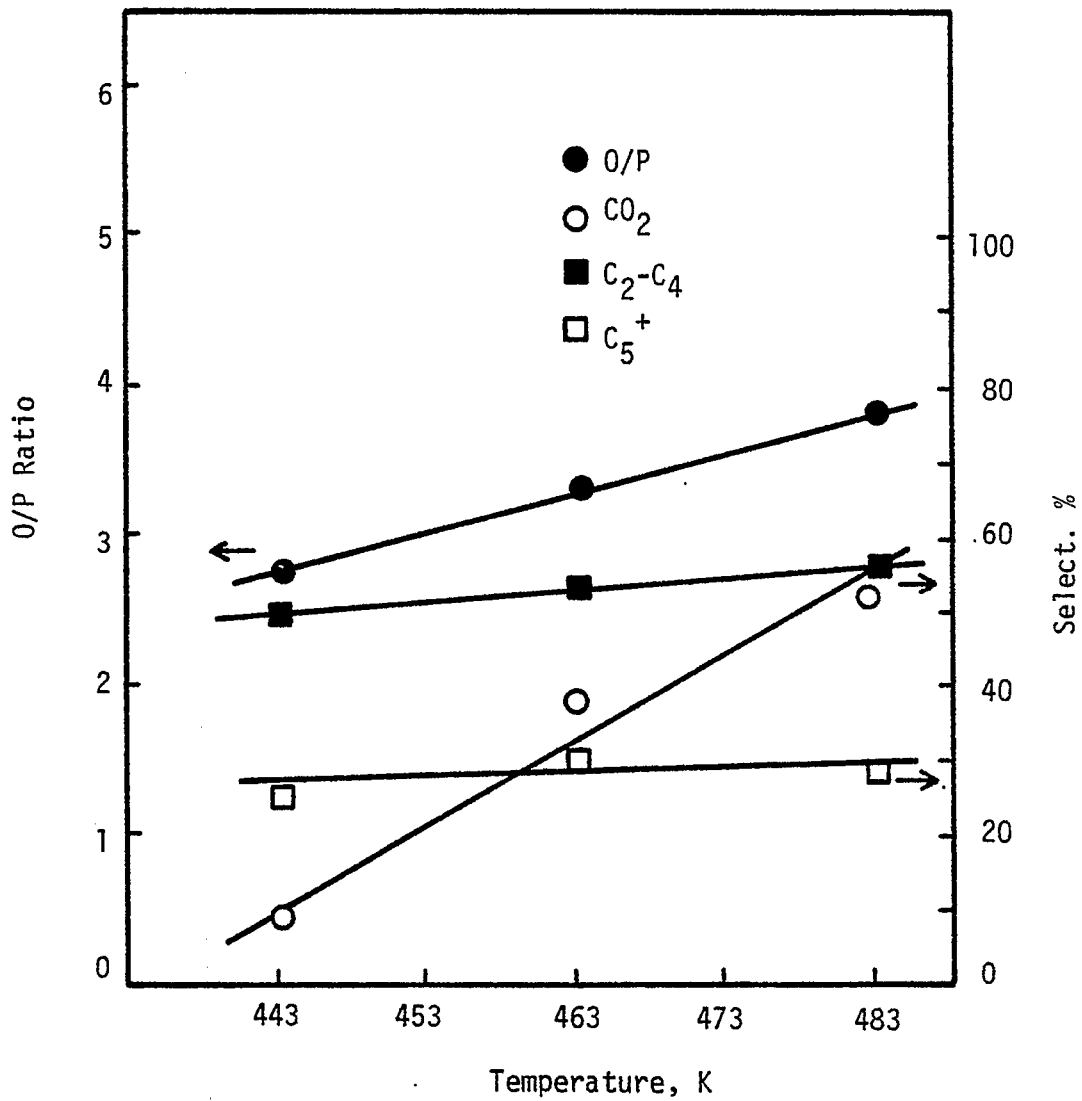


Figure 3. Temperature effect on product selectivity and C₂-C₄ O/P Ratio
 2756 kPa (400 psig), H₂/CO Ratio = 1/1
 Space Velocity = 9 cm³g⁻¹s⁻¹

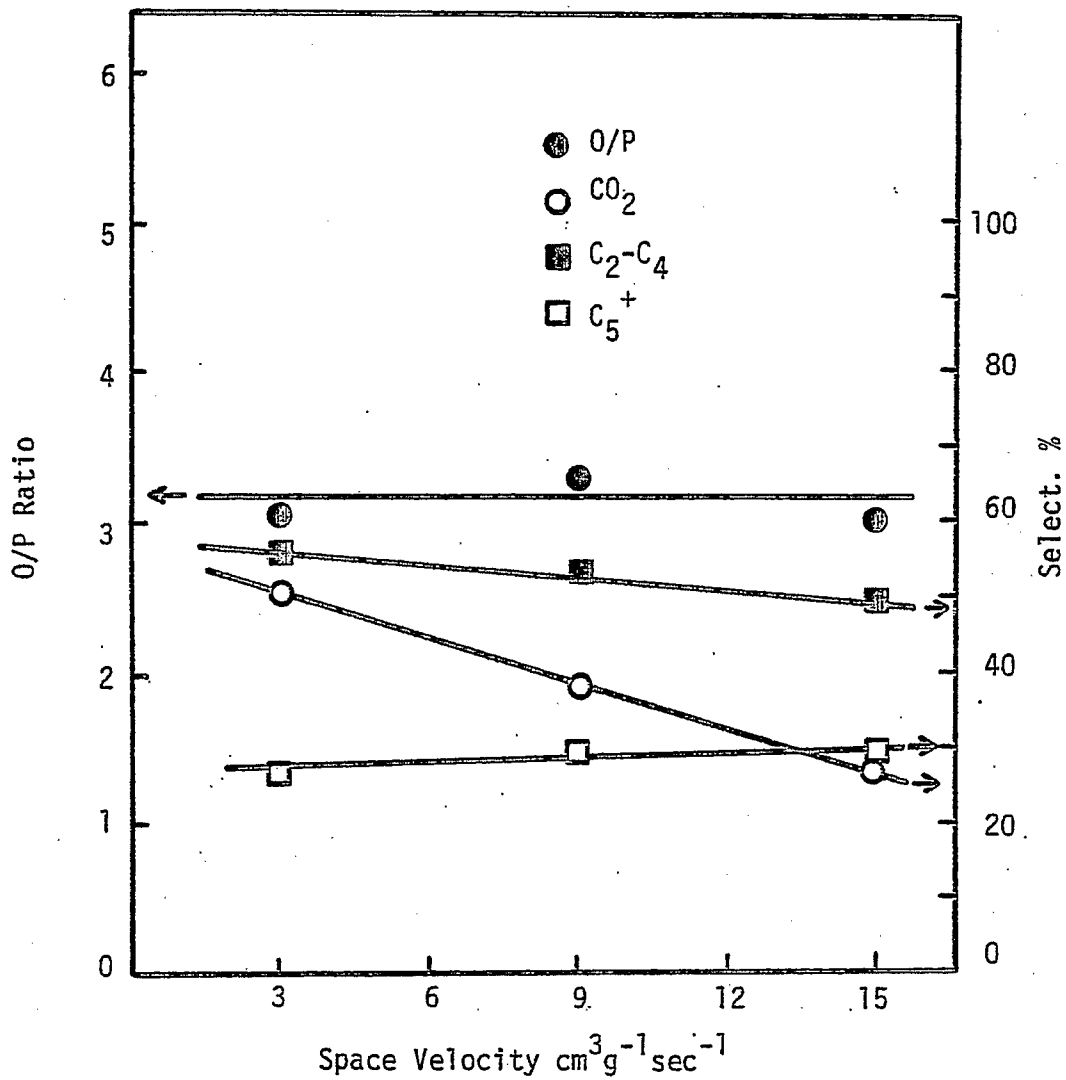


Figure 4. Space velocity effect on product selectivity and C₂-C₄ O/P Ratio
 463 K, H₂/CO Ratio = 1/1
 2756 KPa (400 psig)

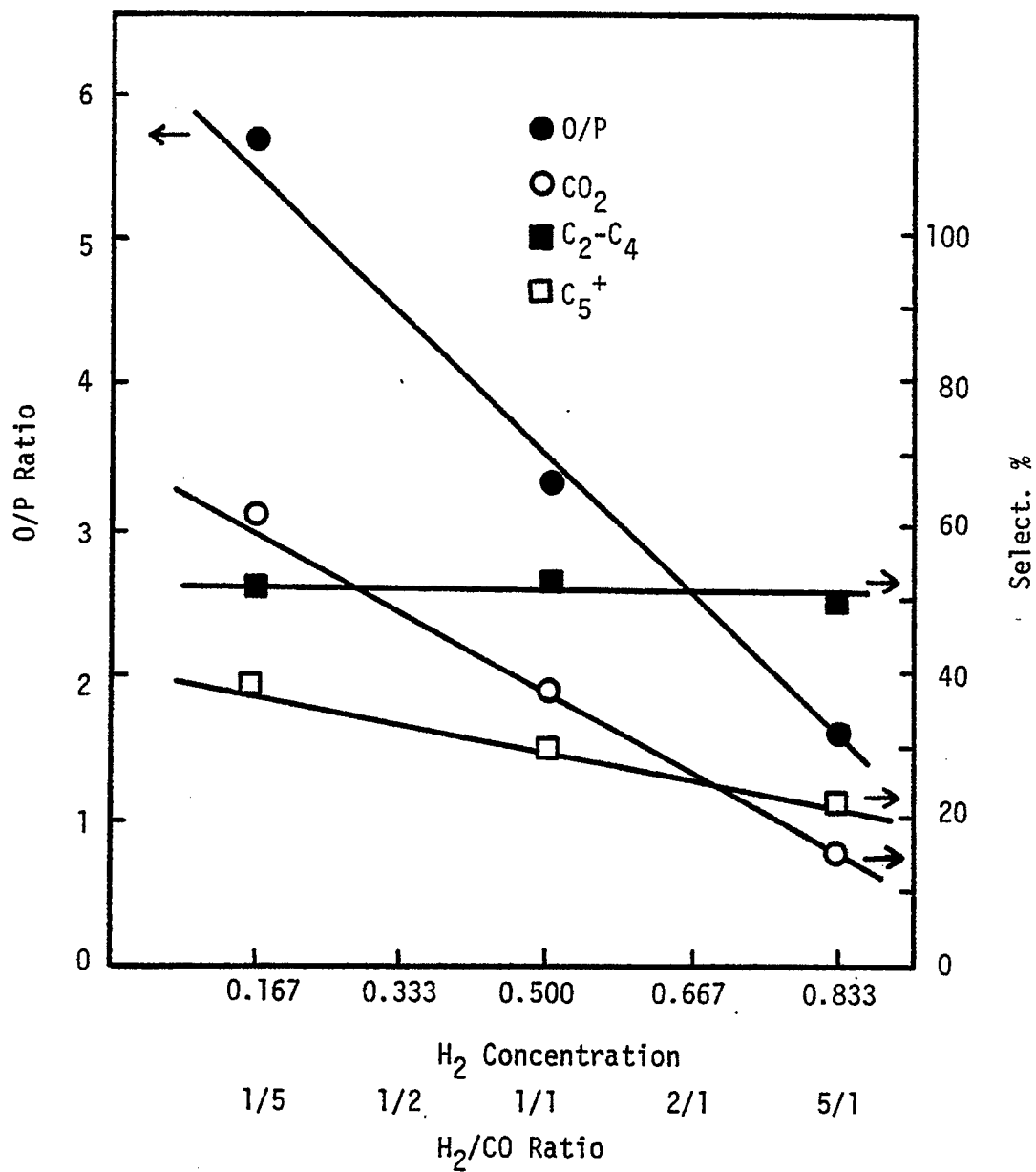


Figure 5. H₂/CO ratio effect on product selectivity and C₂-C₄ O/P Ratio
 463 K, 2756 KPa (400 psig)
 Space Velocity = 9 cm³ g⁻¹ s⁻¹

Table 1 Data of Process Variable Study

No	Pres. Kpa	Temp. °K	SV	H ₂ /CO	C ₂ -C ₄ C/P	C ₁	C ₂ -C ₄	C ₅ ⁺	CO ₂	CO % Conv.
1	3445	473	12	2:1	2.30	0.19	0.53	0.27	0.18	6.27
2	3445	473	12	1:2	4.01	0.15	0.54	0.31	0.27	2.19
3	3445	473	6	2:1	2.50	0.18	0.53	0.28	0.22	13.33
4	3445	473	6	1:2	4.02	0.14	0.55	0.30	0.51	5.74
5	3445	453	12	2:1	2.02	0.20	0.53	0.26	0.11	5.41
6	3445	453	12	1:2	3.11	0.17	0.49	0.29	0.38	1.18
7	3445	453	6	2:1	2.14	0.19	0.55	0.26	0.15	3.61
8	3445	453	6	1:2	3.09	0.15	0.50	0.31	0.30	1.73
9	2067	473	12	2:1	2.42	0.22	0.52	0.26	0.24	5.84
10	2067	473	12	1:2	5.10	0.17	0.51	0.32	0.32	1.80
11	2067	473	6	2:1	2.45	0.21	0.52	0.26	0.29	11.17
12	2067	473	6	1:2	4.90	0.16	0.53	0.31	0.23	2.52
13	2067	453	12	2:1	2.36	0.23	0.53	0.24	0.12	2.71
14	2067	453	12	1:2	3.71	0.19	0.45	0.31	0.44	1.12
15	2067	453	6	2:1	2.35	0.22	0.52	0.26	0.15	4.57
16	2067	453	6	1:2	3.73	0.17	0.49	0.29	0.29	1.48
17	4134	463	9	1:1	2.74	0.16	0.56	0.27	0.32	4.03
18	1378	463	9	1:1	3.77	0.20	0.50	0.29	0.31	2.78
19	2756	483	9	1:1	3.77	0.17	0.55	0.28	0.52	11.86
20	2756	443	9	1:1	2.56	0.20	0.49	0.25	0.09	0.91
21	2756	463	15	1:1	3.00	0.18	0.49	0.29	0.27	2.48
22	2756	463	3	1:1	3.04	0.16	0.56	0.27	0.51	13.59
23	2756	463	9	5:1	1.58	0.27	0.50	0.22	0.15	14.45
24	2756	463	9	1:5	5.61	0.19	0.52	0.28	0.61	3.91
25	2756	463	9	1:1	3.31	0.13	0.53	0.30	0.33	2.97

Table 2 Coefficients of
Process Variable Study

	Coe.	C ₂ -C ₄ O/P	C ₂ -C ₄ Select.	C ₅ + Select.	CO ₂ Select.
	B ₀	3.310	.530	.300	.380
Pres.	B ₁	-.243	.011	-.001	.003
Temp.	B ₂	.319	.012	.006	.049
S.V.	B ₃	-.007	-.010	.001	-.023
H ₂ /CO	B ₄	-.884	.004	-.019	-.092
	B ₁₁	-.034	-.001	-.002	-.030
	B ₂₂	-.057	-.003	-.006	-.033
	B ₃₃	-.093	-.002	-.002	-.012
	B ₄₄	.051	-.004	-.010	-.014
	B ₁₂	-.019	.000	.000	.010
	B ₁₃	-.033	.001	-.001	-.025
	B ₁₄	.164	-.002	.004	-.020
	B ₂₃	.001	.003	.002	-.025
	B ₂₄	-.223	-.014	.000	.030
	B ₃₄	-.031	.005	.004	-.015

Table 3 Reduced Coefficients
of Process Variable Study

	Coe.	C ₂ -C ₄ O/P	C ₂ -C ₄ Select.	C ₅ + Select.	CO ₂ Select.
	B ₀	3.047	.520	.291	.308
Pres.	B ₁	-.243	.011	----	----
Temp.	B ₂	.319	.012	.006	.049
S.V.	B ₃	----	-.010	----	-.023
H ₂ /CO	B ₄	-.884		-.019	-.092
	B ₁₁	.026	----	----	----
	B ₂₂	.003	----	-.004	-.016
	B ₃₃	----	----	----	----
	B ₄₄	.111	----	-.008	.002
	B ₁₂	----	----	----	----
	B ₁₃	----	----	----	----
	B ₁₄	.164	----	----	----
	B ₂₃	----	----	----	----
	B ₂₄	-.223	-.014	----	----
	B ₃₄	----	----	----	----

Task 13

Catalyst Research and Development

Synthesis of Light Hydrocarbons from CO and H₂

Faculty Advisor: F.V. Hanson
Graduate Student: Y.S. Tsai

Introduction

The hydrogenation of carbon monoxide to produce low molecular weight olefins has been investigated over unsupported iron-manganese catalysts. The results from the preliminary tests which were performed in a bench-scale fixed-bed reactor system showed that the unsupported iron-manganese catalysts were very selective in the production of C₂-C₄ olefins.

The catalysts were prepared by coprecipitation in which several steps were involved. However, the effects of the various preparation procedures on the catalyst activity and selectivity has not been determined. Nine Fe/Mn catalysts were prepared for the study of the catalyst preparation effect. Atomic absorption spectroscopy was applied to determine the exact compositions of the catalysts. Some of the catalysts were also analyzed by X-ray diffraction spectroscopy to obtain the average particle size of iron oxide in the catalysts.

In this project in-situ hydrogen reduction has been employed to activate the catalyst for the hydrogenation of carbon monoxide, but other catalyst pretreatments need to be examined to determine the optimum method of the catalyst activation for the production of C₂-C₄ olefins. Hydrogen, carbon monoxide and three synthesis gases with different H₂/CO ratios were used for the pretreatment study. In addition, a series of five Fe/Mn catalysts was tested at a set of standard operating conditions to examine the effect of manganese to promote the iron catalyst for the C₂-C₄ olefin production.

Project Status

Generally, the YST series of Fe/Mn catalysts was prepared by adding iron nitrate and manganese nitrate solutions to ammonium hydroxide to form the precipitates. In the YST-2 catalyst preparation the mixture of iron nitrate and manganese nitrate was added to ammonium hydroxide, however, for the YST-3 catalyst, the iron nitrate was added first, then manganese nitrate. The precipitation procedures for the YST-4 catalyst were just the reverse of those for the YST-3 catalyst. For the FT series of Fe/Mn catalysts, the precipitation of the catalyst was performed by adding ammonium hydroxide to the solution of iron nitrate and manganese nitrate. The procedures for filtration, washing and drying were the same for all catalysts.

Table 1 shows the actual compositions of the catalysts determined by atomic absorption (AA) spectroscopy. The actual composition of all catalysts

was very close to the calculated values. Therefore, the coprecipitation technique was proven to be reliable for preparing a catalyst with a composition very close to the desired value. Data for the average particle size of $\alpha\text{-Fe}_2\text{O}_3$ after the calcination of the Fe/Mn catalysts at 300°C for 16 hours are indicated in Table 2. The more manganese present in the catalyst, the smaller the particle diameter of $\alpha\text{-Fe}_2\text{O}_3$. Any form of manganese oxide was not detected due to the low concentration of Mn in the catalyst.

The catalyst pretreatment studies were conducted over the YST-2 catalyst by using hydrogen, carbon monoxide and synthesis gases of $3\text{H}_2/\text{CO}$, $2\text{H}_2/\text{CO}$ and H_2/CO ratios at 400°C and ambient pressure for 8 hours. Tables 3, 4, 5, 6 and 7 show the effects on the product yield and selectivity due to the different pretreatments. Each experiment lasted up to 20 hours at the following conditions: a $2\text{H}_2/\text{CO}$ ratio, a 200 psig pressure and a $1.0\text{ cm}^3\text{g}^{-1}\text{ sec}^{-1}$ space velocity. The temperature was maintained at either 210°C or at a point corresponding to about 7% CO conversion. Generally, the catalyst reduced by H_2 had a lower CO conversion than others, that is, the CO conversion was about 3.5% at 210°C and 12 hours on stream compared to 8-10% for other catalysts activated by CO or synthesis gases. However, after the close examination of data at 12 hours on stream, the H_2 reduction should still be considered a better catalyst pretreatment for the the research based on the following reasons: (1) The catalyst reduced by hydrogen had a low initial activity, but it showed a stable CO conversion after 12 hours of activation time. For other cases the catalyst activities decreased suggesting an unstable catalyst. (2) Methane and carbon dioxide are generally not desired products for the Fischer-Tropsch synthesis, however, the selectivity of CH_4 and CO_2 was more than 32% for all the cases except for the hydrogen reduced catalyst with a 28% production. (3) The selectivity of $\text{C}_2\text{-C}_4$ hydrocarbons for the hydrogen reduced catalyst was about 50% and the O/P ratio in $\text{C}_2\text{-C}_4$ hydrocarbons was 2.37. Generally, the $\text{C}_2\text{-C}_4$ hydrocarbon selectivities for other cases were lower than 45%. The O/P ratios in $\text{C}_2\text{-C}_4$ hydrocarbons were higher than 2.37 for synthesis gas conditioned catalysts and the ratio for the CO activated catalyst was lower than 2.37.

In the previous TGA study a period of 6 hours was adequate for the reduction of the catalyst by hydrogen. Therefore, the hydrogen pretreatment for 8 hours should be sufficient to activate the catalyst for the production of $\text{C}_2\text{-C}_4$ olefins. Thus, these pretreatment procedures have been adopted for this research. Tables 8, 9, 10, 11 and 12 indicate the catalyst activities and selectivities for the FT series Fe/Mn catalysts. Each catalyst was tested at least up to 12 hours when the catalyst generally reached a stable condition for the synthesis. The catalyst seemed more active in terms of CO conversion with less manganese present, that is, the pure iron catalyst (FT-1) had a CO conversion of 8.5% at 210°C, but the FT-5 catalyst (12.8 Mn/100 Fe) only had 6.8% even at 231°C. The activities for other FT catalysts were in-between. However, the effect of Mn on the production of $\text{C}_2\text{-C}_4$ olefins was significant, that is, the selectivity of $\text{C}_2\text{-C}_4$ hydrocarbons and the O/P ratio for the pure Fe catalyst were 45.7% and 1.07, respectively, but the data for the FT-2 catalyst (2.5 Mn/100 Fe) were 46.1% and 4.69, respectively.

The iron catalyst with a low manganese (i.e., FT-2) content is still evaluated as a more selective catalyst for the production of $\text{C}_2\text{-C}_4$ olefins

due to the following reasons: (1) The CO conversion for the FT-2 catalyst (7.2% at 225°C) was better than those for other FT catalysts at the same conditions. (2) The selectivities of CO₂ and CH₄ for the FT-2 catalyst were less (generally at 35-36%) than those for other FT catalysts (more than 38%). (3) The selectivity of C₂-C₄ hydrocarbons for the FT-2 catalyst was generally above 45% which was higher than those for other FT catalysts (less than 43%). (4) The O/P ratio of the C₂-C₄ hydrocarbons for the FT-2 catalyst was in the range of 4.4 - 5.0. This catalyst performance is very effective for the production of C₂-C₄ olefins because it promoted a more significant olefin production than the other Fe/Mn catalysts.

Future Work

A catalyst characterization study will be initiated. A literature survey on CO hydrogenation as well as heat and mass transfer for the fixed-bed reactor will be continued.

Table 1. Compositions of Fe/Mn catalysts determined by atomic absorption spectroscopy.

<u>Catalyst</u>	<u>Atomic Ratio(Mn/100 Fe)</u>	
	<u>Calculated</u>	<u>Actual</u>
YST-1	0	0
YST-2	3.0	3.6
YST-3	3.0	3.5
YST-4	3.0	3.5
FT-1	0	0
FT-2	2.5	2.5
FT-3	5.0	5.1
FT-4	8.1	8.2
FT-5	12.2	11.8

Table 2. Average particle diameter of α -Fe₂O₃ in Fe/Mn unreduced catalysts analyzed by X-ray diffraction method.

<u>Catalyst</u>	<u>Atomic Ratio (Mn/ 100 Fe)</u>	<u>Particle Size(\AA)</u>
YST-1	0	239
YST-2	3.6	218
FT-1	0	239
FT-2	2.5	224
FT-3	5.4	181
FT-4	8.2	146

Table 3. Product yield and selectivity versus time for YST-2 catalyst; Hydrogen reduction for 8 hours; $H_2/CO = 2/1$; 200 psig; 1.0 cc/g/sec space velocity.

<u>Time on stream(hr.)</u>	<u>0.5</u>	<u>3.0</u>	<u>7.2</u>	<u>11.5</u>	<u>12.5</u>	
<u>Temp.(°C)</u>	210	210	210	210	226	
<u>CO conv.(%)</u>	2.9	3.1	3.4	3.5	7.2	
<u>Selectivity(%)</u>	CO ₂	9.2	5.5	6.8	7.1	12.1
	C ₁	31.3	24.7	21.5	21.0	18.3
	C ₂ -C ₄	42.2	47.5	49.0	49.8	46.7
	C ₅ ⁺	11.3	16.5	18.2	18.0	18.1
	ROH	6.0	5.8	4.5	4.1	4.1
<u>O/P in C₂-C₄</u>	0.94	1.69	2.22	2.37	2.70	

Table 4. Product yield and selectivity versus time for YST-2 catalyst; CO pretreatment for 8 hours; $H_2/CO=2/1$; 200 psig; 1.0 cc/g/sec space velocity.

<u>Time on stream(hr.)</u>	<u>0.5</u>	<u>4.5</u>	<u>6.5</u>	<u>9.0</u>	<u>12.5</u>	
<u>Temp. (°C)</u>	210	210	210	210	210	
<u>CO conv. (%)</u>	21.9	9.4	9.2	9.1	8.4	
Selectivity(%)	CO ₂	2.2	5.6	8.3	9.7	9.3
	C ₁	28.3	26.5	25.0	24.0	23.8
	C ₂ -C ₄	52.1	43.9	43.1	42.2	42.1
	C ₅ ⁺	15.0	21.5	20.4	21.1	22.3
	ROH	2.4	2.5	3.2	3.0	2.5
<u>O/P in C₂-C₄</u>	1.08	1.38	1.52	1.63	1.68	

Table 5. Product yield and selectivity versus time for YST-2 catalyst; $1\text{H}_2/\text{CO}$ pretreatment for 8 hours; $\text{H}_2/\text{CO}=2/1$; 200 psig; 1.0 cc/g/sec space velocity.

<u>Time on stream(hr.)</u>	<u>0.2</u>	<u>3.6</u>	<u>7.5</u>	<u>10.5</u>	<u>12.8</u>	
<u>Temp. (°C)</u>	210	210	210	210	210	
<u>CO conv. (%)</u>	12.1	16.0	9.9	9.3	9.2	
Selectivity (%)	CO ₂	13.8	13.7	12.6	12.6	12.8
	C ₁	46.6	26.4	25.9	26.4	27.1
	C ₂ -C ₄	30.2	42.3	42.1	42.8	42.9
	C ₅ ⁺	7.7	14.9	16.8	15.9	14.9
	ROH	1.7	2.7	2.6	2.3	2.3
<u>O/P in C₂-C₄</u>	2.41	2.84	3.82	3.73	3.84	

Table 6. Product yield and selectivity versus time for YST-2 catalyst; $2\text{H}_2/1\text{CO}$ pretreatment for 8 hours; $\text{H}_2/\text{CO}=2/1$; 200 psig; 1.0 cc/g/sec space velocity.

<u>Time on stream(hr.)</u>	<u>0.4</u>	<u>4.5</u>	<u>7.2</u>	<u>10.2</u>	<u>12.5</u>	
<u>Temp.(°C)</u>	210	210	210	210	210	
<u>CO conv.(%)</u>	9.2	10.5	7.6	7.3	7.1	
<u>Selectivity(%)</u>	CO ₂	5.0	2.8	3.7	9.4	9.7
	C ₁	41.8	31.1	31.5	28.2	27.8
	C ₂ -C ₄	38.3	47.1	46.4	43.5	44.6
	C ₅ ⁺	14.9	16.5	16.0	16.6	15.8
	ROH	0	2.5	2.4	2.3	2.2
<u>O/P in C₂-C₄</u>	3.67	3.10	3.54	3.81	4.09	

Table 7. Product yield and selectivity versus time for YST-2 catalyst; $3\text{H}_2/1\text{CO}$ pretreatment for 8 hours; $\text{H}_2/\text{CO}=2/1$; 200 psig; 1.0 cc/g/sec space velocity.

<u>Time on stream(hr.)</u>	<u>0.5</u>	<u>3.6</u>	<u>5.0</u>	<u>7.5</u>	<u>12.5</u>	
<u>Temp. (°C)</u>	210	210	210	210	210	
<u>CO conv. (%)</u>	8.7	12.4	9.5	8.2	6.6	
Selectivity (%)	CO ₂	8.2	8.8	9.4	9.6	9.8
	C ₁	43.2	31.6	30.3	29.3	28.6
	C ₂ -C ₄	37.5	42.2	43.8	43.6	44.3
	C ₅ ⁺	8.1	15.3	14.7	15.5	15.4
	ROH	3.0	2.1	1.8	2.0	1.9
<u>O/P in C₂-C₄</u>	2.01	2.84	3.12	3.54	3.81	

Table 8. Product yield and selectivity versus time for FT-1 catalyst; hydrogen reduction for 8 hours; $H_2/CO=2/1$; 200 psig; 1.0 cc/g/sec space velocity.

<u>Time on stream(hr.)</u>	<u>3.0</u>	<u>6.5</u>	<u>7.7</u>	<u>9.5</u>	<u>13.5</u>	
<u>Temp. (°C)</u>	210	210	210	210	210	
<u>CO conv. (%)</u>	9.7	8.6	8.4	8.5	8.5	
<u>Selectivity (%)</u>	CO ₂	9.3	10.9	11.5	11.3	11.8
	C ₁	39.3	33.6	32.9	31.3	31.8
	C ₂ -C ₄	38.9	41.5	40.8	42.0	45.7
	C ₅ ⁺	10.0	12.5	12.4	13.3	8.9
	ROH	2.5	1.5	2.4	2.1	1.8
<u>O/P in C₂-C₄</u>	1.16	1.42	1.51	1.65	1.07	

Table 9. Product yield and selectivity versus time for FT-2 catalyst; hydrogen reduction for 8 hours; $H_2/CO=2/1$; 200 psig; 1.0 cc/g/sec space velocity.

<u>Time on stream(hr.)</u>	<u>3.0</u>	<u>8.5</u>	<u>11.0</u>	<u>12.5</u>	<u>17.5</u>	<u>19.0</u>	
<u>Temp.(°C)</u>	210	210	215	221	220	225	
<u>CO conv.(%)</u>	4.1	4.7	4.8	5.9	6.2	7.2	
<u>Selectivity(%)</u>	CO ₂	8.4	8.7	11.5	14.5	13.5	15.8
	C ₁	31.3	23.0	23.7	22.2	22.4	20.8
	C ₂ -C ₄	47.0	50.8	47.4	46.1	45.9	44.9
	C ₅ ⁺	10.8	14.8	15.6	14.9	16.1	15.9
	ROH	2.5	2.7	1.8	2.3	2.1	2.6
<u>O/P in C₂-C₄</u>	2.68	3.42	4.44	4.69	4.56	4.52	

Table 10. Product yield and selectivity versus time for FT-3 catalyst; hydrogen reduction for 8 hours; $H_2/CO=2/1$; 200 psig; 1.0 cc/g/sec space velocity.

<u>Time on stream(hr.)</u>	<u>2.0</u>	<u>4.0</u>	<u>7.7</u>	<u>10.0</u>	<u>11.5</u>	
<u>Temp.(°C)</u>	210	225	225	225	231	
<u>CO conv.(%)</u>	4.4	6.6	5.4	5.2	6.9	
Selectivity(%)	CO ₂	7.8	13.8	14.5	15.0	19.3
	C ₁	33.7	25.8	21.8	20.9	19.8
	C ₂ -C ₄	44.4	43.2	44.8	45.3	43.0
	C ₅ ⁺	12.0	14.7	16.9	16.7	16.0
	ROH	2.1	2.5	2.1	2.1	1.9
<u>O/P in C₂-C₄</u>	2.59	3.55	4.41	4.61	5.05	

Table 11. Product yield and selectivity versus time for FT-4 catalyst; hydrogen reduction for 8 hours; $H_2/CO=2/1$; 200 psig; 1.0 cc/g/sec space velocity.

<u>Time on stream(hr.)</u>	<u>3.0</u>	<u>4.5</u>	<u>7.5</u>	<u>10.5</u>	<u>12.5</u>	
<u>Temp. (°C)</u>	221	221	230	230	230	
<u>CO Conv. (%)</u>	6.5	5.6	7.0	7.2	7.7	
<u>Selectivity (%)</u>	CO ₂	13.2	13.3	19.7	21.1	21.4
	C ₁	28.3	22.5	20.7	19.1	19.1
	C ₂ -C ₄	44.3	46.2	42.8	42.2	42.3
	C ₅ ⁺	11.8	15.6	14.2	15.4	14.8
	ROH	2.4	2.4	2.6	2.2	2.4
<u>O/P in C₂-C₄</u>	2.73	4.04	4.88	5.09	5.03	

Table 12. Product yield and selectivity versus time for FT-5 catalyst; hydrogen reduction for 8 hours; $H_2/CO=2/1$; 200 psig; 1.0 cc/g/sec space velocity.

<u>Time on stream(hr.)</u>	<u>3.3</u>	<u>5.8</u>	<u>7.0</u>	<u>10.0</u>	<u>12.8</u>	
<u>Temp. (°C)</u>	225	231	231	231	231	
<u>CO conv. (%)</u>	7.1	7.3	7.0	6.9	6.8	
<u>Selectivity (%)</u>	CO ₂	13.4	17.5	18.2	19.1	19.7
	C ₁	25.2	21.8	20.4	19.8	19.1
	C ₂ -C ₄	43.2	42.9	43.2	42.7	43.1
	C ₅ ⁺	15.6	15.2	15.8	15.9	15.8
	ROH	2.6	2.6	2.4	2.5	2.3
<u>O/P in C₂-C₄</u>	2.99	4.08	4.61	5.18	5.29	

V. Conclusions

Detailed conclusions are included in the reports for each task. Task 4 is no longer funded and has been discontinued. Task 14 is inactive. No work was done under Task 15.